# Investigations on the use of ionic liquids for superior biomass processing

by

André Pinkert

A Thesis
Submitted to the Department of Chemical and Process Engineering
for the Degree of

DOCTOR OF PHILOSOPHY

March 2011

*"There are many things in life that will catch your eye, but only a few will catch your heart. Pursue those."*

— Dedicated to my parents —

# Acknowledgements

I wish to acknowledge the New Zealand Foundation for Research, Science and Technology for funding the research of my supervisors, who were consequently able to offer me a scholarship for my studies. Further, I wish to acknowledge the assistance from technicians all across the University, with particular focus on the support received from the Department of Chemical and Process Engineering. In addition, I would like to thank my family—and especially my fiancée—for their patience and backup.

It is my desire to express my utmost gratitude to my supervisors Ken Marsh and Shusheng Pang, who earned my deepest respect during the last three years. They supported me in any possible way—constantly focusing on my future career—and treated me as a colleague rather than as a student. I owe them lots, and I consider myself extremely lucky to have such great mentors. Thank you Ken & Shusheng!

On a different note, I would like commemorate the casualties that were claimed by the Christchurch earthquake in February 2011. The series of quakes and its aftermath certainly had an impact on both my studies and my ideology.

# Preface

The content of this thesis is based on research results that have been—or will be—published in international journals. In order to avoid self-plagiarism, I wish to acknowledge that portions of these articles are reproduced in this work. A statement has been signed by the co-authors declaring their approval and also outlining their particular contribution to these publications (see Appendix A).

To comply with copyright regulations, I have obtained permission from the American Chemical Society and the Royal Society of Chemistry to use the content of my original articles for this dissertation (see Appendix B).

This thesis adheres to the referencing style of the American Chemical Society.

# Abstract

Biocompatible composites, generated from renewable biomass feedstock, are regarded as promising materials that could replace synthetic polymers and reduce global dependence on fossil fuel sources. Wood cellulose, the most abundant biopolymer on earth, holds great potential as a renewable biomass feedstock. To unlock the entire scope of potential benefits of this feedstock, the wood components—namely cellulose, hemicellulose and lignin—need to be separated and processed individually. Current methods to separate wood components, such as Kraft pulping for example, suffer considerable drawbacks and cannot be considered environmentally benign. This thesis aims to increase our understanding of the interaction between ionic liquids (ILs) and biomass, in order to develop superior biomass processing techniques necessary to ensure a rapid transformation of our society towards full sustainability.

The first part of this work deals with the particular interaction of ILs with cellulose, and aims to investigate the structural requirements of ILs in order to qualify as a cellulose solvent. The cellulose-dissolving behaviour of selected alkanolammonium ILs was studied, and, combined with the results of an extensive literature review, a novel concept for the interaction of cellulose-dissolving ILs with cellulose was developed. It was postulated that efficient cellulose solvents need to position themselves in a distinct manner—with respect to the cellulose chain—in order to offer H–bond interaction sites with enhanced stability. As a result, alternative ions for cellulose-dissolving ILs were proposed, including oxazolium, 1,3-oxaphospholium, dimethylcarbamate, phosphate, nitrate, and nitrite.

The second part of the work investigated the use of food-additive based ILs for the separation of wood lignin, and studied the influence of selected process parameters, such as extraction time, extraction temperature, IL moisture content, wood particle size, wood species, IL cation species, solvent composition, and IL recyclability on the lignin extraction efficiency. The lignin extract and the wood residues were characterised *via* infrared spectroscopy, elemental analysis, thermogravimetric analysis, differential scanning calorimetry, X-ray diffraction, and gel permeation chromatography. An extraction efficiency of $e = 0.43$ of wood lignin was achieved in one gentle extraction step ($T = 373$ K, $t = 2$ h), and it was found that the presence of a co-solvent increased the extraction efficiency to $e = 0.60$. Gentle conditions during IL treatment did not decrease the crystallinity of the wood sample, and the extracted lignin had both a larger molecular mass and a more uniform molecular mass distribution, compared to commercially available Kraft lignin.

The outcomes of both studies were critically evaluated, addressing existing drawbacks and restrictions that need to be considered, and possibilities for future work were suggested.

# Table of Contents

# 1 Aim and Motivation

The ability of the human species to change the environment to its needs is a key reason for its unprecedented evolutionary success. We are simply shortcutting the time-consuming process of natural selection—which aims to adapt organisms to their environment—by exploiting the resources of our planet. However, if we wish to secure our future, we need to change our attitude and learn to deal with the available resources in a sustainable way.

Today's modern life is based on crude oil. The majority of both our transportation fuels and chemicals is derived from ancient biomass that harvested solar energy millions of years ago. These resources are non-renewable, however, if evaluated on a time scale relevant to human life. The term "peak oil" describes the point in time when global petroleum extraction reaches its maximum, resulting in inevitable subsequent decline.[1] Regardless of when peak oil will happen—or has happened—we need to find sustainable alternatives to be prepared for the future.

One promising alternative to fossil fuel-based transportation energy is fuel cell technology. Its fate, however, will depend on our advances in harvesting the required energy from renewable sources in the first instance. A renewable source for chemicals can be biological material from recently living organisms, commonly referred to as biomass. Plant biomass, and especially wood biomass, is of particular interest due to both its availability and the chemistry of its three major components: cellulose, hemicellulose and lignin.

In 2004, the US Department of Energy identified twelve sugar-derived

chemicals that can serve as building blocks to a number of high-value chemicals or materials.[2] The most abundant biopolymer on earth—cellulose—is entirely composed of sugar monomers, and it is also the main constituent of wood.[3] Combined with the fact that wood is renewable and non-edible for humans, it represents an alternative source to crude oil. In addition, the hexose sugar units contained in cellulose can also be fermented to yield bioethanol, which can be used as additional transportation fuel.[4]

Although wood cellulose has the potential to serve as feedstock for both biochemicals and biofuel, a far more precious asset is hidden in its molecular structure. Wood cellulose contains highly crystalline regions—known as nanocrystals—with tensile properties that rival those of Kevlar®.[5] These nanocrystals can potentially be used to produce biocomposites with outstanding mechanical abilities. However, the presence of lignin is a major barrier for the efficient processing of wood cellulose, and environmentally-benign methods are required to separate wood lignin from its cellulosics, *viz.* cellulose and hemicellulose. Lignin is still considered as a low-value product, but its highly aromatic character qualifies lignin to be regarded as a major renewable source for aromatic chemicals. With the right technology in place, lignin has the potential to become a high-value feedstock for the near future.

Recent research indicated that ionic liquids—a solvent class with unique physical properties—can offer considerable advantages in biomass processing, compared to traditional methods.[6] Little is known about the mechanism of cellulose dissolution in ionic liquids,[7,8] and data on the use of ionic liquids for wood delignification are scarce.[9]

The aim of this thesis is to (i) develop a concept that offers an explanation for the fact that only specific ionic liquids have an ability to dissolve cellulose, and (ii) investigate the use of ionic liquids for the extraction of wood lignin.

# 2 Introduction to Ionic Liquids

## 2.1 Fundamentals

Molten salts with low melting temperatures (< 373 K), commonly referred to as ionic liquids (ILs), attracted first interest in the 1960s at the U.S. Air Force Academy as salt electrolytes for thermal batteries. These first-generation ILs, consisting of binary mixtures of 1-butylpyridinium chlorides ([BPy]Cl) and aluminium chlorides, suffered from serious limitations like easy electrochemical reduction and air-sensitivity.[10] The problems were overcome in the early 1990s with second-generation ILs that were air- and water-stable.[11]

Some examples of these ILs include salts composed of organic cations, such as 1,3-dialkylimidazolium $[R_1R_2IM]^+$, 1-alkylpyridinium $[RPy]^+$, tetraalkylammonium $[NR_4]^+$, or tetraalkylphosphonium $[PR_4]^+$, and inorganic anions, such as hexafluorophosphate $[PF_6]^-$, tetrafluoroborate $[BF_4]^-$, nitrate $[NO_3]^-$, methanesulfonate (mesylate) $[CH_3SO_3]^-$, trifluoromethane sulfonate (triflate) $[CF_3SO_3]^-$, and bis-(trifluoromethanesulfonyl)amide $[Tf_2N]^-$, chloride, bromide, and iodide. (Figure 1)[12–14]

The number of potential ion combinations available is estimated to equate to $10^{12}$ different ILs.[15] Structural characteristics, such as bulky and unsymmetrical ions with a high degree of charge delocalisation, assist IL ions to reduce the attractive Coulomb forces between their cations and anions, resulting in a low melting temperature. If the melting temperature is below room temperature, the IL is called room temperature ionic liquid (RTIL). The

huge variety of possible ion combinations allows for tailoring ionic solvents with specific properties for certain purposes, the so-called task specific ionic liquids (TSILs).[16]

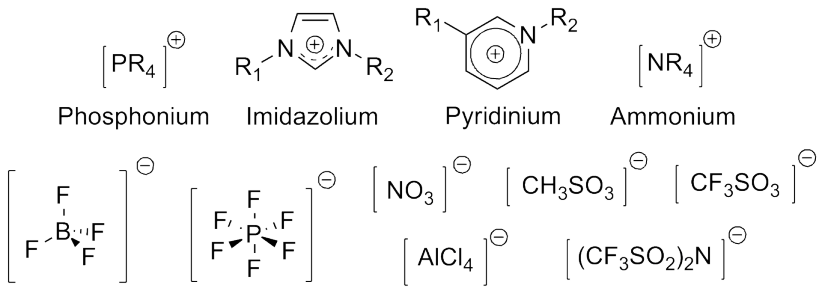


**Figure 1.** Some cations and anions commonly found in ionic liquids.

## 2.2 Synthesis and Purification

The synthesis of imidazolium ILs can generally be split into two steps: the formation of the desired cation and then the exchange of the anion to produce the final product according to the scheme shown in Figure 2. The most common ILs are prepared by quaternising a nitrogen heterocycle with an alkyl halide (Mentschutkin reaction).[17] The anion exchange involves either the direct treatment of a halide salt with a strong Lewis acid to form complex anions, or the formation of the IL by the addition of a metal salt to precipitate the unwanted ion.[18] Other synthesis routes have been developed that include solvent and halide free pathways, microwave or sonochemical methods, or using low-cost industrial products as starting materials, such as the detergent sodium octylsulfate.[19–24]

Depending on the method of synthesis, impurities in the IL can be tertiary amines, alkyl halides, or alkyl sulfates or their side-reaction products, and, after metathesis, residual halide or sulfate. Methods of purification include extraction of the IL with polar solvents (e.g. ethyl acetate), extrac-

tion of the aqueous solution of IL with an immiscible organic solvent (e.g. dichloromethane), flash column chromatography of a solution of IL in an organic solvent, or treatment of the IL with activated charcoal.[18]

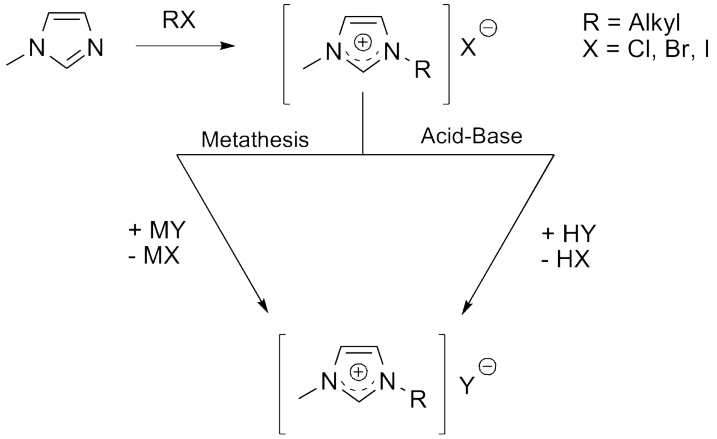


**Figure 2.** Typical synthesis paths for the preparation of ionic liquids.

## 2.3 Properties and Applications

ILs offer a variety of physical properties that make them attractive to a broad field of applications. Some of these properties are common to all ILs and, as such, are defining characteristics. ILs with quaternised nitrogen cations are non-flammable and were initially thought to have negligible vapour pressure, but Earle et al. showed that they can be distilled under low pressure and high temperature.[25] Nevertheless, these desired properties are significant as their negligible vapour pressure means solvent evaporation is limited, thus reducing the need for respiratory protection and exhaust systems. This property also enhances their recyclability and is one reason for them often being called "green solvents". Recent studies have shown that they have a wide range of toxicity and, as a result, the use of the term "green solvents" has been questioned.[26,27]

The diversity of ILs makes them applicable to myriads of applications that include optical thermometers, biocatalysis and separation processes, polymer and catalytic chemistry, electrolytes, biosensors, analytic devices, lubricants, solvent replacement applications, and lunar telescopes.[10,15,16,28–37]

Properties such as melting temperature, thermal stability, refractive index, acid–base character, hydrophilicity, polarity, density, and viscosity can be tailored to a certain degree. However, the presence of reactant impurities, such as halide anions, organic bases and absorbed water, can considerably alter their properties, accounting for much of the variability of published property data.[38]

### 2.3.1 Melting Temperature

The melting temperature ($T_{\text{fus}}$) and viscosity ($\eta$) of ILs depend significantly on the anion type, although the cation does have a minor influence.[39] Most ILs show a glass transition, which occurs when a supercooled liquid forms an amorphous solid.[10] The glassy material can crystallise upon heating, which is followed by subsequent melting of the sample. The thermal properties are governed by van der Waals forces and electrostatic interactions, which are primarily determined by ion size, symmetry, H–bond interactions, and charge delocalisation (Figure 3).[40–42]

### 2.3.2 Symmetry

Low-symmetry cations, such as 1-butyl-3-methylimidazolium $[\text{BMIM}]^+$, possess only $C_1$ symmetry, and their salts melt at lower temperatures than analogous salts with higher symmetry, such as 1-butylpyridinium $[\text{BPy}]^+$ salts with $C_{2v}$ symmetry.[43] Figure 4 shows a correlation between symmetry and melting temperature for a group of tetraalkylphosphonium $[\text{P}_{nnnn}]^+$ ILs. In the series $[\text{P}_{666n}]\text{PF}_6$, the melting temperature reaches a maximum for the

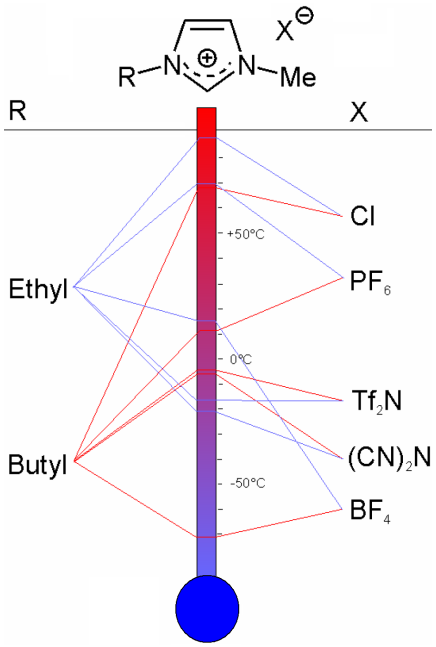


**Figure 3.** Melting temperatures of selected imidazolium-based ionic liquids depending on their ion composition (adapted from Laus et al.).[40]

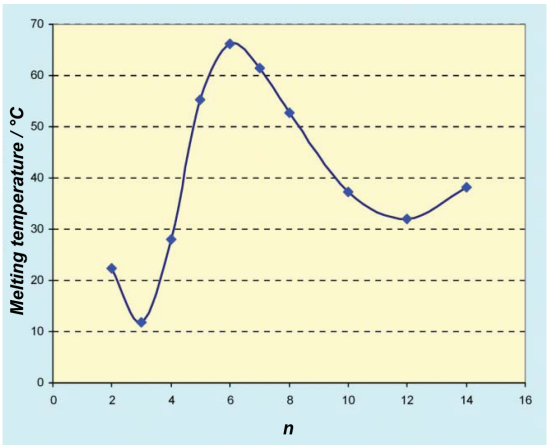


**Figure 4.** The melting temperatures of $[P_{666n}]PF_6$ as a function of $n$ (modified from Plechkova and Seddon).[43]

symmetrical cation $[P_{6666}]^+$, and decreases as one of the chains gets either longer or shorter, with concomitant symmetry lowering to $C_{3v}$.[43]

### 2.3.3 Alkyl Chain Length

The length of the alkyl chain also influences $T_{fus}$. Figure 5 shows an optimised structure of the 1-methyl-3-octadecylimidazolium $[C_{18}MIM]^+$ cation. Such cations, of the general formula $[C_nMIM]^+$, possess a charge-rich imidazolium core and a hydrophobic alkyl side chain. An increasing number of carbon atoms ($n < 7$) in the side chain result in a decrease of the melting temperature due to the lower overall symmetry of the cation (symmetry-breaking region). However, side chains with more than seven carbon atoms lead to an increase of the melting temperature, as attractive van der Waals interactions between the alkyl side chains start outweighing the symmetry effect (hydrophobic region). An example of this symmetry–$T_{fus}$ relationship is shown in Figure 6, illustrating the agreement between experimental results and a computational study using a QSPR (quantitative structure–property relationship) approach.[44,45]

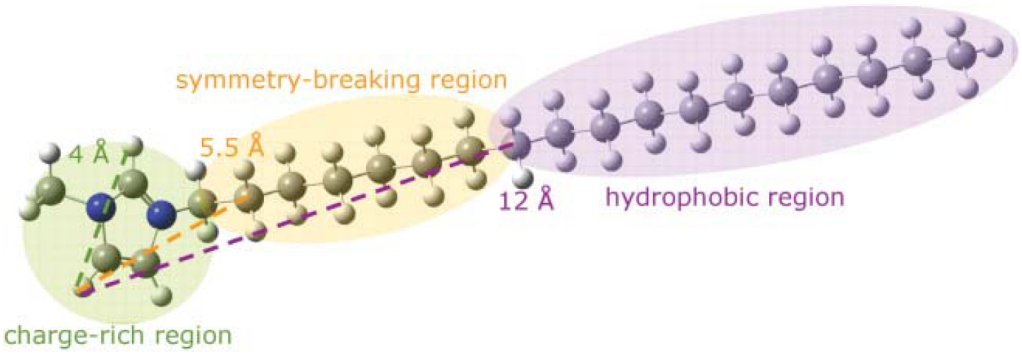


**Figure 5.** Optimised structure of $[C_{18}MIM]^+$ showing its charge-rich imidazolium core and its hydrophobic alkyl side chain (adapted from Plechkova and Seddon).[43]

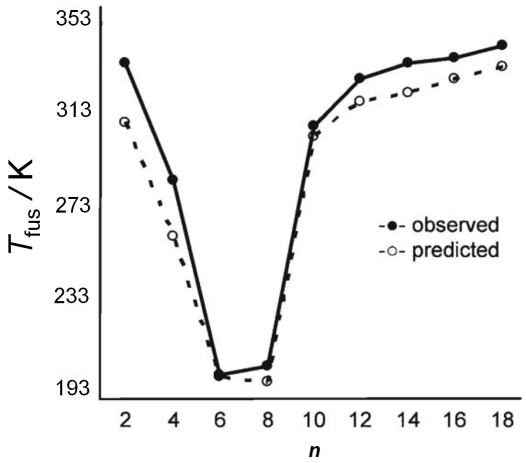


**Figure 6.** Predicted and observed melting temperatures for a series of $[C_nMIM]PF_6$ ILs (modified from Plechkova and Seddon).[43]

### 2.3.4 Hydrogen Bonds

The presence or absence of strong hydrogen bonds (H–bonds) also influences the melting temperature. The existence of H–bonds in imidazolium ILs was first reported in 1986.[46] Traditionally, the C–H$\cdots$X (X = Cl, Br) interaction is characterised as a relatively weak interaction, but it becomes very strong in imidazolium-based halide ILs and can even possess some covalent character.[47] These strong H–bonds involve all three imidazolium ring protons, resulting in a three-dimensional ion-network with aromatic $\pi$-stacking interactions between the imidazolium cores (Figure 7).[48] $[BF_4]^-$ anions can also form H–bonds in imidazolium-based ILs, although the H–bonds are considerably weaker than those of the corresponding halides.[49–51] Hexafluorophosphate anions do not normally participate in H–bonding.[49]

### 2.3.5 Viscosity

The viscosity of ILs is highly sensitive to contaminations. The presence of water decreases the viscosity, whereas chloride impurities have the opposite

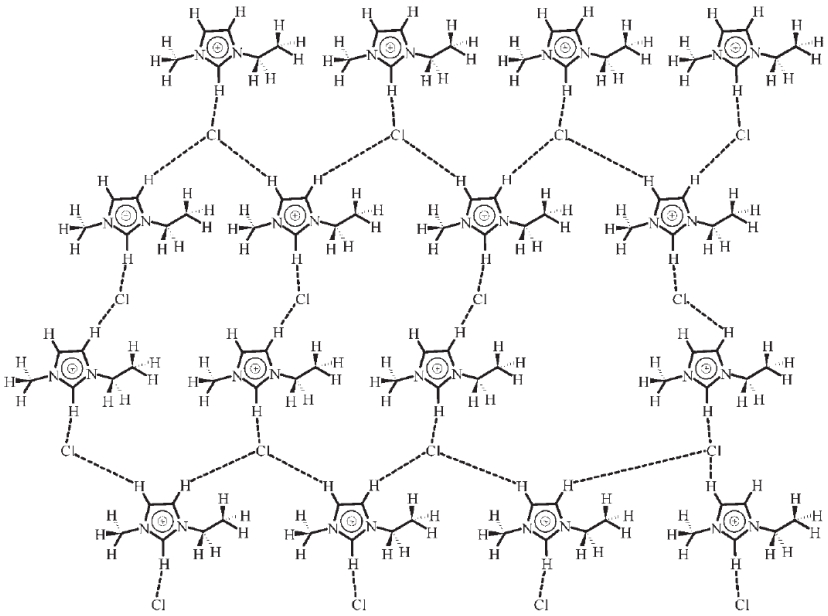

**Figure 7.** Schematic representation of H–bonding in [EMIM]Cl (adapted from Heinze et al.).[18]

effect.[38,52] The presence of co-solvents seems to decrease the aggregation of the ions in the liquid, resulting in a decrease of viscosity, although experimental results indicate that the nature of the co-solvent plays a more important role than its mass fraction.[53,54]

A major barrier to the commercial application of ILs arises from their high viscosity. The viscosity of ILs is higher than water and similar to oils, and the viscosity decreases with increasing temperature.[55–58] The temperature dependence of the viscosity with asymmetric cations and no functional groups in the side chain can generally be described with the Arrhenius equation. For ILs with symmetrical cations and lower molecular weight, the Vogel–Tammann–Fulcher equation appears more suitable. For other ILs, neither model can accurately describe the temperature dependence of viscosity.[55]

Abbott predicted the viscosity behaviour of ILs by the application of the "hole theory". For low viscosity, the ions must be relatively small and the

liquid must contain large free spaces. It is suggested that ILs with a high surface tension have these properties, including imidazolium salts with $C_4$–$C_6$ alkyl moieties.[59] Nitrate ($[NO_3]^-$) based ILs that have a low surface tension are an example of ILs with low viscosity and high electrical conductivity.[60] The same correlation between surface tension and viscosity was observed for $[Tf_2N]^-$ and $[PF_6]^-$ ions.[61]

Furthermore, branching of the alkyl chain in 1-alkyl-3-methylimidazolium salts reduces viscosity, as it reduces the intermolecular dipole–dipole interactions. The same reason accounts for the low viscosity of most polyfluorinated anions.[62] Additional factors to be considered are H–bonding ability and symmetry (see section 2.3.2).[61,63] Concluding, the viscosity of ILs based on the most common anions decreases in the order $Cl^- > [PF_6]^- > [BF_4]^- > [Tf_2N]^-$.

### 2.3.6 Density

Density is one of the most often reported properties of ILs, probably because almost every application requires knowledge of density. In general, ILs are denser than water. The molar mass of the anion significantly affects the overall density of ILs.[62] The bis(methanesulfonyl)amide $[Ms_2N]^-$ salts, for example, have lower densities than the $[Tf_2N]^-$ salts. This is because of the greater mass of the fluorinated $[Tf_2N]^-$ anion, given that the molar volume of both anions is similar.[63] In general, ILs with ions of similar size tend to be denser, because the alternating positive and negative ions can be packed more efficiently.[62]

### 2.3.7 Surface Tension

Little data has been published on the surface tension of ILs.[60,61] In general, the liquid–air surface tensions of ILs are somewhat higher compared to conventional solvents—except for water—and span an unusually wide range.[62]

Surface tension values vary with temperature, and both the surface excess entropy and energy of imidazolium ILs decreases with increasing alkyl chain length. For a specific cation, the compound with the larger anion has, in general, the higher surface tension.[64] However, alkylimidazolium $[PF_6]^-$ salts have a higher surface tension than the corresponding $[Tf_2N]^-$ salts.[62]

### 2.3.8 Thermal Stability

Most ILs exhibit a relatively high thermal stability, with onset decomposition temperatures ($T_D$) between (573 and 673) K. The decomposition appears to be independent of the cation but decreases as the hydrophilicity of the anion increases.[62] In general, it has been suggested that the thermal stability is anion dominated, decreasing in the following order $[PF_6]^- > [Tf_2N]^- \approx [BF_4]^- > X^-$.[65] However other factors can affect the thermal stability. Fluorinated anions such as $[PF_6]^-$ and $[BF_4]^-$, for example, are unstable in the presence of water and decompose to produce HF.[18,26,66] Because some metals catalyse IL decomposition, it is advisable for thermogravimetric analysis experiments to use sample pans made of platinum rather than aluminum.[65,67]

The thermal stability of ILs has been recently revised, because it was shown that degradation occurs at much lower temperatures if the temperature is held at that elevated level for a longer period of time ($\approx$ 10 h). On the basis of these observations, the introduction of a new parameter describing the maximum operating temperature without degradation was suggested.[67,68] The anions usually decompose via dealkylation, whereas the cations undergo primarily alkyl migration and elimination reactions.[67] In general, imidazolium salts tend to be more stable than tetraalkylammonium salts.[65]

### 2.3.9 Polarity

For molecular solvents, the term "polarity" is often related to its ability to dissolve other compounds. The precise definition of "solvent polarity" is complex, since this term encompasses many molecular properties responsible for interactions between solvent and solute molecules (e.g. Coulombic, directional, inductive, dispersion, H–bonding, electron pair donor, and electron pair acceptor forces). Hence, the quantitative characterisation of "solvent polarity" remains a problem not completely solved for molecular solvents.[62]

The most common method to describe the polarity of ILs is the solvatochromic determination of the Kamlet–Taft parameters, but fluorescence spectra, refractive indices, or organic reactions were also used to determine polarity.[10,69–72] The linear solvation–energy relationship parameters are empirical and attempts to describe both H–bond basicity+acidity and polarity+polarisability.

As a rule of thumb, ILs are polar solvents similar to short- to medium-chain alcohols.[10,69] Water impurities do not greatly influence the polarity. Anions have the greatest effect on the H–bond basicity, and the polarity of ILs depend to some extent on the polarity of their environment.[69,71,73]

### 2.3.10 Permittivity

The relative dielectric permittivity, previously known as dielectric constant ($\epsilon_s$), cannot be used for the quantitative characterisation of solvent polarity, because this property does not provide an adequate correlation with much of the experimental data of molecular solvents. Conventional methods for measurement of $\epsilon_s$ are not applicable due to the high electrical conductivity of ILs, although measuring the permittivity at high frequencies ($f > 5$ GHz) and subsequent extrapolation to zero frequency provides an estimate of the relative permittivities.[74–82] Huang and Weingaertner conclude that the relative permittivities of 1,3-dialkylimidazolium ILs at ambient temperature

vary little ($\epsilon_s$ = 10 to 15) compared to those of molecular solvents. Even though $\epsilon_s$ of ILs can range from about 11 to 57, $\epsilon_s$ values of ILs are significantly lower than those of common polar solvents.[74,75]

The influence of the anion on $\epsilon_s$ appears to be minor, and H–bonding influences the permittivity—and consequently the polarity—in very much the same way as in molecular liquids.[75] Table 1 shows the relative dielectric permittivities of some ILs. Molten salts with fluoride-containing anions are poor cellulose solvents and also have low permittivities. In contrast, 2-hydroxyethylammonium formate ([HEA]Fmt) displays the highest permittivity measured for an IL so far, and a high affinity to interact with cellulose was reported.[75] However, it will be shown later that [HEA]Fmt is not a solvent for cellulose (see 3.2 on page 35). The relationship between permittivity and cellulose-dissolving power of ILs has yet to be systematically studied.

**Table 1. Relative Dielectric Permittivities $\epsilon_s$ of some Ionic Liquids at 293 K.**

| Ionic liquid[a] | $\epsilon_s$ |
|---|---|
| [HEA]Fmt[75] | 57.3 |
| [EMIM]$EtOSO_3$[74] | 27.9 |
| [EMIM]$BF_4$[74] | 12.9 |
| [EMIM]$Tf_2N$[74,76] | 12.3 |
| [BMPyr]$Tf_2N$[77] | 11.7 |
| [BMIM]$BF_4$[74] | 11.7 |
| [BMIM]$PF_6$[74] | 11.4 |

[a] See Glossary for IL ion explanation

### 2.3.11 Miscibility with Water

The hydrophilic or hydrophobic nature of an IL determines its solvation properties in other solvents, and it consequently affects its miscibility with water. Many applications require knowledge of the degree of water misci-

bility of a solvent, especially with regard to phase separation processes or possible wastewater contamination. A recent publication indicates a route for separating water-miscible ILs from the aqueous phase.[83] The miscibility of ILs with water depends mainly on the hydrophilic nature of the anion and the hydrophobic nature of the cation, which is primarily determined by the length of the imidazolium alkyl chains.[62] In general, the solubility of water decreases with decrease in temperature. All ILs are hygroscopic to some extent and absorb water from the atmosphere.

Spectroscopic studies indicate that the water dissolved in ILs is mostly present in the "free" state, bonded via H–bonds to two anions. Cammarata et al. suggested that the degree of hydrophilicity of the IL can be used as an indicator for the strength of these H–bond interactions.[84] Nuclear magnetic resonance (NMR) studies suggest that water molecules prefer to interact with the H-2, H-4, and H-5 protons of the imidazolium core (see Figure 21 on page 58) and that the three-dimensional ion network of the IL is weakened as a result.[85]

### 2.3.12 Toxicity

ILs quickly gained attention as new solvents within the green chemistry community. Initially there were few environmental and ecological studies, but the cytotoxic, environmental, and microbial toxicity of the most common ILs has only been studied since a few years.[27,86–90] The effect of [BMIM]Cl, the most widely used IL, on marine algae, *Vibrio Fischeri*, luminescent bacteria, leukaemia cell lines, or enzymes like acetylcholinesterase—which plays an essential role in the nervous system of all higher organisms—showed that the IL was not acutely toxic ($EC_{50}$ ≈13 $\mu$M).[86]

However, the toxicity of imidazolium ILs increases dramatically with increasing length of the alkyl side chains, due to an increase in lipophilicity. The cation dominates the toxic effect of ILs, although some influence of the

anion was shown.[87] In general, imidazolium ILs are more toxic than the more bulky phosphonium ILs, and it is recommended to work with short alkyl side chains on the cation core wherever possible.[88,89] Nevertheless, there is still a lack of *in vivo* investigations on IL biouptake, and it was suggested to emphasise recycling issues in IL life-cycle analyses.[87,88,91]

### 2.3.13 Thermophysical Property Database

Easy access to the exponentially increasing rate of publications on ILs during the past decade requires a data collection of as many properties as possible.[10] The most comprehensive data collection of IL properties—covering the years from 1984 to 2004—with 1680 data entries was published by Zhang et al. in 2006,[92] prior to the establishment of the IUPAC operated—and freely accessible—online database "IL Thermo". It is regularly updated and contains, at the time of writing, property data of 339 ILs with a total number of 212 different ions and more than 25 000 property data points for pure ILs.[93] Property data for binary and ternary IL systems is also included in the database.

# 3 Ionic Liquids and their Interaction with Cellulose

Wood cellulose can be used for producing biofuels and biopolymers, thus offering a solution to global concerns on the excessive use of fossil fuels. Efficient processing of cellulose requires a solvent for the biopolymer, preferably one that is easy to handle and that facilitates ecofriendly processing. In ideal solvent would be nontoxic, noncorrosive, of low cost, of low viscosity, with negligible vapour pressure, and with a superior ability to dissolve cellulose at moderate temperatures.

Some ILs have shown promising results as cellulose solvents, with many advantages compared to traditional approaches. It is agreed that their ionic nature is responsible for cleaving H–bonds between cellulose chains, resulting in dissolution of the biopolymer. The mechanism of cellulose dissolution in ILs, however, is still unclear, and no theories are available that explain why only certain IL ion combinations are able to dissolve the biopolymer.

This chapter aims to analyse the structural similarities that are shared by the most common cellulose solvents, particularly focusing on ILs, in order to discover a structural feature that is beneficial for the dissolution of cellulose. As a result, a mutual relationship between IL anions and IL cations is postulated, offering an explanation for the ability—or disability—of certain ion combinations to dissolve the biopolymer.

# 3.1 Literature Review

## 3.1.1 Cellulose

Cellulose is the most common organic polymer, and it is considered an almost inexhaustible source of raw material for the increasing demand for environmentally friendly and biocompatible products. Wood consists of up to 47 % of cellulose, which is the main structural component of the primary cell walls of plants.[94] Although wood pulp remains the most important raw material source for cellulose, the biopolymer can also be extracted from algae, bacteria, and annual crops.[95]

Cellulose is a linear polymer of cellobiose—which is composed of two glucose sugar units—linked by glycosidic linkages (C—O—C) at the $C_1$ and $C_4$ positions (Figure 8). The polymer chain length depends on the degree of polymerisation (DP), which is the number of repeating units of glucose. The DP can vary considerably from about 20, in the case of laboratory-synthesised cellulose, to 10 000 or more for bacterial cellulose.[95,96] Each glucose unit is rotated by 180° with respect to its neighbour, so that the structure repeats itself every cellobiose unit. Wood cellulose contains approximately $10^4$ units, and the polymer can reach a length of about 5 $\mu$m in the highly crystalline regions.[94] One chain end has a hemiacetal group at the $C_1$ position, known as the reducing-end, while the other side has an alcoholic hydroxy (OH–) group on the $C_4$ carbon position, referred to as nonreducing end.

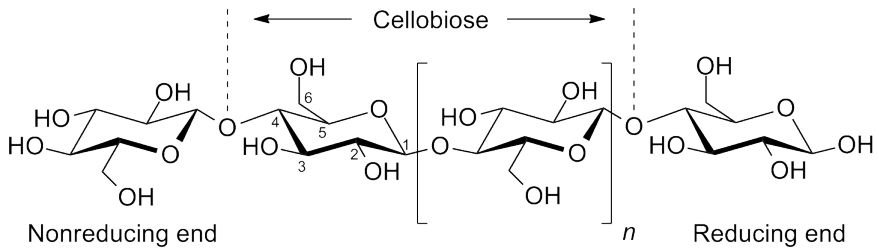


**Figure 8.** Schematic structure of a cellulose polymer chain.

At least seven different crystal structures of cellulose are known: $I_\alpha$, $I_\beta$, II, $III_I$, $III_{II}$, $IV_I$, and $IV_{II}$. These cellulose allomorphs differ mainly in their unit-cell dimensions, chain-packing, and H–bond interactions. Cellulose I and II are the most common forms. Native cellulose—or cellulose I—consists of parallel aligned chains, while regenerated cellulose—or cellulose II—has antiparallel alignment. Although being thermodynamically more stable than cellulose I, the conformation of the hydroxymethyl group in cellulose II is not suitable for intermolecular H–bonding, resulting in this allomorph being more susceptible to solvent attack.[97] Native cellulose is a linear but semicrystalline polymer, consisting of highly structured crystalline regions—known as microfibrils—and amorphous parts. Other plant components, such as lignin or hemicellulose, have branched structures.[98] The very stable $\beta$-(1→4)-link is reinforced by intrachain H–bonds between (i) the OH–group at position $C_3$ and the adjacent in-ring oxygen, and (ii) between the OH–group at position $C_2$ and the hydroxymethyl group oxygen at position $C_6$ (Figure 9).[99]

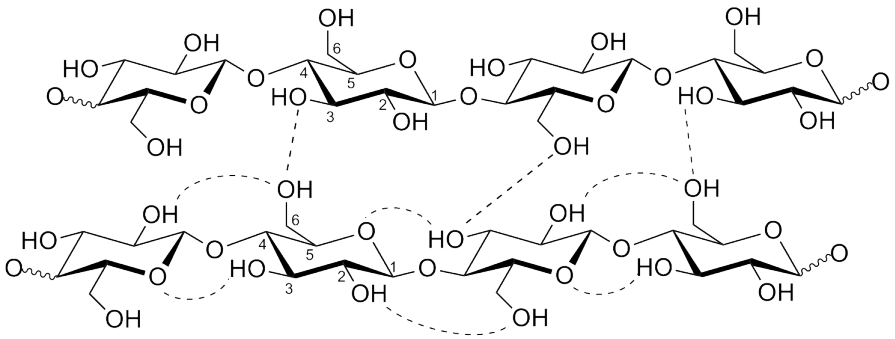

**Figure 9.** Intra- and intermolecular hydrogen bonds in cellulose.

In the natural state, about 40 to 70 cellulose chains are interconnected by H–bonds—between the hydroxymethyl at position $C_6$ and the OH–group at position $C_3$ of the adjacent chain—to form a microfibril.[100] These microfibrils are extremely stiff, with an elastic modulus of approximately 220 GPa in

fibre direction and about 15 GPa perpendicular to it.[101] Both the strong glycosidic bonds and the large degree of intra- and intermolecular H–bonds in cellulose are responsible for its great chemical and mechanical stability. The hydrophilic character of cellulose is due to its numerous OH–groups.[96]

### 3.1.2 Dissolving Cellulose with Ionic Liquids

ILs appear to be highly polar due to their ionic character, resulting in their enhanced biopolymer dissolving capacity. Table 2 gives an overview of the cellulose-dissolving capacity of ILs reported in the literature.

A number of factors influence the IL's ability to dissolve cellulose, and it is important to note that Table 2 deals only with the dissolution capacity of these solvents, and not with the kinetics. Low viscosity ILs promote the dissolution process—mainly due to the higher mobility of the ions—and longer dissolution times ($>$ 12 h) do not always lead to better results, especially at higher temperatures.[102–104] The risk of partial degradation at elevated temperatures may account for the fact that the favoured dissolution temperature is very often 10 K above the melting temperature of the IL.[105,106]

Impressive results have been obtained when (3 to 5) s microwave pulses were used instead of thermal heating. For example, the solubility of cellulose with a DP of 1000 could be increased by 150 %.[107] Microwave heating is characterised by an internal heating process, due to the direct absorption of energy by polar molecules, and differs significantly from conventional heating methods that are based on heat transfer. Internal heating may be responsible for the more effective breakdown of the H–bond network between the microfibrils, although care must be taken because heating occurs rapidly and can easily lead to pyrolysis of the biopolymer.[108] Sonication-assisted IL treatment of cellulose does not seem to significantly influence the dissolution process.[107] Additional factors influencing the dissolution are the DP of the biopolymer and the solvent structure.[103]

The most successful cations for cellulose dissolution are based on methylimidazolium and methylpyridinium core structures, with allyl-, ethyl-, or butyl- side chains. Even numbers of carbon atoms in the side chain are more favourable for cellulose dissolution than odd numbers.[109] The maximum dissolution power is reached with the butyl side chain, and it was reported that OH–groups in the side chain can enhance cellulose solubility.[108] This could be due to the additional polarity in the heteroatomic substituents on the imidazolium ring. Imidazolium ILs with double bond containing side chains can show reduced viscosity. The same effect was observed if one of the alkyl chain carbon atoms was replaced by an oxygen atom, although those ILs do not tend to dissolve cellulose.[20,40] The most promising IL anions for cellulose dissolution are chloride, acetate, and formate. $^{13}C$ and $^{35/37}Cl$ NMR relaxation studies indicate there is a stoichiometric interaction between the chloride anions and the cellulose OH–groups.[110]

It is thought that both anions and cations are involved in the dissolution process. Figure 10 shows the proposed interaction between IL ions and cellulose during dissolution. The oxygen and hydrogen atoms of the cellulose form electron donor–electron acceptor complexes with the IL ions. It has been suggested that this occurs primarily between the OH–groups at positions $C_3$ and $C_6$ of neighboured cellulose chains, resulting in chain separation and subsequent dissolution of biopolymer.[108,111,112]

Heinze et al. investigated the interactions of IL cations using low DP cellooligomers as simplified cellulose model systems.[18] They propose that [EMIM]Ac forms a covalent bond between the C-1 carbon of the glucose unit and the C-2 carbon of the imidazolium core, because NMR studies showed that the C-1 carbon signal of the glucose unit disappeared after dissolution in [EMIM]Ac (Figure 11). Ebner et al. verified this hypothesis by means of labelling experiments with $^{13}C$ isotopes or fluorescence markers, suggesting the formation of a covalent bond between the C-2 carbon of 1-alkyl-3-methyl-imidazolium ILs and the reducing end of cellulose.[113]

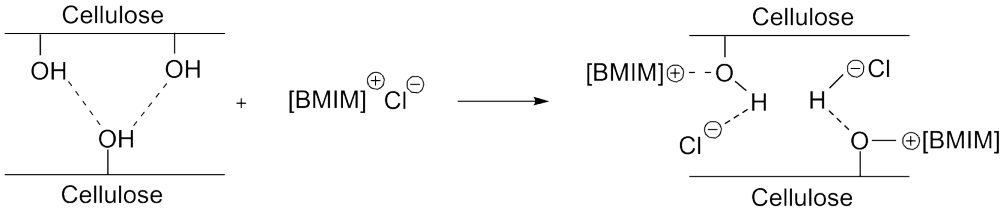


**Figure 10.** Proposed interaction between [BMIM]Cl and cellulose chains during dissolution of the biopolymer (redrawn from Feng and Chen).[108]

Surprisingly, this is not the case when the oligomer was dissolved in [EMIM]Cl.[18] Considering that the suggested bond formation between the IL and cellulose is base-catalysed, the presence of residual imidazolium impurities in the [BMIM]Ac could be a possible explanation of this observation. Another reason for this phenomenon might be the proposed H–bond network within [EMIM]Cl (see Figure 7), as this would result in a saturated coordination sphere of the cation. Leipner et al. studied the dissolution of cellulose in molten salt hydrates, and concluded that an unsaturated coordination sphere of the cation is necessary to interact successfully with the cellulose.[114] However, the similar dissolution power for cellulose of both ILs—[BMIM]Cl and [EMIM]Cl—does not agree with those conclusions (Table 2). It has been suggested that dissolved cellulose can exist in many different states, depending on the solvent and other factors.[95,111] Varying dissolution states of cellulose are another possible reason for the differing reactivity of IL cations with regard to cellulose.

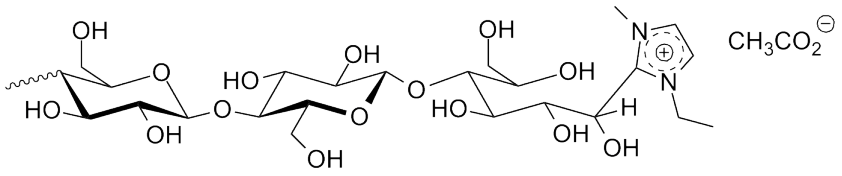


**Figure 11.** Structure proposed for a covalent binding of [EMIM]Ac to cello-oligomer.[18]

Contaminations can also influence the cellulose dissolution capacity of an IL. It has been shown that a mass fraction ($w$) of water of 0.01 in [BMIM]Cl is sufficient to prevent biopolymer dissolution.[107] Elevated pressures of (0.2 to 0.9) MPa can assist the dissolution process, and adding co-solvents can either reduce the dissolution rate (e.g. with carbon disulfide) or decrease the viscosity of the mixture (e.g. with DMSO, $CHCl_3$, or DMF).[102,115–118]

**Table 2. Biopolymer-Dissolving Capacity of Ionic Liquids and Other Solvents in Mass Fraction ($w$), Focusing on Cellulose with Different Degrees of Polymerisation (DP).**

| Ionic liquid | Cellulose solubility | DP[a] (DP)[b] | Solution conditions | | Reference |
|---|---|---|---|---|---|
| | 100 $w$ | | $\theta$/°C | $t$/h | |
| [BMIM]$CF_3SO_3$ | > 50 | lignin[c] | 90 | 24 | Lee[119] |
| [MMIM]$MeSO_4$ | > 50 | lignin[c] | 90 | 24 | Lee[119] |
| [BMPy]Cl | 39 | 286 (172) | 105 | 12 | Heinze[105,120] |
| [BMPy]Cl | 37 | 593 (412) | 105 | 12 | Heinze[105,120] |
| [BMPy]Cl | 12 | 1198 (368) | 105 | 12 | Heinze[105,120] |
| [BMPy]Cl | > 5 | $\alpha$-cellulose | 105 | 12 | Zavrel[121] |
| $H_3PO_4$ | 38 | cellulose | nn | nn | Boerstoel[122] |
| [HEA]Fmt | 30 | cellulose | nn | 24 | Bicak[123] |
| $[IM]_2Al_xCl_y$ | 25 | wood | 110 | 25 min | Xie[124] |
| [BMIM]Cl | 25 | 1000 | mwh | mwh | Swatloski[107] |
| [BMIM]Cl | 11–25 | 1175 | nn | nn | Laus[40] |
| [BMIM]Cl | ≈ 20 | nn | 100 | 2 | Erdmenger[109] |
| [BMIM]Cl | 18 | 286 (307) | 83 | 12 | Heinze[105,120] |
| [BMIM]Cl | 13.6 | 569 | nn | nn | Kosan[111] |
| [BMIM]Cl | 13.4 | 454 | nn | nn | Kosan[111] |
| [BMIM]Cl | 13 | 593 (544) | 83 | 12 | Heinze[105,120] |
| [BMIM]Cl | 11 | keratin[d] | 130 | 10 | Xie[125] |

Continued on next page...

**Table 2. Continued**

| Ionic liquid | Cellulose solubility | DP[a] (DP)[b] | Solution conditions | | Reference |
|---|---|---|---|---|---|
| | 100 $w$ | | $\theta$/°C | $t$/h | |
| [BMIM]Cl | 10 | 1198 (812) | 83 | 12 | Heinze[105,120] |
| [BMIM]Cl | 10 | cellulose | 100 | 5 mg/h | Zhao[126] |
| [BMIM]Cl | 10 | 1000 | 100 | nn | Swatloski[107] |
| [BMIM]Cl | > 10 | lignin[c] | 90 | 24 | Lee[119] |
| [BMIM]Cl | 8 | wood[e] | 110 | 8 | Kilpelainen[103,127] |
| [BMIM]Cl | 8 | keratin[d] | 130 | 10 | Xie[125] |
| [BMIM]Cl | 7 | wood[f] | 130 | 8 | Kilpelainen[103,127] |
| [BMIM]Cl | > 5 | $\alpha$-Cellulose | 90 | 12 | Zavrel[121] |
| [BMIM]Cl | 5 | wood[g] | 130 | 8 | Kilpelainen[103,127] |
| [BMIM]Cl | 5 | 1000 | 80 | uss | Swatloski[107] |
| [BMIM]Cl | 3 | 1000 | 70 | nn | Swatloski[107] |
| [BMIM]Cl | 3 | 1000 | 70 | nn | Swatloski[107] |
| [BMIM]Cl | > 3 | wood[h] | 80 | 24 | Lee[119] |
| [BMIM]Cl | > 3 | wood[i] | 105 | nn | Kilpelainen[103] |
| [BMIM]Cl | sls | wood[i] | 130 | 15 | Kilpelainen[103,127] |
| [BMIM]Cl | 4 | nn | 130 | 8 | Aaltonen[104] |
| [BMIM]Cl | 4 | nn | 130 | 27 | Aaltonen[104] |
| [BMIM]Cl | 3 | nn | 130 | 4 | Aaltonen[104] |
| [BMIM]Cl | 1 | nn | 130 | 4 | Aaltonen[104] |
| [BMIM]Cl | 4 | wood | 130 | 4.5 | Aaltonen[104] |
| [BMIM]Cl | 3 | wood | 130 | 10 | Aaltonen[104] |
| [BMIM]Cl | 3 | wood | 130 | 21 | Aaltonen[104] |
| [BMIM]Cl | 3 | lignin | 130 | 3 | Aaltonen[104] |
| [BMIM]Cl | 3 | lignin | 130 | 2 | Aaltonen[104] |
| [BMIM]Cl | 2 | lignin | 130 | 27 | Aaltonen[104] |

Continued on next page...

**Table 2. Continued**

| Ionic liquid | Cellulose solubility | DP[a] (DP)[b] | Solution conditions | | Reference |
|---|---|---|---|---|---|
| | 100 $w$ | | $\theta$/°C | $t$/h | |
| [BMIM]Cl | 2 | lignin | 130 | 4 | Aaltonen[104] |
| [BMIM]Cl | 1.4 | lignin | 130 | 8 | Aaltonen[104] |
| [BMIM]Cl | 1.3–2.6 | wood[j] | 110 | 16 | Sun[9] |
| [BMIM]Cl | 2 | xylan | 130 | 8 | Aaltonen[104] |
| [BMIM]Fmt | $< 20$ | 250 | 85 | nn | Fukaya[128] |
| [BMIM]Fmt | 8 | 225 | 110 | nn | Zhao[126] |
| NMMO | 17 | 454 (444) | nn | nn | Kosan[111] |
| NMMO | 14.4 | 569 (537) | nn | nn | Kosan[111] |
| [BMIM]Ac | 13.2 | 569 | nn | nn | Kosan[111] |
| [BMIM]Ac | 12 | 398 | 100 | 1 | Vitz[129] |
| [BBIM]Ac | 9 | 300 | 100 | nn | Zimmermann[130] |
| [EMIM]Ac | $> 30$ | lignin[c] | 90 | 24 | Lee[119] |
| [EMIM]Ac | 15 | 225 | 110 | nn | Zhao[126] |
| [EMIM]Ac | 13.5 | 569 | nn | nn | Kosan[111] |
| [EMIM]Ac | 8 | 398 | 100 | 1 | Vitz[129] |
| [EMIM]Ac | $> 5$ | $\alpha$-cellulose | 90 | 12 | Zavrel[121] |
| [EMIM]Ac | $> 5$ | wood[k] | 90 | 12 | Zavrel[121] |
| [EMIM]Ac | $< 5$ | wood[h] | 80 | 24 | Lee[119] |
| [EMIM]Ac | 4.9–5.0 | wood[l] | 110 | 16 | Sun[9] |
| [EMIM]Ac | 4.6–4.9 | wood[j] | 110 | 16 | Sun[9] |
| [EMIM]Cl | 15.8 | 569 | nn | nn | Kosan[111] |
| [EMIM]Cl | 12 | 268 (329) | 90 | 12 | Barthel[106,120] |
| [EMIM]Cl | $\approx 10$ | cellulose | 100 | 2 | Erdmenger[109] |
| [EMIM]Cl | 6 | 593 (580) | 90 | 12 | Barthel[106,120] |
| [EMIM]Cl | $> 5$ | $\alpha$-cellulose | 90 | 12 | Zavrel[121] |

Continued on next page...

**Table 2. Continued**

| Ionic liquid | Cellulose solubility | DP[a] (DP)[b] | Solution conditions | | Reference |
|---|---|---|---|---|---|
| | 100 $w$ | | $\theta$/°C | $t$/h | |
| [EMIM]Cl | 4 | 1198 (1129) | 90 | 12 | Barthel[106,120] |
| [AMIM]Cl | > 30 | lignin[c] | 90 | 24 | Lee[119] |
| [AMIM]Cl | 14.5 | 220 | 80 | < 0.5 | Zhang[112] |
| [AMIM]Cl | 14.5 | 650 | 80 | < 0.5 | Zhang[112] |
| [AMIM]Cl | 12.5 | 1085 | nn | nn | Laus[40] |
| [AMIM]Cl | 11 | 250 | 100 | nn | Fukaya[128] |
| [AMIM]Cl | 10 | 250 | 100 | nn | Fukaya[128] |
| [AMIM]Cl | 10 | 1175 | nn | nn | Laus[40] |
| [AMIM]Cl | 8 | 1600 | 80 | < 0.5 | Zhang[112] |
| [AMIM]Cl | 8 | wood[m] | 80 | 8 | Kilpelainen[103,127] |
| [AMIM]Cl | 8 | wood[e] | 110 | 8 | Kilpelainen[103,127] |
| [AMIM]Cl | 7 | wood[f] | 130 | 8 | Kilpelainen[103,127] |
| [AMIM]Cl | > 5 | $\alpha$-Cellulose | 90 | 12 | Zavrel[121] |
| [AMIM]Cl | > 5 | wood[n] | 90 | 12 | Zavrel[121] |
| [AMIM]Cl | 5 | wood[e] | 80 | 24 | Kilpelainen[103,127] |
| [AMIM]Cl | 5 | wood[g] | 130 | 8 | Kilpelainen[103,127] |
| [AMIM]Cl | 2 | wood[g] | 110 | 8 | Kilpelainen[103,127] |
| [AMIM]Cl | > 3 | wood[h] | 80 | 24 | Lee[119] |
| [AMIM]Cl | > 3 | 1176 | nn | nn | Laus[40] |
| [AMIM]Br | — | 398 | 100 | 1 | Vitz[129] |
| [AEIM]Cl | 5 | 306 | 90 | nn | Guo[131] |
| [AMIM]Fmt | 21.5 | 250 | 85 | nn | Fukaya[128] |
| [AMIM]Fmt | 20 | 250 | 80 | nn | Fukaya[128] |
| [BDMIM]Cl | 12.8 | 569 | nn | nn | Kosan[111] |
| [BDMIM]Cl | 9 | 286 (377) | 90 | 12 | Barthel[106,120] |

Continued on next page...

**Table 2. Continued**

| Ionic liquid | Cellulose solubility | DP[a] (DP)[b] | Solution conditions | | Reference |
|---|---|---|---|---|---|
| | 100 $w$ | | $\theta$/°C | $t$/h | |
| [BDMIM]Cl | 6 | 593 (580) | 90 | 12 | Barthel[106,120] |
| [BDMIM]Cl | 4 | 1198 (1129) | 90 | 12 | Barthel[106,120] |
| [BDMIM]Cl | ≈ 3 | 1176 | nn | nn | Laus[40] |
| [ADMIM]Br | 12 | 286 (320) | 80 | 12 | Barthel[106] |
| [ADMIM]Br | 4 | 593 (599) | 80 | 12 | Barthel[106] |
| [ADMIM]Br | 4 | 1198 (1203) | 80 | 12 | Barthel[106] |
| [EMIM]DMP | 16.2 | MCC | 90 | nn | Yang[132] |
| [EMIM]DMP | 13.0 | MCC | 80 | nn | Yang[132] |
| [EMIM]DMP | 9.4 | MCC | 70 | nn | Yang[132] |
| [EMIM]DMP | 7.2 | MCC | 60 | nn | Yang[132] |
| [EMIM]DMP | 6.4 | MCC | 50 | nn | Yang[132] |
| [EMIM]DMP | 5.1 | MCC | 40 | nn | Yang[132] |
| [EMIM]DMP | 10 | 250 | 65 | 0.5 | Fukaya[133] |
| [EMIM]DMP | 8 | 250 | 60 | 0.5 | Fukaya[133] |
| [EMIM]DMP | 6 | 250 | 55 | 0.5 | Fukaya[133] |
| [EMIM]DMP | 6 | 250 | 40 | 1 | Fukaya[133] |
| [EMIM]DMP | 4 | 250 | 50 | 0.5 | Fukaya[133] |
| [EMIM]DMP | 2 | 250 | 45 | 0.5 | Fukaya[133] |
| [EMIM]DEP | 11.5 | MCC | 90 | nn | Yang[132] |
| [EMIM]DEP | 9.6 | MCC | 80 | nn | Yang[132] |
| [EMIM]DEP | 9.0 | MCC | 70 | nn | Yang[132] |
| [EMIM]DEP | 6.2 | MCC | 60 | nn | Yang[132] |
| [EMIM]DEP | 5.1 | MCC | 50 | nn | Yang[132] |
| [EMIM]DEP | 3.8 | MCC | 40 | nn | Yang[132] |
| [MMIM]DMP | 10.6 | MCC | 90 | nn | Yang[132] |

Continued on next page...

**Table 2. Continued**

| Ionic liquid | Cellulose solubility | DP[a] (DP)[b] | Solution conditions | | Reference |
|---|---|---|---|---|---|
| | 100 $w$ | | $\theta$/°C | $t$/h | |
| [MMIM]DMP | 9.8 | MCC | 80 | nn | Yang[132] |
| [MMIM]DMP | 8.8 | MCC | 70 | nn | Yang[132] |
| [MMIM]DMP | 7.4 | MCC | 60 | nn | Yang[132] |
| [MMIM]DMP | 5.3 | MCC | 50 | nn | Yang[132] |
| [MMIM]DMP | 4.7 | MCC | 40 | nn | Yang[132] |
| [EMIM]MPh | 10 | 250 | 45 | 0.5 | Fukaya[133] |
| [EMIM]MPh | 8 | 250 | 40 | 0.5 | Fukaya[133] |
| [EMIM]MPh | 6 | 250 | 30 | 1 | Fukaya[133] |
| [EMIM]MPh | 4 | 250 | 30 | 0.5 | Fukaya[133] |
| [EMIM]DMPh | 10 | 250 | 55 | 0.5 | Fukaya[133] |
| [EMIM]DMPh | 8 | 250 | 50 | 0.5 | Fukaya[133] |
| [EMIM]DMPh | 6 | 250 | 45 | 0.5 | Fukaya[133] |
| [EMIM]DMPh | 6 | 250 | 35 | 1 | Fukaya[133] |
| [EMIM]DMPh | 4 | 250 | 40 | 0.5 | Fukaya[133] |
| [EEIM]DEP | 9.1 | MCC | 90 | nn | Yang[132] |
| [EEIM]DEP | 5.9 | MCC | 80 | nn | Yang[132] |
| [EEIM]DEP | 2.1 | MCC | 70 | nn | Yang[132] |
| [EEIM]DEP | 1.2 | MCC | 60 | nn | Yang[132] |
| [AMIM]DMP | 9.1 | MCC | 90 | nn | Yang[132] |
| [AMIM]DMP | 7.9 | MCC | 80 | nn | Yang[132] |
| [AMIM]DMP | 6.2 | MCC | 70 | nn | Yang[132] |
| [AMIM]DMP | 3.0 | MCC | 60 | nn | Yang[132] |
| [AMIM]DMP | 1.8 | MCC | 50 | nn | Yang[132] |
| [AMIM]DMP | 0.6 | MCC | 40 | nn | Yang[132] |
| [AEIM]DEP | 6.3 | MCC | 90 | nn | Yang[132] |

Continued on next page...

**Table 2. Continued**

| Ionic liquid | Cellulose solubility | DP[a] (DP)[b] | Solution conditions | | Reference |
|---|---|---|---|---|---|
| | 100 $w$ | | $\theta$/°C | $t$/h | |
| [AEIM]DEP | 5.3 | MCC | 80 | nn | Yang[132] |
| [AEIM]DEP | 4.5 | MCC | 70 | nn | Yang[132] |
| [AEIM]DEP | 2.0 | MCC | 60 | nn | Yang[132] |
| $[MMIM](MeO)_2PO_2$ | 10 | 398 | 100 | 1 | Vitz[129] |
| $[EMIM](EtO)_2PO_2$ | 12 | 398 | 100 | 1 | Vitz[129] |
| $[BMIM](BuO)_2PO_2$ | — | 398 | 100 | 1 | Vitz[129] |
| [HEMIM]Cl | 6.8 | cellulose | 70 | 12 | Luo[134] |
| ECOENG™ | $> 5$ | $\alpha$-Cellulose | 90 | 12 | Zavrel[121] |
| $[Bu_4P]$Fmt | 6 | 225 | 110 | nn | Zhao[126] |
| $[(C_6)_3C_{14}P]$Dca | $< 0.5$ | 225 | 110 | nn | Zhao[126] |
| [BzDTA]Cl | 5 | 286 (327) | 62 | 12 | Heinze[105,120] |
| [BzDTA]Cl | 2 | 593 (527) | 62 | 12 | Heinze[105,120] |
| [BzDTA]Cl | 1 | 1198 (966) | 62 | 12 | Heinze[105,120] |
| $[Bu_4N]$Fmt | 1.5 | 225 | 110 | nn | Zhao[126] |
| [Amm110]Cl | 0.5 | 225 | 110 | nn | Zhao[126] |
| [Amm110]Fmt | 0.5 | 225 | 110 | nn | Zhao[126] |
| [Amm110]Ac | 0.5 | 225 | 110 | nn | Zhao[126] |
| [Amm110]Dca | $< 0.5$ | 225 | 110 | nn | Zhao[126] |
| [BzMIM]Cl | $> 10$ | wood[h] | 80 | 24 | Lee[119] |
| [BzMIM]Cl | $> 10$ | lignin[c] | 90 | 24 | Lee[119] |
| [BzMIM]Cl | 5 | wood[g] | 130 | 8 | Kilpelainen[103,127] |
| [BzMIM]Cl | 5 | wood[f] | 130 | 8 | Kilpelainen[103,127] |
| $[M(OEt)_2EtIM]$Ac | 12 | 225 | 110 | nn | Zhao[126] |
| $[M(OEt)_3EtIM]$Ac | 12 | 225 | 110 | nn | Zhao[126] |
| $[M(OEt)_4EtIM]$Ac | 10 | 225 | 110 | nn | Zhao[126] |

Continued on next page...

**Table 2. Continued**

| Ionic liquid | Cellulose solubility | DP[a] (DP)[b] | Solution conditions | | Reference |
|---|---|---|---|---|---|
| | 100 $w$ | | $\theta$/°C | $t$/h | |
| [M(OEt)$_2$Et$_3$N]Ac | 10 | 225 | 110 | nn | Zhao[126] |
| [M(OEt)$_3$Et$_3$N]Ac | 10 | 225 | 110 | nn | Zhao[126] |
| [H(OEt)$_2$MIM]Ac | 5 | 225 | 110 | nn | Zhao[126] |
| [M(OMe)BzIM]Cl | 5 | wood[g] | 130 | 8 | Kilpelainen[103,127] |
| [M(OEt)$_7$EtIM]Ac | 3 | 225 | 110 | nn | Zhao[126] |
| [H(OEt)$_3$MIM]Ac | 2 | 225 | 110 | nn | Zhao[126] |
| [M(OMe)BzIM]Cl | 2 | wood[g] | 130 | 8 | Kilpelainen[103,127] |
| [H(OEt)$_2$MIM]Cl | 2 | 225 | 110 | nn | Zhao[126] |
| [M(OEt)$_3$MEMIM]Ac | 0.5 | 225 | 110 | nn | Zhao[126] |
| [M(OPr)$_3$EtIM]Ac | 0.5 | 225 | 110 | nn | Zhao[126] |
| [M(OEt)$_3$BuIM]Ac | $< 0.5$ | 225 | 110 | nn | Zhao[126] |
| [MM(EtOH)NH]Ac | $< 0.5$ | 225 | 110 | nn | Zhao[126] |
| [(MeOEt)$_2$NH$_2$]Ac | $< 0.5$ | 225 | 110 | nn | Zhao[126] |
| [MM(MeOEt)NH]Ac | $< 0.5$ | 225 | 110 | nn | Zhao[126] |
| [M(MeOEt)$_2$NH]Ac | $< 0.5$ | 225 | 110 | nn | Zhao[126] |
| [BzMIM]Dca | 2 | wood[g] | 130 | 8 | Kilpelainen[103,127] |
| [BMIM]Br | 5-7 | 1000 | mwh | mwh | Swatloski[107] |
| [BMIM]Br | — | $\alpha$-cellulose | 90 | 12 | Zavrel[121] |
| [E(CN)MIM]Br | 3.4 | cellulose | 90 | 0.3 | Lateef[135] |
| [E(CN)MIM]Br | 9.5 | lignin | 90 | 0.3 | Lateef[135] |
| [BMIM]I | — | $\alpha$-cellulose | 90 | 12 | Zavrel[121] |
| [BMIM]SCN | 5-7 | 1000 | mwh | mwh | Swatloski[107] |
| [BMIM]BF$_4$ | — | 1000 | mwh | mwh | Swatloski[107] |
| [BMIM]BF$_4$ | — | $\alpha$-cellulose | 90 | 12 | Zavrel[121] |
| [BMIM]BF$_4$ | 4 | lignin[c] | 90 | 24 | Lee[119] |

Continued on next page...

**Table 2. Continued**

| Ionic liquid | Cellulose solubility | DP[a] (DP)[b] | Solution conditions | | Reference |
|---|---|---|---|---|---|
| | 100 $w$ | | $\theta$/°C | $t$/h | |
| [BMIM]$PF_6$ | — | 1000 | mwh | mwh | Swatloski[107] |
| [BMIM]$PF_6$ | — | $\alpha$-cellulose | 90 | 12 | Zavrel[121] |
| [BMIM]$PF_6$ | 0.1 | lignin[c] | 90 | 24 | Lee[119] |
| [$C_6$MIM]$BF_4$ | 5 | 1000 | mwh | mwh | Swatloski[107] |
| [$C_8$MIM]$BF_4$ | sls | 1000 | mwh | mwh | Swatloski[107] |
| [$C_2$MIM]F | 2 | 398 | 100 | 1 | Vitz[129] |
| [$C_2$MIM]Cl | 10 | 398 | 100 | 1 | Vitz[129] |
| [$C_2$MIM]Cl | ≈ 10 | cellulose | 100 | 2 | Erdmenger[109] |
| [$C_2$MIM]Br | 1 | 398 | 100 | 1 | Vitz[129] |
| [$C_3$MIM]Cl | ≈ 0.5 | cellulose | 100 | 2 | Erdmenger[109] |
| [$C_3$MIM]Cl | — | 398 | 100 | 1 | Vitz[129] |
| [$C_3$MIM]Br | 1.7 | cellulose | 90 | 0.3 | Lateef[135] |
| [$C_3$MIM]Br | 1 | 398 | 100 | 1 | Vitz[129] |
| [$C_3$MIM]Br | 6.2 | lignin | 90 | 0.3 | Lateef[135] |
| [$C_4$MIM]Cl | ≈ 20 | cellulose | 100 | 2 | Erdmenger[109] |
| [$C_4$MIM]Cl | 1.8 | cellulose | 90 | 0.3 | Lateef[135] |
| [$C_4$MIM]Br | 2 | 398 | 100 | 1 | Vitz[129] |
| [$C_4$MIM]Cl | 8.8 | lignin | 90 | 0.3 | Lateef[135] |
| [$C_5$MIM]Cl | ≈ 1.5 | cellulose | 100 | 2 | Erdmenger[109] |
| [$C_5$MIM]Cl | 1 | 398 | 100 | 1 | Vitz[129] |
| [$C_5$MIM]Br | 1 | 398 | 100 | 1 | Vitz[129] |
| [$C_6$MIM]Cl | ≈ 6.5 | cellulose | 100 | 2 | Erdmenger[109] |
| [$C_6$MIM]Cl | 6 | 398 | 100 | 1 | Vitz[129] |
| [$C_6$MIM]Cl | — | $\alpha$-cellulose | 90 | 12 | Zavrel[121] |
| [$C_6$MIM]Br | 1 | 398 | 100 | 1 | Vitz[129] |

Continued on next page...

**Table 2. Continued**

| Ionic liquid | Cellulose solubility | DP[a] (DP)[b] | Solution conditions | | Reference |
|---|---|---|---|---|---|
| | 100 $w$ | | $\theta$/°C | $t$/h | |
| [$C_7$MIM]Cl | $\approx 5$ | cellulose | 100 | 2 | Erdmenger[109] |
| [$C_7$MIM]Cl | 5 | 398 | 100 | 1 | Vitz[129] |
| [$C_7$MIM]Br | 1 | 398 | 100 | 1 | Vitz[129] |
| [$C_8$MIM]Cl | $\approx 4$ | cellulose | 100 | 2 | Erdmenger[109] |
| [$C_8$MIM]Cl | 4 | 398 | 100 | 1 | Vitz[129] |
| [$C_8$MIM]Br | 1 | 398 | 100 | 1 | Vitz[129] |
| [$C_8$MIM]Cl | — | $\alpha$-cellulose | 90 | 12 | Zavrel[121] |
| [$C_8$MIM]Dca | $< 1$ | 225 | 110 | nn | Zhao[126] |
| [$C_9$MIM]Cl | $\approx 2.5$ | cellulose | 100 | 2 | Erdmenger[109] |
| [$C_9$MIM]Cl | 2 | 398 | 100 | 1 | Vitz[129] |
| [$C_9$MIM]Br | 1 | 398 | 100 | 1 | Vitz[129] |
| [$C_{10}$MIM]Cl | $\approx 0.5$ | cellulose | 100 | 2 | Erdmenger[109] |
| [$C_{10}$MIM]Cl | — | 398 | 100 | 1 | Vitz[129] |
| [$C_{10}$MIM]Br | — | 398 | 100 | 1 | Vitz[129] |
| [ABIM]Cl | $> 3$ | 1176 | nn | nn | Laus[40] |
| [DAIM]Cl | $> 3$ | 1176 | nn | nn | Laus[40] |
| [APIM]Cl | $< 3$ | 1176 | nn | nn | Laus[40] |
| [BMIM]Dca | — | 1176 | nn | nn | Laus[40] |
| [BMIM]Dca | 1 | 225 | 110 | nn | Zhao[126] |
| [EMIM]Dca | — | 398 | 100 | 1 | Vitz[129] |
| [EMIM]Ts | 1 | 398 | 100 | 1 | Vitz[129] |
| [BMIM]Ts | — | 1176 | nn | nn | Laus[40] |
| [BMIM]Ts | — | 1176 | nn | nn | Laus[40] |
| [BMIM]$Tf_2N$ | $< 0.5$ | 225 | 110 | nn | Zhao[126] |
| [BMIM]$NO_3$ | — | 398 | 100 | 1 | Vitz[129] |

Continued on next page...

**Table 2. Continued**

| Ionic liquid | Cellulose solubility | DP[a] (DP)[b] | Solution conditions | | Reference |
|---|---|---|---|---|---|
| | 100 $w$ | | $\theta$/°C | $t$/h | |
| [BMIM]$Tf_2N$ | — | 398 | 100 | 1 | Vitz[129] |
| [BMIM]OTf | — | 398 | 100 | 1 | Vitz[129] |
| [BMIM]Sac | — | 1176 | nn | nn | Laus[40] |
| [BMIM]$EtOSO_3$ | — | $\alpha$-cellulose | 90 | 12 | Zavrel[121] |
| [BMIM]$HSO_4$ | — | 1176 | nn | nn | Laus[40] |
| [BDMIM]SCN | — | 1176 | nn | nn | Laus[40] |
| [ABIM]Dca | — | 1176 | nn | nn | Laus[40] |
| [AOMIM]Dca | — | 1176 | nn | nn | Laus[40] |
| [AOMIM]Cl | — | 1176 | nn | nn | Laus[40] |
| [Ch]Cl+urea | — | 1176 | nn | nn | Laus[40] |
| [BMPyr]Cl | — | $\alpha$-cellulose | 90 | 12 | Zavrel[121] |
| [BMPyr]$Tf_2N$ | — | $\alpha$-cellulose | 90 | 12 | Zavrel[121] |
| [EMIM]$Tf_2N$ | — | $\alpha$-cellulose | 90 | 12 | Zavrel[121] |
| [EMIM]$EtOSO_3$ | — | $\alpha$-cellulose | 90 | 12 | Zavrel[121] |
| [EMIM]$EtOSO_3$ | — | 398 | 100 | 1 | Vitz[129] |
| [EMIM]$BF_4$ | — | $\alpha$-cellulose | 90 | 12 | Zavrel[121] |
| [HMIM]$BF_4$ | — | $\alpha$-cellulose | 90 | 12 | Zavrel[121] |
| [HEMIM]$BF_4$ | — | $\alpha$-cellulose | 90 | 12 | Zavrel[121] |
| [TBPM]Cl | — | $\alpha$-cellulose | 90 | 12 | Zavrel[121] |
| [MMIM]I | — | 398 | 100 | 1 | Vitz[129] |

[a] Before regeneration. [b] After regeneration. [c] Indulin AT (Kraft lignin). [d] wool keratin fibers. [e] Norway spruce sawdust. [f] Norway spruce thermomechanical pulp. [g] Southern pine thermomechanical pulp. [h] maple wood flour. [i] wood chips. [j] Southern yellow pine. [k] spruce, beech, chestnut. [l] red oak. [m] Southern pine powder. [n] spruce, fir, beech, chestnut. Mwh = microwave heating, nn = Not known by the author, sls = slightly soluble, uss = ulatrsound sonication, ECOENG = 1,3-dimethylimidazolium dimethylphosphate. **Cations** [ABIM] = 1-allyl-3-butylimidazolium, [ADMIM] = 1-allyl-2,3-dimethylimidazolium, [AEIM] = 1-allyl-3-ethylimidazolium, [AMIM] = 1-allyl-3-methylimidazolium, [Amm110]Cl = AMMOENG™, [AOMIM] = 1-allyloxy-3-methylimidazolium, [APIM] = 1-allyl-3-propargylimidazolium, [BBIM] = 1,3-dibutylimidazolium, [BMIM] = 1-butyl-3-methylimidazolium, [BDMIM] = 1-butyl-2,3-dimethylimidazolium, [BzDTA] = benzyldimethyl(tetradecyl)ammonium, [BMPyr] = 1-butyl-3-methylpyrrolidinium, [BMPy] = 3-methyl-N-butylpyridinium, [DAIM] = 1,3-diallylimidazolium, [E(CN)MIM] = 1-(2-

cyanoethyl)-3-methylimidazolium, [EEIM] = 1,3-diethylimidazolium, [EMIM] = 1-ethyl-3-methylimidazolium, [HEA] = 2-hydroxyethylammonium, [HEMIM] = 1-(2-hydroxymethyl)-3-methylimidazolium, $[IM]_2$ = imidazolium dication, [BzMIM] = 1-methyl-3-benzylimidazolium, [MMIM] = 1-methyl-3-methylimidazolium, [M(OMe)BzIM] = 1-methyl-3-m-methoxylbenzylimidazolium, $[M(OEt)_3MEMIM]$ = 1-ethoxy-(methoxy)methyl-3-triethoxymethylimidazolium, [TBPM] = tetrabutylphosphonium. **Anions** Ac = acetate, $Al_xCl_y$ = chloroaluminates, $BF_4$ = tetrafluoroborate, $CF_3SO_3$ = trifluoromethanesulfonate, Cl = chloride, Dca = dicyanamide, $EtOSO_3$ = ethylsulfate, F = fluoride, Fmt = formate, I = iodide, $MeSO_4$ = methanesulfate, DEP = diethylphosphate, DMP = dimethylphosphate, MPh = methylphosphonate, DMPh = dimethylphosphonate, $NO_3$ = nitrate, OTf = triflate, $PF_6$ = hexafluorophosphate, $(RO)_2PO_2$ = dialkylphosphates, Sac = saccharinate, SCN = thiocyanate, $Tf_2N$ = bis-(trifluoromethanesulfonyl)amide, Ts = tosylate. **Other solvents:** [Ch]Cl+urea = choline chloride : urea (1 : 2 mixture), NMMO = *N*-methylmorpholine-*N*-oxide.

### 3.1.3 Regenerating Dissolved Cellulose

Independent on the solvent type for dissolving cellulose, regeneration of the biopolymer is always based on the same concept. The dissolved cellulose precipitates after adding an excess of a polar solvent such as water, acetone, dichloromethane, acetonitrile, or mixtures of thereof.[40,102,103,107,120,136,137] Deionised water is often preferred if precipitated from *N*-methylmorpholine-*N*-oxide (NMMO) solvent systems, because the coagulated fibres show a higher degree of crystallinity and consequently a higher strength.[138,139] Some IL dissolution studies report a decreased DP of regenerated cellulose compared to the initial sample (see Table 2 on page 23), but the reason for this observation is not clear.[140] Although proton NMR studies on regenerated cellulose fibres—in the hydrated state—have shown a rapid proton exchange between the surface OH–groups of the biopolymer and the surrounding water, this interaction is not sufficient to fully reestablish the stiff H–bond network of microcrystalline cellulose.[141] Recent studies indicate that the final hydrogel is free of IL residues that may count for the lower degree of crystallinity.[142] One possible method to determine changes in the H–bond network of cellulose after IL treatment is X-ray photoelectron spectroscopy.[143]

The morphology of the recovered cellulose depends on the method that was used to regenerate the biopolymer. Thin films of (0.1 to 0.2) mm are obtained by casting the cellulose solution on glass plates prior to leaching

with water.[144] Other groups sprayed water on the surface of the gel, in order to fix the shape of the final sample, prior to immersing the gel in water for several days.[145] Duchemin et al. characterised all-cellulose composites and investigated the influence of process parameters, such as dissolution time, precipitation rate, or the initial cellulose concentration of the solvent, on the resulting material properties.[145] All these parameters were shown to affect the mechanical properties of all-cellulose composites through their influence on crystallinity, void formation, and laminated microstructure. The stiffest gels were obtained following a slow and gentle precipitation. However, if the order of adding the solutions is reversed, and the coagulation solvent is added to the cellulose solution instead of the other way around, the cellulose can be recovered in the form of flocs, which can be separated by filtration.[140]

Kosan et al. shaped cellulose dopes via a dry–wet spinning process, and spun the fibre directly into a coagulation bath.[111] Microscopy, rheometry and laser analysis results indicated that the solution state of cellulose (i) depends on the solvent type and (ii) affects the properties of the regenerated polymer.

Finally, nanofibrillar cellulose aerogels can be prepared if the regenerated gel is washed with liquid carbon dioxide prior to drying under supercritical conditions. The released carbon dioxide leaves a porous polymer structure resulting in an aerogel.[104] Similar methods can be applied to obtain hydro- and methanogels.[146]

## 3.2 Investigations on the Cellulose-Dissolving Ability of Alkanolammonium Ionic Liquids

### 3.2.1 Why Alkanolammonium Ionic Liquids?

The solubility of cellulose in ILs is a field of high interest, because dissolved cellulose is very accessible for enzymatic hydrolysis, resulting in single sugar

units that can be fermented to serve as feedstock for biofuels.[147] Once dissolved, cellulose can also be processed into composites that possess desirable properties for biomedical engineering.[148–151]

In 2004, it was reported that dispersions of up to 0.3 mass fraction of cellulose can be prepared in ethanolammonium formate—an alkanolammonium IL (AAIL)—but without obtaining a clear solution.[123] However, no information was given regarding the IL water content, the mixing conditions, or the crystallinity of the cellulose, and all those factors are known to influence an IL's ability to dissolve the biopolymer.[152]

Because ethanolammonium formate is a low-viscous, protic AAIL that can be prepared easily from cheap starting materials, it was decided to investigate whether protic AAILs can dissolve microcrystalline cellulose and to determine the influence of the ion structure on the dissolution ability. All the AAILs in this study were prepared *via* proton exchange reactions between amines and organic acids (Figure 12). Five different amines and four different acids were selected for the synthesis (Figure 13), and Table 3 explains the acronyms that were used for describing the AAILs.

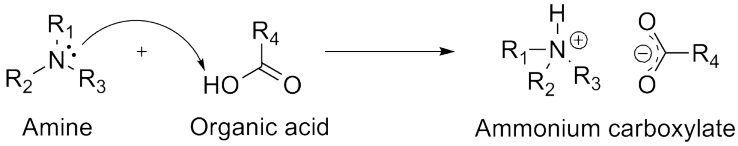


**Figure 12.** Synthesis of alkanolammonium ionic liquids: proton exchange reactions between organic acids and amines result in ammonium carboxylates.

Structural variations on the cation include (i) the number of carbon atoms between the OH–group and the nitrogen atom (HEA < HPA), (ii) the number of alkanol substituents on the nitrogen atom (HEA < DEA < TEA), and (iii) the replacement of alkanol substituents with allyl groups (DAA). Although not representing an alkanolamine, we decided to include the diallylammonium cation in our study due to reports of 1,3-diallylimidazolium ILs being very

good cellulose solvents.[112,133,136] The studied anions are formate, acetate, and malonate, and vary in both their number of $-CO_2H$ groups (Fmt = Ac < Mal) and their number of $\alpha$-carbons (Fmt < Ac = Mal).

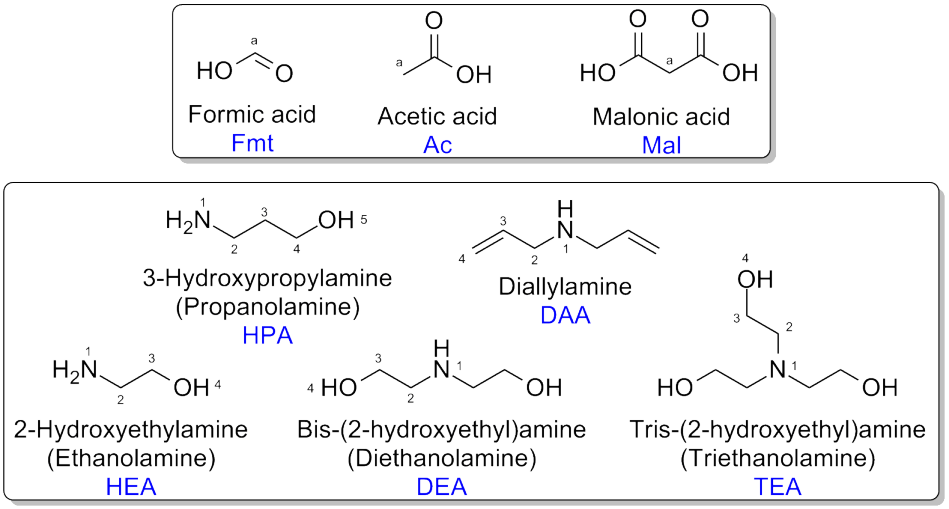


**Figure 13.** Organic acids and amines used for the synthesis of alkanolammonium ionic liquids. Atoms are labelled to assist $^1$H NMR assignment. Acronyms are introduced to facilitate the description of the resulting ionic liquid products.

**Table 3. Acronyms of Ionic Liquids.**

| acronym | explanation |
|---|---|
| [HEA] | 2-hydroxyethylammonium |
| [HPA] | 3-hydroxypropylammonium |
| [DEA] | bis(2-hydroxyethyl)ammonium |
| [TEA] | tris(2-hydroxyethyl)ammonium |
| [DAA] | diallylammonium |
| Fmt | formate |
| Ac | acetate |
| Mal | malonate |

In addition, the physical properties of the studied AAILs, such as density, viscosity and electrical conductivity, were measured in order to establish a

structure–property relationship. However, these studies are out of the scope of this thesis, and it was decided not to discuss the results but to include them in the appendix (see Appendix C).

### 3.2.2 Literature Study on Alkanolammonium Ionic Liquids

The first AAIL, ethanolammonium nitrate, was synthesised in 1888.[153] Since then, many more studies on AAILs have been reported, mainly focusing on ethanolammonium formate and ethanolammonium acetate.[75,123,154,154–168] Less data are available on the diethanolammonium and triethanolammonium cations.[154,156,157,165,167–171] Several patents that mention alkanolammonium malonates and diallylammonium or propan-1-olammonium ILs have been issued, but no articles have been published on these compounds.[172–181]

Angell and co-workers have shown that the ionicity of protic ILs can differ from the ionicity of aprotic ILs, because of the ease of proton back-transfer.[60,182,183] It has been argued that the difference in p$K_a$ values—which is a logarithmic measure of the acid dissociation constant—of the aqueous starting materials can be used to estimate the Gibbs energy of the proton transfer between acid and base.[182] Other authors, however, raised concerns, arguing that the aqueous p$K_a$ data are only of remote relevance to the nature of the IL.[184] However, $^{15}$N NMR studies on mono-, di-, and triethanolammonium acetates and formates strongly suggest that the proton transfer is complete if the starting materials were used in a stoichiometric ratio.[170] Our own studies on the ionicity of these AAILs support these findings (see Appendix C).[185,186]

### 3.2.3 Results and Discussion

#### Purity and Water Content

Impurities can significantly influence the ability of an IL to dissolve cellulose (see 3.1.2 on page 23). There are two major sources of possible impurities in AAILs: (i) water, attracted and retained due to the hygroscopic nature of the ILs, and (ii) ethers, which can be formed during the synthesis due to condensation reactions at elevated temperatures. To minimise these impurities, the AAILs have been synthesised with pre-dried starting materials in a moisture-free atmosphere. Ice or water cooling was applied during synthesis in order to minimise the temperature rise due to the exothermic nature of the proton exchange reaction between amines and organic acids. After IL synthesis, molecular sieves were used to gently reduce their water content to a minimum, without promoting condensation reactions or decomposition due to proton back-transfer.

Figure 14 compares the $^{1}$H NMR spectra of the IL diethanolammonium acetate with the spectra of its starting materials acetic acid and diethanolamine. The chemical shift differences of the nonlabile protons between the starting materials and the resulting IL are attributed to the ionic nature of the product. Peaks of rapidly exchanging protons appear further downfield, outside the ppm range shown in the figure. The lack of additional signals in the spectra, which would result from the asymmetric condensation product or unreacted starting materials, shows that the reaction is complete and without byproduct. The $^{1}$H NMR coupling constants of the triplets in the IL spectra are larger compared to the spectra of the starting materials, which is attributed to the increased viscosity of the ILs (see Appendix D).

Both the viscosity and the hygroscopic nature of these ILs are mainly governed by the number of their OH–groups. The higher the number of OH–groups present in the IL, the higher its viscosity and water affinity. Some AAIL syntheses did require increased stirring temperatures to counteract

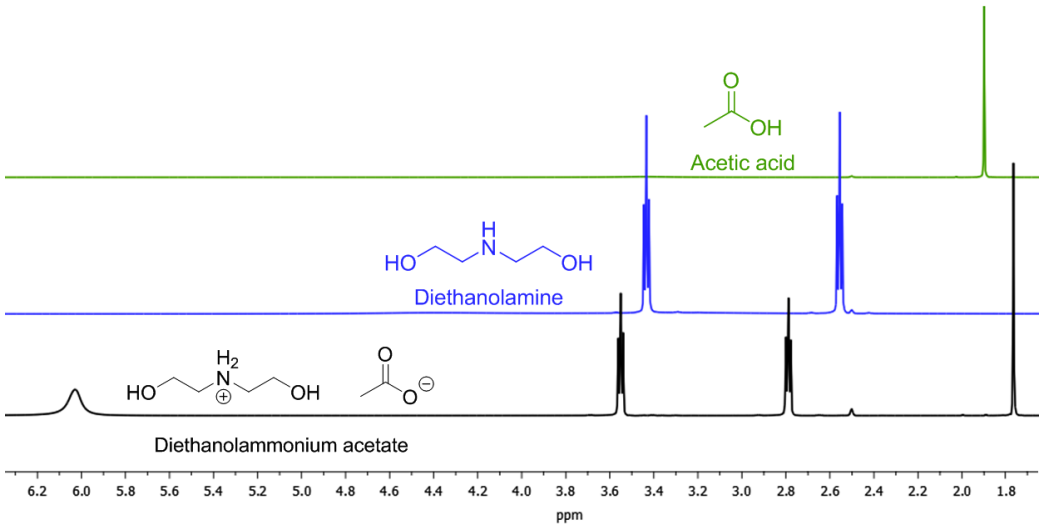


**Figure 14.** $^{1}$H NMR spectra of acetic acid and diethanolamine as starting materials, compared to their reaction product diethanolammonium acetate in DMSO-$d_6$. The number of signals and the chemical shift difference between starting materials and product shows that only the ionic liquid, and no condensation byproduct, is formed.

the high viscosities and to ensure a complete reaction. As a consequence, NMR data reveals small amounts of condensation byproduct in $[DEA]^+$ and $[TEA]^+$ malonates. A pH value of 7 for all but one of the synthesised AAILs is an additional indication that the starting materials have reacted completely. Diallylammonium formate ([DAA]Fmt) had a pH value of 5, suggesting an incomplete reaction of the starting materials. This assumption was confirmed by (i) the lack of H-1 proton peaks in the $^{1}$H NMR spectra of [DAA]Fmt, and (ii) the fact that the signal of the acid proton H-a appeared further upfield compared to the other alkanolammonium formates. Furthermore, the presence of carboxylic acid stretches around 1700 $cm^{-1}$ in the case of the diallylammonium ILs indicates that the ionicity of these ILs varies (see Appendix D). A more detailed assessment of their ionic character was derived from correlating their electrical conductivity with their viscosity in the form

of a Walden plot. The results are presented and discussed in the appendix (see Appendix C).

The hygroscopic trend of the ILs can be seen in Table 4, summarising the water content and the optical appearance of the dried products at 298 K. Preliminary experiments showed that condensation of volatile IL starting materials—at cooler areas of the reaction flask—occurred during water removal at elevated temperatures (353 K) and decreased pressures (<100 Pa), concluding that conventional drying techniques are not suitable for this type of protic ILs. This observation is in agreement with the monitored thermogravimetric behaviour of these ILs, confirming their limited thermal stabilities.

**Table 4. Water Mass Fractions $w_{H_2O}$ and Optical Appearances of Dried Alkanolammonium Ionic Liquids at 298 K.**

| ionic liquid | $10^3$ $w_{H_2O}$ | optical appearance |
|---|---|---|
| [HEA]Fmt | 4.3 | colorless liquid |
| [HEA]Ac | 6.1 | colorless liquid |
| [HEA]Mal | 6.6 | colorless liquid |
| [HPA]Fmt | 6.6 | colorless liquid |
| [HPA]Ac | 7.2 | colorless liquid |
| [HPA]Mal | 6.4 | colorless liquid |
| [DEA]Fmt | 4.3 | colorless liquid |
| [DEA]Ac | 4.6 | colorless liquid |
| [DEA]Mal | 39.4 | colorless liquid |
| [TEA]Fmt | 6.0 | colorless solid |
| [TEA]Ac | 6.6 | orange liquid |
| [TEA]Mal | 33.6 | colorless liquid |
| [DAA]Fmt | 0.7 | orange liquid |
| [DAA]Ac | 0.7 | orange liquid |
| [DAA]Mal | 0.1 | orange liquid |

### Thermal Stability

Table 5 shows the AAIL decomposition temperatures $T_D$ at a fractional mass loss of 0.1 at two different heating rates $\dot{T}_{1K}$ = 1 K·min$^{-1}$ and $\dot{T}_{10K}$ = 10 K·min$^{-1}$. $T_D$ varies significantly with the heating rate of the thermogravimetric experiment, and both the inconsistent definition of $T_D$ in the literature and poorly defined experimental conditions can be responsible for differences in reported data.[123,154,169] Consequently, slow heating rates of preferably 1 K·min$^{-1}$ and well defined decomposition temperatures, such as fractional mass loss, are recommended to obtain representative information about thermal stability of ILs. All ILs in this study show very limited thermal stability, especially those with the diallylammmonium cation. Elevated temperatures promote the dissociation of the protic ILs, resulting in proton back-transfer from the cation to the acid anion. The resulting acids are either volatile (e.g. formic acid or acetic acid) or are prone to decomposition (e.g. decarboxylation of malonic acid).

**Table 5. Decomposition Temperatures $T_D$ of Alkanolammonium Ionic Liquids at a Fractional Mass Loss of 0.1 at Two Different Heating Rates $\dot{T}_{1K}$ = 1 K·min$^{-1}$ and $\dot{T}_{10K}$ = 10 K·min$^{-1}$.**

| | [DAA] | [HEA] | [HPA] | [DEA] | [TEA] |
|---|---|---|---|---|---|
| | $T_{D,\ 1K,10K}$ | $T_{D,\ 1K,10K}$ | $T_{D,\ 1K,10K}$ | $T_{D,\ 1K,10K}$ | $T_{D,\ 1K,10K}$ |
| | K | K | K | K | K |
| Fmt | 323, 363 | 363, 336 | 373, 424 | 393, 431 | 383, 427 |
| Ac | 311, 335 | 368, 405 | 373, 415 | 379, 417 | 357, 392 |
| Mal | 334, 371 | 381, 409 | 381, 414 | 370, 415 | 379, 409 |

### Cellulose Solubility

The main intention of this work was (i) to investigate the ability of the selected ILs to dissolve microcrystalline cellulose (MCC), and (ii) to determine how

certain structural aspects influence this dissolution ability. In general, IL cellulose solvents are able to dissolve a reasonable amount of cellulose—mass fraction of 0.05 or more—at a temperature of $T \approx 353$ K within 24 h or less, regardless of the crystallinity of the biopolymer.[152,187]

Here, the solubility of MCC, with a DP of 163, at temperatures of up to 353 K was investigated. A cellulose mass fraction of 0.01, 0.05, or 0.1 was added to the IL in a dry atmosphere, and stirred for at least 12 h. None of the studied ILs with cationic OH–groups were able to produce a clear solution of cellulose after stirring for at least 24 h, yielding turbid dispersions. Only the ILs without cationic OH–groups—the diallylammonium ILs—showed no interaction with the cellulose at all, resulting in a clear IL supernatant and cellulose powder at the bottom of the flask. Several centrifugation steps were necessary to separate the finely dispersed cellulose from the ILs with cationic OH–groups (see Figure 15). After separation of the dispersed cellulose from the IL, excess of distilled water was added to the clear IL to regenerate any dissolved cellulose. No precipitation could be detected, neither visually nor with the assistance of an optical microscope.

In contrast, experiments with the cellulose-dissolving ILs, such as [EMIM]Ac, showed that the precipitation of a 0.01 cellulose mass fraction can be clearly identified, even without a microscope. With the exception of the two AAIL malonates [DEA]Mal and [TEA]Mal, all the investigated ILs display water a mass fraction that is low enough to ensure that their residual water is not responsible for their nondissolving behaviour. An excess of dissociated protons, possibly interfering with the dissolution of cellulose, was excluded because of the neutral pH value of 7 for all of the cellulose-dispersing ILs (see 3.2.3 on page 40).

**Figure 15.** Instead of dissolving, microcrystalline cellulose forms a turbid dispersion in alkanolammonium ionic liquids with cationic OH–groups, such as propan-1-olammonium formate [HPA]Fmt (left). Centrifugation results in a cellulosic residue and an ionic liquid supernatant (right). Several centrifugation cycles are necessary to remove all of the dispersed cellulose.

## 3.2.4 Experimental

### Materials and Instruments

**Materials** Formic acid, acetic acid, malonic acid, 3-hydroxypropylamine, microcrystalline cellulose (MCC), and chemicals for Karl Fischer titrations were obtained from Merck. Diallylamine was purchased from Sigma Aldrich. 2-Hydroxyethylamine and tris(2-hydroxyethyl)amine were from Unilab, and bis(2-hydroxyethyl)amine from AnalaR. The commercial IL 1-ethyl-3-methylimidazolium acetate ([EMIM]Ac) was from Fluka. It was dried at 353 K for 48 h prior to use, resulting in a water mass fraction of $8{\cdot}10^{-4}$. Molecular sieve type 4A was from Fluka, and nylon syringe filters—with a pore size of 0.45 $\mu$m and a diameter of 13 mm—were from Raylab. All reagents were analytical-grade purity where possible. Liquid reagents were dried with a molecular sieve prior to use. Microcrystalline cellulose, with a particle size of (20 to 160) $\mu$m and a degree of polymerisation of 163,[138] was dried at 353 K

for 72 h to reduce the initial water content by 90 % to a final water mass fraction of $2.9 \cdot 10^{-3}$.

**Instruments** Fourier transform infrared (FT-IR) spectra were recorded on a Perkin–Elmer Spectrum One FT-IR spectrometer over a range of (4000 to 450) $cm^{-1}$. A total of 20 scans at a resolution of 4 $cm^{-1}$ was taken for each sample. Liquid samples were sandwiched between two polished KBr plates, and solid samples were pelletised with KBr containing a sample mass fraction of 0.01. $^1$H NMR spectra were recorded on a Varian INOVA 500 spectrometer (500 MHz), using the signals of the residual solvent protons as internal references ($\delta_H$ 2.6 for DMSO-$d_6$). Water content was determined with a Radiometer Analytical TIM550 Volumetric Karl Fischer Titrator, using Karl Fischer Reagent 5 from Merck. The titrant was calibrated with a 0.01 % Apura® water standard. Thermogravimetric analysis (TGA) was conducted on a SDT Q600 from TA Instruments by heating (5 to 10) mg of sample in a platinum pan under a nitrogen atmosphere ($N_2$ flow rate 100 $ml \cdot min^{-1}$). The decomposition temperatures $T_D$ were determined at a fractional mass loss of 0.1 at two different heating rates $\dot{T}_{1K} = 1$ $K \cdot min^{-1}$ and $\dot{T}_{10K} = 10$ $K \cdot min^{-1}$. Microscopy was performed with an Olympus PX60 microscope.

## Synthesis

The ILs were prepared according to the synthesis of 2-hydroxyethylammonium formate described in the literature.[123] A three-necked 500 mL flask was equipped with a reflux condenser, a dropping funnel, a nitrogen gas source, and a magnetic stirring bar. Moisture-free conditions in the flask were ensured by repeating the following cycle three times: (i) apply vacuum, (ii) heat flask surface with a heat gun while vacuum is applied, and iii) flush with nitrogen. Subsequently, the flask was kept under a dry nitrogen gas atmosphere at all times. The flask was mounted in an ice bath to control the exothermic

reaction, and the alkanolamine was stirred vigorously while the acid was added dropwise. In the case of the acid being a solid at ambient temperatures, the alkanolamine was added dropwise to the acid. Very viscous products required the use of an oil bath to control the temperature. After mixing, stirring was continued at the lowest suitable temperature for at least 12 h. Finally, the ILs were stirred for at least 12 h with a molecular sieve to reduce the water content to a minimum. Prior to use, the ILs were filtered through nylon syringe filters—under nitrogen atmosphere—to the remove molecular sieve residues.

### Cellulose Solubility

All experiments were conducted in a dry $N_2$ atmosphere. Five grams of dried IL was transferred to a moisture-free 25 mL flask. MCC was added in mass fractions of either 0.01, 0.05, or 0.1 and stirred at 353 K for 12 h. The stirring temperature was kept below the thermal decomposition temperature ($T_{\mathrm{D,1K}}$) of the IL if $T_{\mathrm{D,1K}} < 353$ K. In this case, if no dissolution occurred after 12 h, the experiment was repeated with a stirring temperature of 353 K. To determine whether any cellulose has dissolved, the turbid mixtures were centrifuged at 10 000 rpm for 30 min at 313 K in a dry atmosphere. The supernatant was separated and centrifuged again. This process was repeated until no further residue was formed after centrifugation. The obtained IL supernatant was then mixed with distilled water to regenerate and identify any dissolved cellulose. In addition, all IL+water mixtures were analysed with an Olympus PX 60 microscope with varying magnification (10×, 50×, 100×) for the existence of regenerated cellulose.

### Characterisation of Ionic Liquids

See Appendix D for characterisation of the studied AAILs.

### 3.2.5 Conclusions

Qualitative cellulose-dissolving experiments with protic ILs consisting of ammonium cations (ethanolamine, diethanolamine, triethanolamine, propan-1-olamine, and diallylamine) and organic acid anions (formic acid, acetic acid, and malonic acid) allow to conclude the following:

(i) protic alkanolammonium acetates or formate cannot dissolve crystalline cellulose;

(ii) cellulose disperses very finely in these AAILs, most likely due to the presence of the cationic OH–group;

(iii) cationic allyl groups do not interact with cellulose per se, and consequently do not participate in the cellulose-dissolution process.

The last observation is especially interesting due to the fact that the allyl-containing IL 1-allyl-3-methylimidazolium chloride is a powerful cellulose solvent, but it has not been clarified yet whether it is the decreased viscosity of the IL—due to the presence of cationic allyl groups—or the allyl group itself that promotes cellulose dissolution.[112,133,136]

Although none of the investigated ILs turned out to be cellulose solvents, these results are important towards the understanding of the cellulose dissolution process in ILs. In addition, the ability to disperse cellulose in these types of ILs may allow for further useful applications in other areas, such as the selective extraction of wood hemicellulose for example. The next section is going to combine the information, gained from both the extensive literature study (see 3.1) and the dissolution experiments with AAILs, in order to suggest a mechanism for the dissolution of cellulose that can explain the ability or inability of certain IL ion combinations to dissolve the biopolymer.

## 3.3 Reflections on the Solubility of Cellulose

### 3.3.1 The Importance of Superior Cellulose Solvents

A solvent is commonly defined as a substance—usually a liquid—that possesses the power of dissolving other substances. Water is undoubtedly the most universal solvent, as it is involved in all biological processes that enable life on our planet. The discovery of novel solvents with advantageous properties has always been of interest to mankind. The alchemists of the Middle Ages were already aspiring for an universal solvent for everything, the so-called "Alkahest". Although the Alkahest was never found, a solvent for gold—aqua regia—has been discovered a millennia earlier than a suitable solvent for cellulose.[188,189] This fact certainly reflects the changing aspirations of scientists.

The necessity to face present problems, such as shortage of fossil fuels, environmental changes, and rapidly growing population, attracted extensive research to find a suitable solvent for dissolving cellulose from natural biomaterials, such as wood. Cellulose is the most abundant biopolymer on earth. It regenerates quicker than fossil fuels, and it does not represent a human food source.[127] Once extracted, the cellulosic biomass is a desirable feedstock for a variety of applications. One example is the production of biofuel by fermenting the sugars that are left after hydrolysing cellulose.[147] Another option is the engineering of biocompatible high-tech composites for use in medicine. Some cellulose composites are desirable materials for tissue replacements in brain and heart surgery, or as scaffolds for both joint replacement and bone regeneration.[148–151]

Especially with regard to biocomposites production it is important to dissolve and process cellulose without degradation.[152,190] As a consequence, harsh dissolution conditions need to be avoided for disrupting the highly ordered structures in native cellulose, which are responsible for the biopolymer's

recalcitrance towards dissolution in most solvents. Several traditional solvent systems possess the potential to dissolve cellulose, but concerns regarding their toxicity and recyclability have motivated the search for alternatives.[152]

In 2002, Swatloski et al. reported the solubility of cellulose in some ILs.[107] Their ionic nature is responsible for a number of desirable properties that distinguishes ILs from most molecular solvents. Not all ILs, however, possess the ability to dissolve cellulose, and their dissolution efficiency can vary considerably.[152] It is very likely that the most effective IL cellulose solvents have not yet been discovered amongst the postulated $10^{12}$ possible ILs.[15] Although the first cellulose solvent was already reported in 1921,[189] the mechanism responsible for the dissolution of cellulose is still unclear, and this lack of understanding is still a major barrier in developing more effective cellulose solvents. The motivation to improve such solvents originates from the desire to both optimise possible industrial applications and enable the preparation of cellulose composites with enhanced mechanical properties.[138] The following section aims to:

(i) analyse the extensive data set from the literature review on the cellulose-dissolving ability of ILs (see Table 2 on page 23);

(ii) combine this knowledge with the information gained from the AAIL experiments (see 3.2);

(iii) derive new perspectives on the dissolution process of cellulose, offering an explanation why only certain IL ion combinations are potent cellulose solvents.

### 3.3.2 Facts about the Solubility of Cellulose

Native cellulose is recalcitrant towards its dissolution due to its high crystallinity, but also because of its high molecular weight and the presence of additional wood polymers, such as lignin.[152] Its ordered structure is the

result of a three-dimensional H–bond network between the OH–groups that surround each polymer chain. Successful cellulose solvents must possess the ability to compete for the existing intermolecular H–bond interactions in order to separate the polymer chains from each other, resulting in the dissolution of the biopolymer.[108] The exact mechanism of cellulose dissolution is still under debate.[110,187,191–193]

A desirable cellulose solvent needs to comply with additional requirements beyond its good dissolving power, such as low viscosity and low toxicity, ease of recycling, low melting temperature, and high thermal stability. However, those additional attributes are not expected to have an influence on the dissolution mechanism of cellulose, and are therefore omitted in the subsequent discussions. The success of the dissolution process depends on variables such as mixing time, mixing temperature, cellulose crystallinity, and the degree of polymerisation of the biopolymer. For this reason, the following discussion will only focus on solvents with the ability to dissolve cellulose regardless of its crystallinity or degree of polymerisation, without pretreatment, and without degrading or derivatising the biopolymer. Furthermore, those solvents should be efficient at ambient pressures and moderate temperatures ($< 393$ K).

Many traditional solvent systems are known to dissolve cellulose with varying efficiency. They can be categorised into derivatising and nonderivatising solvent systems. The latter ones are of special interest to this study, as those solvents possess the ability to dissolve cellulose in its natural state. Nonderivatising solvent systems include aqueous inorganic transition-metal complexes, aqueous bases, mineral acids, melts of inorganic salt hydrates, mixtures of organic liquids and inorganic salts, mixtures of organic liquids with amines and sulfur dioxide, and mixtures of ammonia and ammonium salts.[194] However, some of those solvents are only able to dissolve cellulose with short polymer chain lengths, or they dissolve cellulose *via* deprotonation of its OH–groups.[114,194–196]

Three nonderivatising solvent systems are considered in this study, rep-

resenting different structural types of solvents that dissolve cellulose without degradation: *N*,*N*-dimethylacetamide+lithium chloride (DMA+LiCl), dimethylsulfoxide+tetrabutylammonium fluoride (DMSO+TBAF), and *N*-methylmorpholine-*N*-oxide (NMMO). In Figure 16, these solvents are deliberately drawn with charge distributions—any associated hydrates are not considered—in order to visualise both their polar character and the presence of small electronegative anions, such as chloride or fluoride. The role of associated water molecules for the dissolution of cellulose is not agreed upon, but strong indications exist that water–solvent clusters facilitate the H–bond cleavage between the cellulose chains.[197,198]

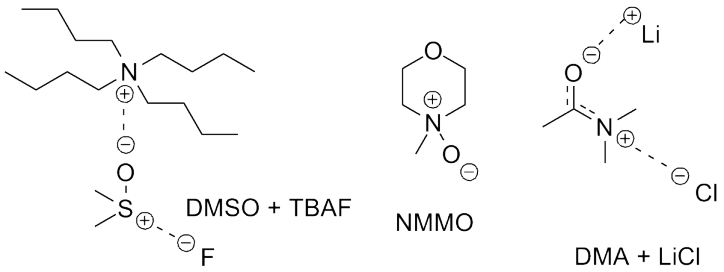


**Figure 16.** Simplified visualisation of the polar character of traditional cellulose solvents: *N*,*N*-dimethylacetamide+lithium chloride (DMA+LiCl) , dimethylsulfoxide+tetrabutylammonium fluoride (DMSO+TBAF), and *N*-methylmorpholine-*N*-oxide (NMMO).

Cellulose degradation due to reactive solvent intermediates—formed at elevated temperatures—and limited dissolution efficiencies are drawbacks shared by some of the solvents displayed in Figure 16.[199–201] The most successful traditional cellulose solvent is probably *N*-methylmorpholine-*N*-oxide (NMMO). It displays a low toxicity, it is biodegradable, and the recovery rate in large scale systems is greater than 99 %. Depending on the water content, it can dissolve up to 0.3 mass fraction of cellulose.[202] However, the use of NMMO in commercial fibre processing (Lyocell process) leads to side reactions that affect the recyclability and toxicity of the solvent. In addition,

some of the side reactions are exothermal and can cause runaway reactions.[202] Those and other drawbacks explain the ongoing search for alternative cellulose solvents, such as ILs.

Although a wide range of different ionic liquids has been synthesised and characterised for specific purposes, only limited data are available on their ability or disability to dissolve cellulose. To shed light on the dissolution mechanism of cellulose in ionic liquids, it is important to know which ILs cannot dissolve the biopolymer. It proves difficult to compare the reported cellulose-dissolving ability of ILs, because many factors influence the efficiency of the dissolution process (*vide supra*). Particularly important are the viscosity and the water content of the IL. Both increasing water content and increasing viscosity inhibit cellulose dissolution.[9,105,107,136,203] This can be explained with the regenerating effect of water as an antisolvent for cellulose, and with the increased ion mobility in low-viscous ILs.

Based on the literature study investigating reports on the ability or disability of ILs to dissolve cellulose, it is obvious that only certain combinations of IL ions are effective cellulose solvents (see Table 2 on page 23). To give an example, the 1-butyl-3-methylimidazolium cation is able to dissolve cellulose if paired with a chloride anion, but not if paired with the bis(trifluoromethanesulfonyl)amide anion ($[Tf_2N]^-$). On the other hand, the chloride anion cannot dissolve cellulose if paired with a pyrrolidinium or piperidinium cation.[204] Based on these observations, it is the author's opinion that both IL ions—cation and anion—participate in the dissolution process, although other research has attributed most of the dissolution ability to the anion.[110,133,133,136,205–209] However, the idea that both IL ions participate in the dissolution process has been mentioned in the literature several times.[108,112,191] Some data even suggested that hydrophobic interactions between the IL cation and the cellulose are responsible for the dissolution of cellulose.[192,193]

Figure 17 summarises ions that can be found in ILs that have the po-

tential to dissolve cellulose.[152] In general, ILs are nonderivatising solvents for cellulose, although it has been reported that acetate anions can react with cellulose in the presence of *p*-toluenesulfonyl chloride.[113,210,211] The most common cations involved in cellulose dissolution are imidazolium and pyridinium.[152] The nature of the alkyl side chains on the imidazolium cation does not play an active role in the dissolution of cellulose but it can assist in decreasing the viscosity of the IL, resulting in enhanced dissolving ability for the biopolymer.[112,134,203] In the case of imidazolium chlorides, it was shown that even-numbered alkyl side chains on the imidazolium cation are better-suited for dissolving cellulose than odd-numbered chains, but this could not be confirmed for the corresponding bromides.[129] It has been argued that the delocalised 3-centres–4-electrons configuration of the imidazolium cation might be responsible for its cellulose dissolution capacity, but trials with nonaromatic cyclic cations, such as pyrrolidinium or piperidinium, failed.[74,204] Common IL anions with a strong potential to dissolve cellulose are chloride, acetate, formate, and dialkylphosphate.[129,132,133,152] Bromide and thiocyanate are less efficient but are known to be able to dissolve cellulose with low DP values.[107,203,204] Only limited data are available for IL fluorides.[129]

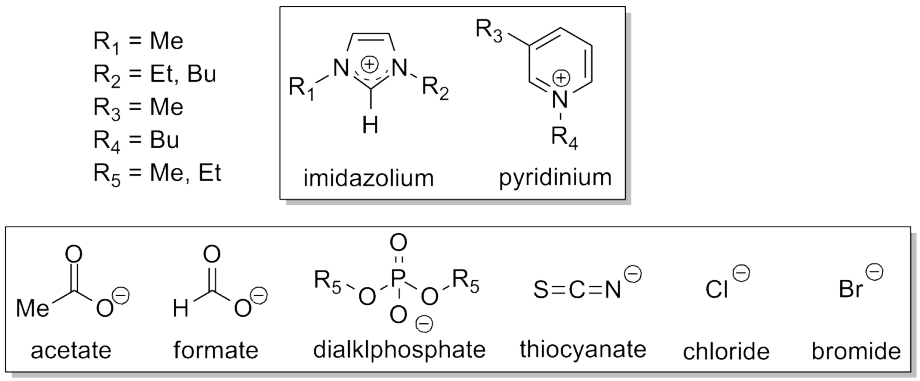


**Figure 17.** Ionic liquid ions with the potential to dissolve cellulose: 1,3-dialkylimidazolium, 1,3-dialkylpyridinium, acetate, formate, dialkylphosphate, thiocyanate, chloride and bromide.

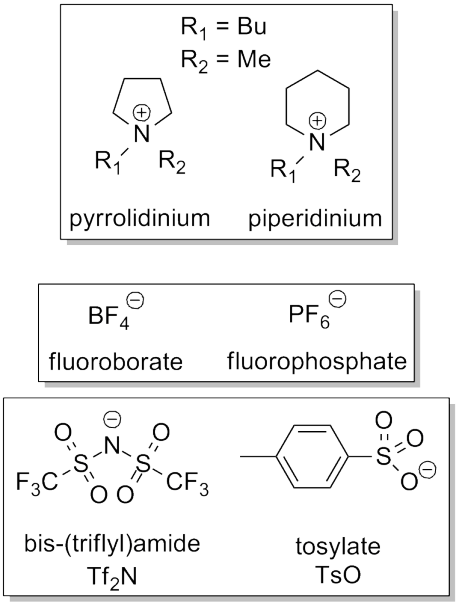


**Figure 18.** Ionic liquid ions with poor ability to dissolve cellulose: pyrrolidinium, piperidinium, tetrafluoroborate, hexafluorophosphate, bis-(trifluoromethanesulfonyl)amide ($[Tf_2N]^-$), and tosylate ($[TsO]^-$).

On the other hand, some IL ions are known for their inability to dissolve cellulose (Figure 18). Those include pyrrolidinium and piperidinium cations, as well as the anions tetrafluoroborate, hexafluorophosphate, bis-(trifluoromethanesulfonyl)amide ($[Tf_2N]^-$), and tosylate ($[TsO]^-$).[152,204] There have been reports that ILs containing noncyclic ammonium- and phosphonium-based cations possess dissolving capacity for the biopolymer.[121,126] However, their dissolution efficiency is very poor, especially for celluloses with elevated DP values. Turbid dispersions of up to a cellulose mass fraction of 0.3 in 2-hydroxyethylammonium formate has been reported.[123] Further studies on alkanolammonium ILs with organic acid anions did show that these types of ILs are only capable of forming fine dispersions of undissolved cellulose without any dissolution (see 3.2 on page 35).[212] As mentioned earlier, it is the author's belief that both IL ions must be suitable to efficiently dissolve

cellulose. The poor cellulose solubility of the aforementioned ammonium- and phosphonium-based ILs is—in the author's view—to be attributed to the IL cation.

### 3.3.3 Comparing Cellulose-Dissolving Ionic Liquids

Based on this temporary classification of IL ions, one can now look for structural similarities that distinguish ions with good cellulose-dissolution ability from those with poor ability. Dissolving cations seem to consist of planar, nitrogen-containing rings with the ability to delocalise their positive charge within their aromatic $\pi$-system (Figure 19). This is in contrast to poorly dissolving cations (Figure 20). The nonaromatic ring structure of these compounds results in a tetrahedral-like nitrogenium heteroatom without the ability to delocalise the positive charge. Poorly dissolving IL cations, such as noncyclic ammonium and phosphonium cations (*vide supra*), also display their localised positive charge at a $sp^3$ hybridised nitrogen centre. Cellulose-dissolving anions cover a wider structural variety than the dissolving-cations, and include planar, tetrahedral, linear, and spherical geometries.

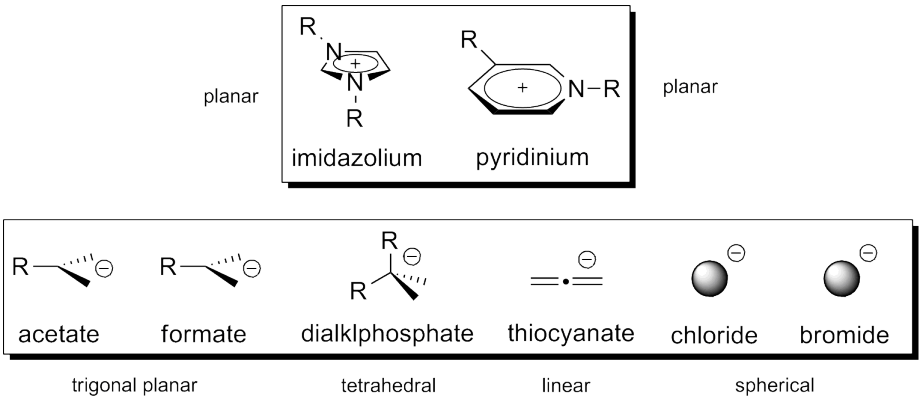


**Figure 19.** Geometry of cellulose-dissolving ionic liquid ions: Planar ring cations, as well as trigonal planar, tetrahedral, linear, and spherical anions.

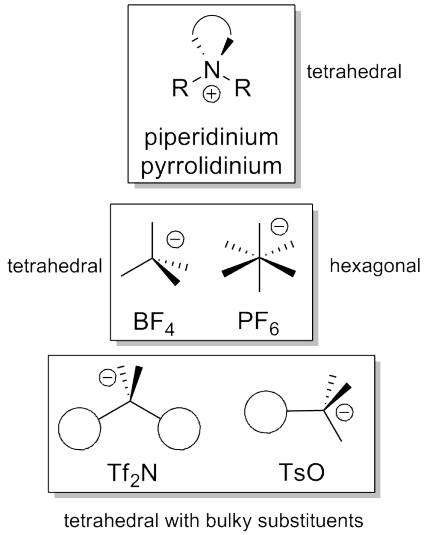


**Figure 20.** Geometry of non-cellulose-dissolving ionic liquid ions: Tetrahedral cations, as well as hexagonal and tetrahedral anions.

The obvious differences between dissolving and nondissolving cations originate from their structure, which governs their ability to delocalise their positive charge. Such differences are not as obvious with regard to the anions. Tetrahedral structures and charge delocalisation can be found within both dissolving and nondissolving anions. However, the two groups of anions differ in their H–bonding ability. All of the nondissolving anions display poor to negligible H–bond donor or acceptor characteristics. This is especially true for the $[BF_4]^-$ and the $[PF_6]^-$ anions. The $[Tf_2N]^-$ and $[TsO]^-$ anions are theoretically qualified for H–bonding but their bulky substituents impede those interactions, especially with regard to the highly cross-linked H–bond network in cellulose.

This is in contrast to cellulose-dissolving anions, which are all moderate to excellent H–bond acceptors. The H–bond acceptor ability of the anion is partially reflected in its ability to dissolve cellulose: thiocyanate < bromide < dialkylphosphate < formate ≈ acetate ≈ chloride.[69,128,133,206,207] Comparing

cellulose-dissolving anions with the ability to delocalise their charge between two O atoms, dialkylphosphate ILs do not perform as well as formates or acetates. This is possibly due to the larger anion size, resulting from additional substituents on the P atom that hinders efficient interaction with the H–bond network of cellulose. Similar charge delocalisation can be found within the $SO_3^-$ of the $[TsO]^-$ anion, with the bulky phenyl substituent facing the opposite direction. However, both the hydrophobic character of the phenyl group and its rigidity are not favourable for interacting with the interwoven H–bond network of hydrophilic cellulose.

A difference in H–bonding ability can also be found between dissolving and nondissolving cations. Because of the aromatic character of the dissolving cations, all of the ring protons are capable of H–bonding to some extent. This is not true for the tetrahedral nondissolving cations. Another aspect to consider is the cation polarity. Although difficult to quantify in some cases, it is without doubt that the heteroatoms in the imidazolium and pyridinium rings induce a dipolar character into these cations.[62,70,77,81] The presence of water molecules can decrease the effective dipole moment of the IL, resulting in the precipitation of dissolved cellulose.[213] This raises the question whether cationic dipoles are favourable for the dissolution of cellulose. AAILs, for example, can be very polar (see Table 1 on page 14) and they are able to participate in H–bonding, but they cannot dissolve cellulose.[212] As a consequence, IL ions must meet a number of requirements to efficiently dissolve cellulose:

- Cation characteristics favourable for cellulose dissolution:
  - (i) aromatic heterocycle with a $sp^2$ nitrogen heteroatom;
  - (ii) ability to delocalise the positive charge;
  - (iii) ability to participate in H–bonding;
  - (iv) dipolar ring character.

- Anion characteristics favourable for cellulose dissolution:
  - (i) ability to act as H–bond acceptor;
  - (ii) substituents should not be bulky or hydrophobic.

### 3.3.4 Attempts to Find Similarities Amongst Cellulose-Dissolving Solvents

The objective of this section is to identify structural similarities between traditional cellulose solvents and cellulose-dissolving ionic liquids. As mentioned above, ILs are nonderivatising solvents for cellulose. For this reason, only nonderivatising traditional cellulose solvents are considered for comparison (*vide supra*). The proposed similarities are derived from three observations which are outlined below.

First, NMR studies of imidazolium-derived ILs, with varying water content, indicate that the chemical shift of the H-2 proton on the imidazolium cation (Figure 21) can vary according to the water content of the IL.[214] A low water mass fraction ($w_{H_2O}$) can result in a greater downfield shift of the H-2 signal, compared to elevated $w_{H_2O}$. Consequently, an increasing $w_{H_2O}$ in the IL can result in a decreased acidity of the imidazolium H-2 proton. This can be explained by the competing effect of water molecules as H–bond partners for the anions. Regarding the fact that $w_{H_2O} = 0.01$ in cellulose-dissolving ILs can be sufficient to prevent dissolution of the biopolymer,[107] it is likely that the acidic H-2 proton of imidazolium-derived ILs is involved in the cellulose dissolution process.[191,207]

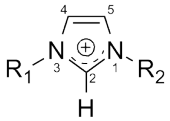


**Figure 21.** Atom labelling of the imidazolium cation

Second, NMR and density functional theory studies by Balevicius et al. showed that the acidic proton of piccolinic acid *N*-oxide (Figure 22) can experience chemical downfield shifts of up to 20 ppm, depending on the surrounding bulk media. In addition, they observed that the H–bond state in IL media is largely governed by the dielectric properties of the bulk media.[215] This means that polar water molecules, as immediate H–bond competitors, can hinder the formation of intermolecular H–bonds between the imidazolium cations. Furthermore, Balevicius et al. postulated the formation of a six-membered cyclic state that involves the acid proton of piccolinic acid *N*-oxide as a shared bridge proton.[215] The question arises as to whether cyclic states with polar characteristics—as shown in Figure 24 on page 62—are responsible for the increased H-2 downfield shift in dry imidazolium-derived ILs. The proposed cyclic arrangement of IL ions can potentially have the same effect on the IL imidazolium H-2 acidity.

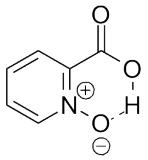


**Figure 22.** Piccolinic acid *N*-oxide

Third, it has been suggested that the permittivity of ILs can be correlated with their ability to dissolve cellulose.[152] Although the ionic nature of ILs impedes the determination of their permittivities, recent studies demonstrated that the molecular polarisations of IL ions can be of importance for solvation processes.[216] The fact that all cellulose solvents display highly polar characteristics also suggests that solvent polarity is a key factor for its dissolution.

Inspired by these three observations (*vide supra*), it is suggested that all nonderivatising cellulose solvents can hypothetically be arranged in cyclic structures of varying ring size. Important to stress at this point, is that

the discussed ring formations (*vide infra*) are not intended to represent the true nature of these solvents, but they are to be regarded as an attempt to assign a structural similarity between them. It is the aim of Figure 23 to demonstrate that the selected traditional solvents for cellulose are all able to arrange themselves in hypothetical ring formations. The ring sizes vary from five to six atoms, and small ions or polar characteristics assist in the arrangement.[217] Larger molecules, such as NMMO or tetrabutylammonium, seem to be less-suited for this purpose. However, one must consider that two-dimensional drawings do not represent the three dimensional reality, which allows the solvent components to arrange in a more favourable manner with reduced steric hindrance. NMMO inherits a N–O dipole, which may assist in theoretically assigning a ring formation, but this is harder to imagine for the tetrabutylammonium cation. In addition, associated water molecules are potentially helpful to form the cyclic arrangements proposed in Figure 23. However, the very small fluoride anion and the assistance of an additional dipolar molecule (DMSO) could theoretically compensate for the unfavourable steric geometry of the cation. It was reported that tetrabutylammonium chloride or bromide are unable to dissolve cellulose.[218]

The inherited ionic nature of cellulose-dissolving ILs allows an easy arrangement of hypothetical ring structures (Figure 24). Depending on whether one decides to involve the acidic H-2 proton of the imidazolium cation for the ring formation, six- to eight- membered cyclic structures are possible. Three ion pairs are necessary for the [BuMePy]Cl to form a six-membered ring, but only two pairs are needed in the case of imidazolium chlorides. If anions such as formate, acetate, or phosphate derivatives are considered together with imidazolium cations, an increased stability can be assigned to the cyclic arrangement. This is because these anions possess a second O atom that can interact with the imidazolium cation. Although ions with little steric hindrance are more favourable for dissolving cellulose, IL formates or acetates are more efficient in dissolving cellulose than phosphate derivatives. A valid

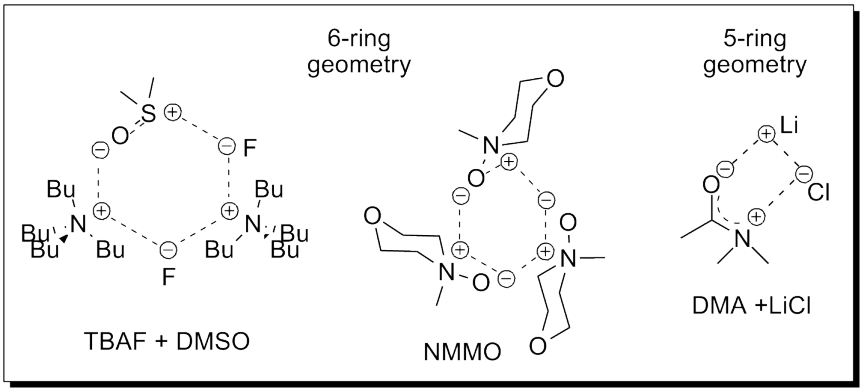


**Figure 23.** Hypothetical ability of traditional nonderivatising cellulose solvents to arrange in cyclic formations: Tetrabutylammonium fluoride+dimethylsulfoxide (TBAF+DMSO), *N*-methylmorpholine-*N*-oxide (NMMO), and *N*,*N*-dimethylacetamide+lithium chloride (DMA+LiCl).

point for criticism, at this point, is the sterically hindered structure of the pyridinium cation. This issue will be resolved later in this discussion, but it is important to note that the efficiency of [BuMePy]Cl to dissolve cellulose must be questioned, because this solvent significantly degrades the biopolymer during dissolution.[105]

Because of the acidic character of their H-2 proton, imidazolium cations appear to be more suitable for participating in the hypothetical arrangement.[191] The higher the H-2 acidity, the more polar the resulting imidazolium cation and the easier the hypothetical formation of the cyclic arrangement. Complete dissociation of the H-2 proton would result in Arduengo carbene-like structures with high polarity, and Arduengo carbenes are known to be relatively stable. However, imidazolium cations with methyl substituents at the C-2 position are also able to dissolve cellulose, demonstrating that the presence of the imidazolium H-2 proton is actually not a requirement for dissolving cellulose with imidazolium ILs.[106,111,120,126]

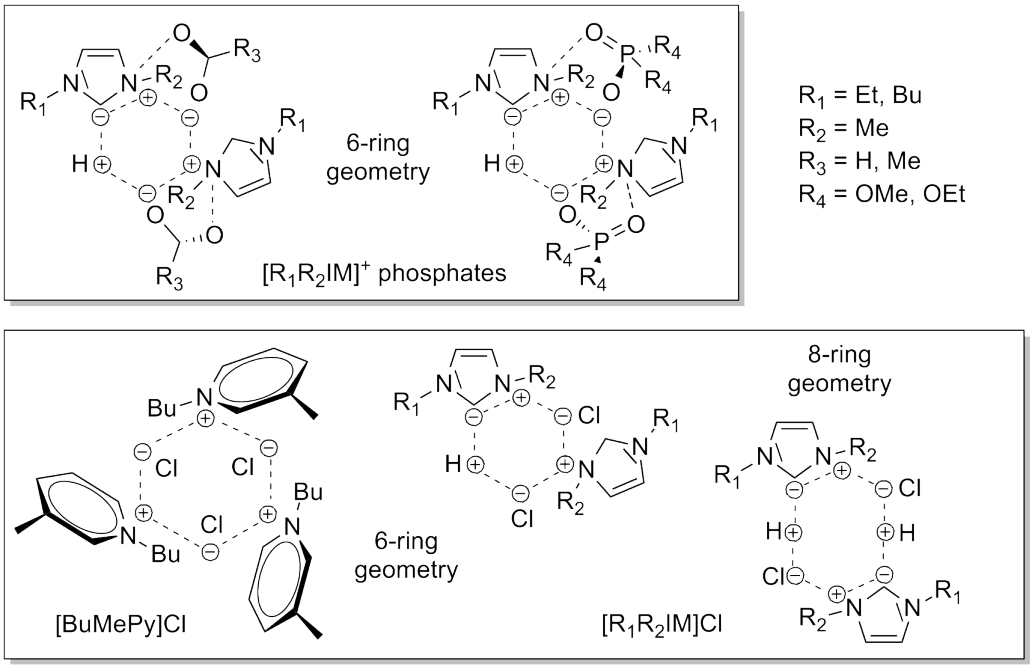


**Figure 24.** Hypothetical ability of ionic liquid cellulose solvents to arrange in cyclic formations: 1,3-dialkylimidazolium ($[R_1R_2IM]^+$) formates ($R_3$ = H) and acetates ($R_3$ = Me), $[R_1R_2IM]^+$ dialkylphosphates ($R_4$ = OMe, OEt), 1-butyl-3-methylpyridinium chloride ([BuMePy]Cl), and $[R_1R_2IM]^+$ chlorides.

### 3.3.5 Structural Investigations on the Cellulose Crystal Lattice

After identifying a common characteristic between traditional and IL cellulose solvents, a closer look at the structure of crystalline cellulose is required to explore whether the proposed similarities can be responsible for the dissolution of the biopolymer. Due to the fact that cellulose consists of cellobiose monomers, every second glucose unit is rotated by 180° (see Figure 8 on page 18). Consequently, only the OH–groups at positions C-3 and C-6 are responsible for the attractive intermolecular forces that hold the cellulose chains together. The OH–group at position C-2 is only responsible for

intrachain H–bonds (see Figure 9 on page 19). As a result, cellulose solvents do only need to attack the H–bonds between the OH–groups at positions C-3 and C-6 to dissolve cellulose (Figure 25).

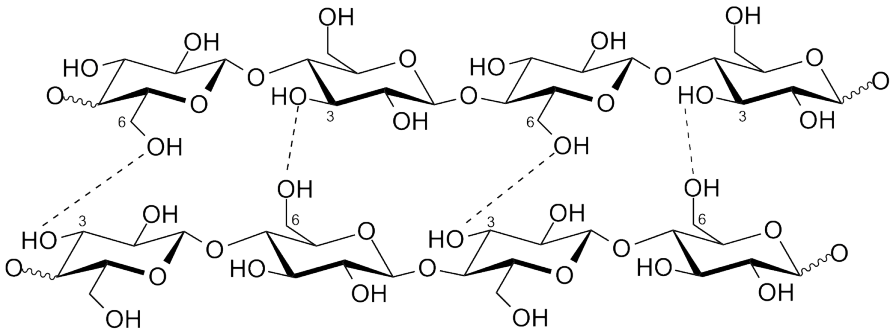


**Figure 25.** Only the OH–groups at positions C-3 and C-6 are responsible for intermolecular hydrogen bonding in cellulose.

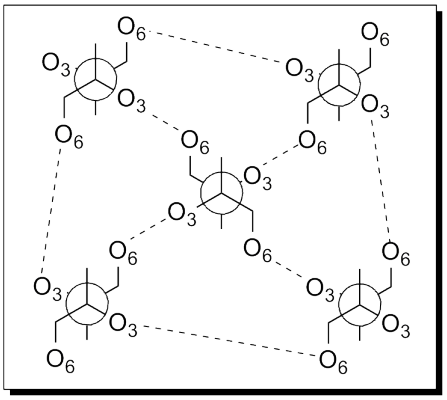


**Figure 26.** Simplified axial view of interchain hydrogen bonding in crystalline cellulose microfibrils.

Figure 26 shows a simplified axial view of the interchain H–bonding in crystalline cellulose microfibrils. Imagining a rectangular shape of the crystalline regions, the chains at the corner positions of the rectangle are most prone to solvent attack. This is because they are most exposed to the surrounding environment, and because they interact least with adjacent OH–groups.

The crystal structure of native cellulose has been determined by X-ray diffraction (XRD) experiments.[100] Gardner and Blackwell have stated that the H–bond network in native cellulose is completely contained within the (020) plane, and that it is compatible with both parallel and antiparallel chains.[100] Although the bond angles and atom distances are known, it is difficult to envisage the precise three-dimensional structure of aligned cellulose chains in the crystal lattice. For better visualisation purposes, Figure 27 shows a simplified projection of the (020) plane of native cellulose, only focusing on the H–bond network involving the positions C-3 and C-6. This results in 9-membered cyclic structures within each polymer chain and 14-membered rings between the cellulose chains.

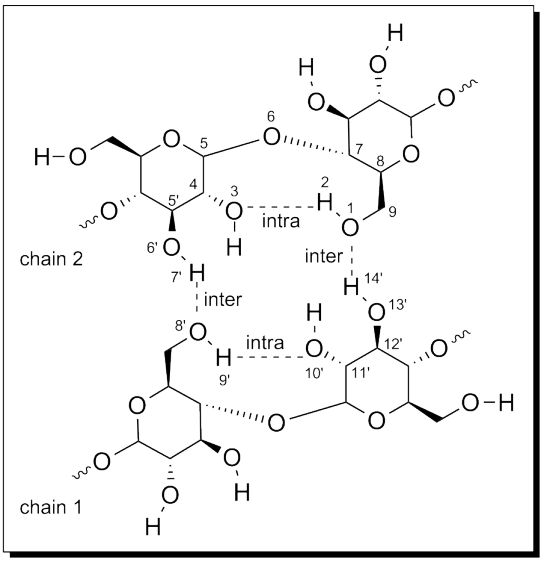


**Figure 27.** Simplified projection of the (020) plane of native cellulose, only showing the hydrogen bonds at the relevant C-3 and C-6 positions. This results in 9-membered cyclic structures within each polymer chain and in 14-membered rings between the cellulose chains.

It has been suggested that, during the dissolution of cellulose in ILs, the cellulosic interchain H–bonds are broken apart, because of the formation

of new H–bonds with the solvent (see Figure 10 on page 22).[108,191,207] The OH–groups in native cellulose, however, do already form very strong H–bonds between each other. Consequently, the main reason why cellulose solvents can successfully compete with the H–bonds of native cellulose is—in the author's opinion—that the solvent can offer H–bond interactions that are at least of the same stability compared to the native interchain H–bonds of cellulose. Cyclic transition states—especially with six members—are very common in chemical reactions because of their increased thermodynamic stability. As a result, the author proposes that an efficient cellulose solvent is able to compete with the H–bonds of native cellulose because of its ability to arrange itself in a favourable geometry with enhanced thermodynamic stability. The following section is going to discuss this possibility.

### 3.3.6 Speculations on Cellulose-Dissolving Ionic Liquids

The previous discussions revealed structural similarities among cellulose solvents and offered explanations for the general ability of these solvents to compete successfully with the strong H–bond network in native cellulose. The objective in this section is now to link these two components together to provide a theory on the dissolution mechanism of cellulose. As mentioned earlier, the solvent is only required to attack the cellulosic OH–groups at positions C-3 and C-3 to separate the polymer chains (Figure 27 on page 64). However, considering that the OH–group at position C-6 also interacts with intrachain C-2 hydroxyls, additional H–bond attack at C-2 can assist in breaking the interchain H–bonds that involve the OH–group.

Prior to discussing selected cellulose solvents, three assumptions are now made: (i) cyclic arrangements consisting of six members are favourable; (ii) at least two cellulose OH–groups are involved in solvent interactions; and (iii) each cellulose OH–group does not interact with more than two H–bond partners at the same time. Figure 28 demonstrates possible interactions

between a solvent dipole and a cellulosic OH–group. Required is a dipolar solvent character, with favourably $n = 2$ bridging atoms between the dipoles, to form a six-membered cyclic state. Fewer bridging atoms result in five-membered ($n = 1$) or four-membered ($n = 0$) arrangements.

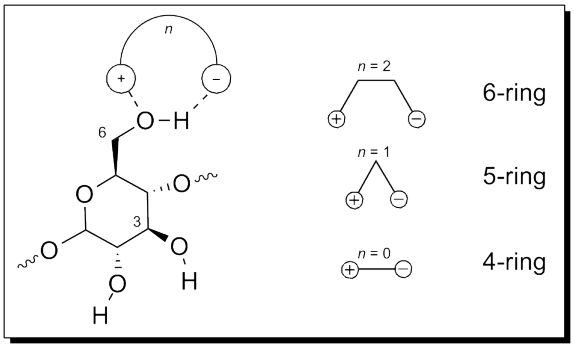


**Figure 28.** Scheme for the possible interaction between a cellulose OH–group and a solvent dipole: The amount of bridging molecules $n$ determines the size of the resulting cyclic state.

The question arises as to whether any nonderivatising cellulose solvents fit into this scheme. First of all, traditional solvent systems are going to be investigated with respect to their number ($n$) of bridging atoms between their dipoles (Figure 29). One can find everything from zero to two bridging atoms, resulting in the hypothetical formation of four- to six-membered cyclic arrangements. The bulky tetrabutylammonium cation is expected to depend on the presence of both a very small anion and an additional solvent molecule, which must be polarisable and nonbulky, in order to qualify for the required geometry. Admittedly, it does seem odd that NMMO, as an efficient cellulose solvent, is only able to form a four-membered cyclic arrangement because of its lack of bridging atoms between its dipoles. To resolve this issue, however, it is first necessary to take a closer look at cellulose-dissolving ILs.

At a first glance, only $n = 0$ or 2 bridging atoms are found for cellulose-dissolving ILs (Figure 30). However, the ability to delocalise the positive

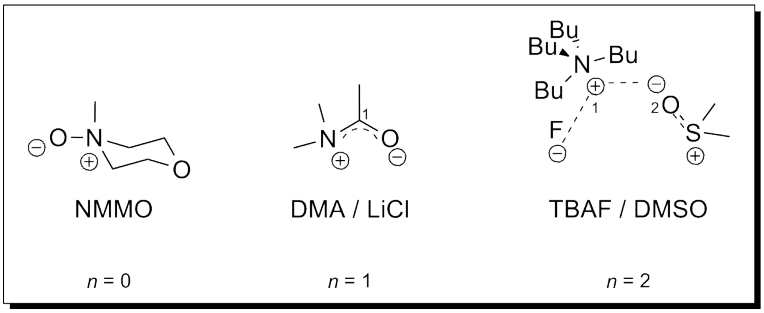


**Figure 29.** Traditional nonderivatising cellulose solvents ordered according to their number ($n$) of bridging atoms between their dipoles: *N*-methylmorpholine-*N*-oxide (NMMO), *N*,*N*-dimethylacetamide+lithium chloride (DMA+LiCl), and tetrabutylammonium fluoride+dimethylsulfoxide (TBAF+DMSO).

charge in the cation heterocycle allows these ILs to adjust their dipolar geometry appropriately, according to their needs. The acidity—or the presence—of the imidazolium H-2 proton is not important in this respect. As shown before, small ions that are capable of H–bonding are crucial for any cellulose solvent. The ability to H–bond is important to break down the intermolecular H–bonds in cellulose. Ion size governs ion mobility, and the mobility affects the ion's ability to penetrate and attack the cellulose network: the smaller the ion, the more favourable. This explains why the addition of salts that are composed of small ions, such as lithium chloride for example, is favourable for cellulose dissolution. Many traditional cellulose solvents rely on the presence of these salts, and ILs can also benefit of their presence.[207,219]

In this respect, ILs have one disadvantage. To be molten salts at low temperatures, they must meet certain structural criteria for decreasing the attractive Coulombic forces between their cations and anions. This dictates that at least one ion cannot be of small size anymore. Requiring that one ion, usually the cation, must be of larger size can impede the ILs dissolution ability, because it restricts the ion to efficiently penetrate the cellulosic H–bond network. The advantage of the ILs shown in Figure 30, on the

other hand, is their ability to delocalise the charge of their more bulky ion, allowing them to adapt a favourable dipole geometry. Computational studies of Sashina and Novoselov support this conclusion, suggesting that the degree of charge delocalisation in IL ions plays a major role in the dissolution process of natural polymers.[213]

Many traditional nonderivatising cellulose solvents share the drawback that their active components—small ions—are usually dissolved in, or associated with, an antisolvent for cellulose, such as DMSO or water.[194,218] Formate, acetate, and phosphate derivatives can also delocalise their negative charge to a certain extent. This may help to compensate for their bigger size. The presence of two good H–bond acceptor atoms (oxygen) in intermediate proximity of each other on one side of the molecule, and the nonfavourable substituents facing away on the opposite side, can explain why those ions are still found in cellulose-dissolving ILs. However, it will always be a tradeoff between the size of the ion and its ability to present its H–bonding components at a favourable location.

The possible existence of the proposed arrangements between IL ions and cellulose polymer chains still needs to be validated. Spectroscopic techniques, such as NMR or Raman experiments, can possibly give hints about the changes in the immediate environment of the solvent. Furthermore, the energetic aspects of the proposed interactions between solvent and polymer must be considered. Both entropic effects and the thermodynamic stability of the H–bonds are expected to influence the dissolution process.

The conclusions drawn from IL cellulose solvents shed a different light on the NMMO dissolution process. According to the proposed dissolution mechanism, it is the flexible arrangement of dipoles that is crucial for efficient attack of the native H–bond network between cellulose polymer chains. The special arrangement of heteroatoms in the morpholine ring, together with its nonaromaticity, can explain the ability of NMMO to interact favourably with cellulose. First, the lack of a delocalised $\pi$-system within the ring

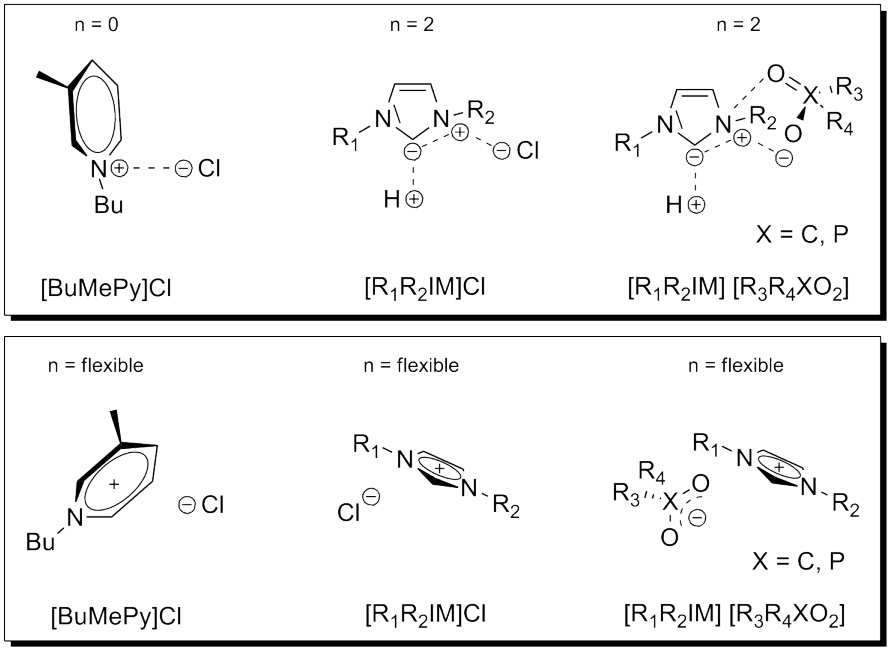


**Figure 30.** Cellulose-dissolving ionic liquids ordered according to their number ($n$) of bridging atoms between their dipoles (top). However, their ability to delocalise their charges enables them to adopt a flexible dipolar geometry (bottom).

keeps the heterocycle sufficiently flexible to adopt various conformations. Second, the oxygen in para position to the N atom in the heterocycle can potentially interact with two cellulose OH–groups at the positions C-2 and C-3 simultaneously, thus competing for both intramolecular and intermolecular interactions (Figure 31).

Attacking the cellulose intrachain H–bond at position C-6 can assist in cleaving the interchain H–bond that originates from the same OH–group at position C-6. Consequently, the simultaneous interaction of NMMO with three OH–groups of the same polymer chain (at positions C-2, C-3, and C-6) can facilitate the separation of adjacent cellulose chains. It is likely that the C-2 and C-3 OH–groups are most prone to solvent attack, because they only interact with one adjacent OH–group. Once deprived of its intrachain

bonding partner, the hydrogen of the C-6 OH–group is potentially available to interact with the oxygen substituent of NMMO. The final step can be the cleavage of the C-6 interchain H–bond and subsequent interaction with the new bonding partner NMMO. Assuming that one OH–group does not take part in more than two H–bond interactions at the same time, the resulting cyclic state is likely to be more stable than the initial one, because only three H–bonds are broken and four new ones are formed between NMMO and one unit of the polymer chain.

Little is known about the dissolution mechanism of cellulose in NMMO. Although calculational studies do not support the idea of H–bond interactions that involve the ring oxygen in NMMO, it is interesting that the postulated cyclic state, between the heterocyclic core of NMMO and the cellulose OH–groups, consists of 14 atoms (Figure 31).[220] This is identical to the interchain ring size in native cellulose (see Figure 27 on page 64), indicating that the resulting cyclic arrangement, between NMMO and cellulose, is of similar stability than the H–bond arrangement in native cellulose. As a consequence, NMMO can also be regarded as a dipole with $n = 2$ bridging atoms, and it is concluded that a second heteroatomic species, at a favourable position in the IL cation, enhances cellulose dissolution.

Based on the analysis of NMMO, and in agreement with other studies, it is further concluded that one solvent unit can interact with multiple OH–groups simultaneously, including those that do not participate in interchain H–bonding.[191] This allows the cellulose solvent to potentially cleave three H–bonds while establishing four new ones. Summarising these conclusions, the refined structural characteristics of IL ions for enhanced cellulose dissolution are:

- Cation characteristics for enhanced cellulose dissolution:
  - (i) aromatic heterocycle;
  - (ii) ability to delocalise the positive charge;

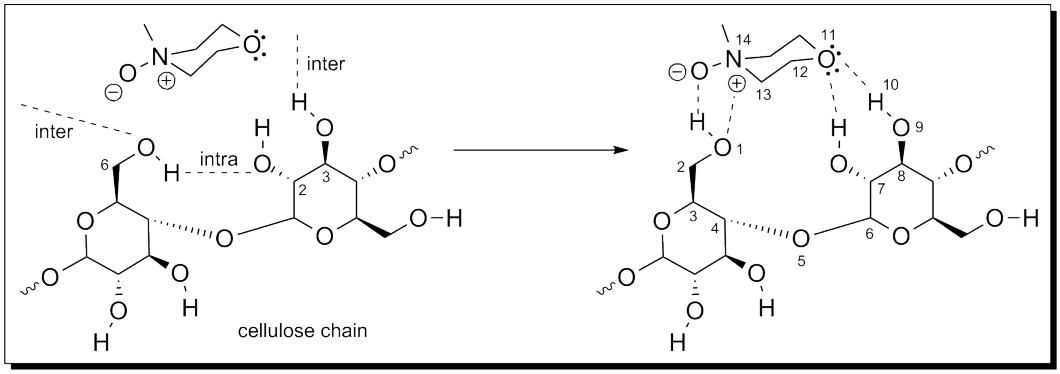


**Figure 31.** Possible H–bond interactions between *N*-methylmorpholine-*N*-oxide (NMMO) and cellulose: three cellulosic hydrogen bonds can theoretically be attacked simultaneously.

(iii) second heteroatom in aromatic ring;

(iv) inherited dipolar characteristics.

- Anion characteristics for enhanced cellulose dissolution:

  (i) ability to act as H–bond acceptor;

  (ii) substituents should not be bulky or hydrophobic;

  (iii) either small in size or ability to offer several H–bond acceptor sites.

### 3.3.7 Alternatives for Cellulose-Dissolving Ionic Liquids

To reflect on the previous conclusions (*vide supra*) is the most interesting part of this particular work. The objective of this section is to take advantage of the newly gained insights and to propose novel cellulose solvents. Alternative IL ions for dissolving cellulose will be suggested and discussed.

Suitable cations, for dissolving cellulose, are heterocycles that can at least partially delocalise their positive charge. The presence of an inherited dipole is expected to be favourable. Dipolar characteristics can be introduced with

heteroatoms positioned at opposite sides of the ring. The larger the difference in electronegativity of the heteroatom, the larger the resulting dipole (Figure 32). It remains to be seen what is most beneficial for dissolving cellulose: (a) two heteroatoms that are more electronegative than the connecting C atoms, such as N and O for example, or (b) two heteroatoms with the largest difference in electronegativity possible, such as P and O. The imidazolium cation is an example of (a), whereas *N*-methylmorpholine-*N*-oxide follows (b) by exploiting its N–O dipole. An unsaturated equivalent to morpholine is 1,4-oxazine, but oxazine as a six-membered ring is not an aromatic compound, because of the presence of an $sp^3$ ring carbon. Similar difficulties are encountered if P and O are to be paired in a six-membered heterocycle to introduce a large difference in electronegativity ($\Delta$EN). Promising heterocycles, however, are the two five-membered rings oxazole and 1,3-oxaphosphole (Figure 33).

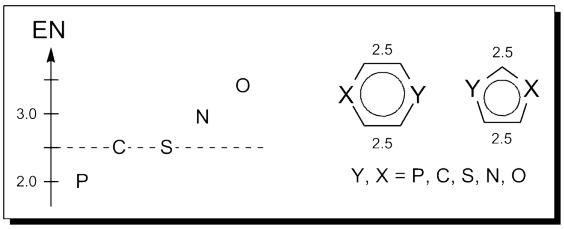


**Figure 32.** The dipolar character of heterocycles is affected by the nature and the position of the heteroatoms in the ring. Carbon has a electronegativity (EN) value of 2.5, and the EN values of other possible heteroatoms increase from phosphor to oxygen.

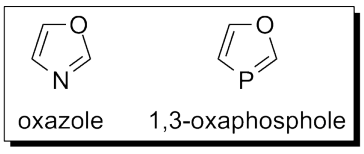


**Figure 33.** Heterocycles with different dipolar character: nitrogen and oxygen are both more electronegative, and phosphorus is less electronegative, than carbon.

Suitable IL anions—for the dissolution of cellulose—are always good H–bond acceptors, preferably small in size and without any hydrophobic substituents. The presence of several H–bond acceptor sites can be an advantage. Possibilities include fluoride ($F^-$), chloride ($Cl^-$), formate ($[HCO_2]^-$), acetate ($[MeCO_2]^-$), phosphate ($[PO_4]^{3-}$), peroxide ($[O_2]^{2-}$), superoxide ($[O_2]^-$), hydroxide ($[OH]^-$), nitrite ($[NO_2]^-$), or nitrate ($[NO_3]^-$).

Only limited data are available for IL fluorides, and their cellulose-dissolution ability is not convincing.[129] A possible explanation would be that the fluoride-containing IL has a highly ordered structure in the liquid state, due to the small and very electronegative fluoride anions. This could inhibit the penetration of the cellulosic H–bond network, and other studies have shown that a high degree of dissociation in ILs is favourable to dissolve cellulose.[191] Most IL chlorides are good cellulose solvents, but their increased viscosity and their corrosive behaviour is not desirable.[152] Alkali superoxides are known to be unstable and to react with traces of water to form oxygen, hydrogen peroxide, and hydroxide. In addition, peroxides must be handled with care, because of their combustive nature, and IL peroxides are also most likely to be unstable. Because of the nature of the hydroxide anion, corresponding ILs are expected to be hygroscopic and viscous. Ionic liquid formates and acetates pose an alternative to the chlorides, although their long-term stability at elevated temperatures must still be established.

However the $[CO_2]^-$ synthon can assist in finding anions with similar dissolution ability—compared to the acetate ion—but with increased thermal stability. Dimethylcarbamate (Figure 34) could qualify as such, and the mesomeric effect of the N atom also offers the possibility of two H–bond acceptor sites. It remains to be seen whether the bulkiness of the anion is an issue. The nitrogen equivalent to the $[CO_2]^-$ synthon is $[NO_2]^-$. Consequently, nitrite and nitrate are additional ions that must be considered as alternatives. Furthermore, anions based on phosphate derivatives are known to show moderate dissolution ability for cellulose and exhibit reasonable thermal

stability.[221] The phosphate anion can offer multiple O atoms that qualify as H–bond acceptors, and its triple negative charge enables the anion to be paired with three cations.

More promising cellulose solvents may be not pure ILs, but mixtures of substances. One example would be to mix cellulose-dissolving heterocyclic cations with very small cations, such as lithium for example. These cations can potentially be paired with phosphate to form an IL, combining the desirable effects attributed to these ions for dissolving cellulose. The possibilities are manifold and need to be explored. In conclusion, Figure 35 summarises the suggested alternatives for IL ions that are expected to show enhanced cellulose solubility.

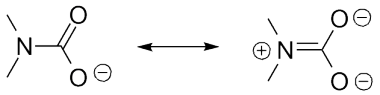

**Figure 34.** Mesomeric structure of dimethylcarbamate.

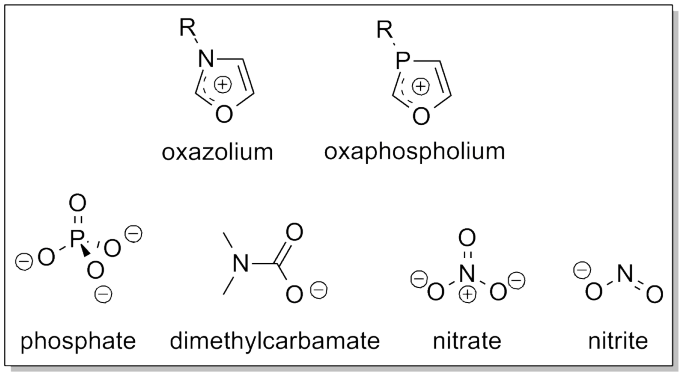


**Figure 35.** Proposed IL ions for enhanced cellulose dissolution: oxazolium, 1,3-oxaphospholium, phosphate, dimethylcarbamate, nitrate, and nitrite.

### 3.3.8 Conclusion

Until now, the search for ILs with cellulose-dissolving ability has mainly been based on trial and error. The objective of this work was to identify structural similarities among cellulose solvents in order to propose alternative ILs for enhanced dissolution. It is reasoned that both IL cations and IL anions are important for the efficient dissolution of cellulose. IL ions that are found in cellulose-dissolving ILs were identified and compared to both nondissolving ILs and traditional cellulose solvents. It was found that all nonderivatising cellulose solvents share one similarity: they can form hypothetical cyclic arrangements with themselves. Structural analysis of the native cellulose crystal lattice reveals that only one specific type of H–bond must be cleaved to achieve polymer chain separation.

It is proposed that efficient cellulose solvents are able to arrange their dipoles in a favoured geometry, allowing them to successfully compete with the strong H–bonds network of native cellulose. Cation characteristics that are expected to enhance cellulose dissolution are (i) an aromatic heterocycle with the ability to sufficiently delocalise the positive charge, and (ii) a second heteroatom in the aromatic ring that increases the dipolar character of the cation. Anion characteristics that are expected to enhance cellulose dissolution are (i) being an H–bond acceptor of small size, (ii) having substituents that are neither bulky nor hydrophobic, and (iii) possessing the ability to offer several H–bond acceptor sites.

Proposed alternatives for cellulose-dissolving IL ions are oxazolium, 1,3-oxaphospholium, dimethylcarbamate, phosphate, nitrate, and nitrite. In addition, it is suggested that mixtures of ILs and salts, with small-sized ions such as lithium chloride, could result in highly efficient cellulose solvents that are more environmentally friendly than traditional cellulose solvents.

# 4 Extracting Wood Lignin with Ionic Liquids

Facilitating a more efficient access to natural biopolymers—which subsequently enables fuel and material technology platforms based on renewable resources—is a key challenge towards sustainability and is generally recognised as a worldwide goal. However, it lacks environmentally benign technologies to separate the major components of lignocellulosic biomass without compromising product quality.

The excellent mechanical properties of crystalline wood cellulose rival those of Kevlar® and are due to its highly crystalline structure. Preserving this crystallinity during delignification processes is crucial for the transfer of these mechanical properties to cellulose-based biocomposites. However, traditional delignification methods do not completely adhere to the Principles of Green Chemistry, and recently suggested alternatives face considerable drawbacks, including loss or degradation of cellulosic material.

This chapter's work aims to explore the possibility to extract wood lignin with ILs, while retaining the crystalline integrity of the cellulosic-rich residues. A class of food-additive based ILs, with the ability to dissolve wood lignin but not cellulose, has been identified and the efficiency of IL lignin extractions, at varying extraction conditions, has been investigated.

## 4.1 The Importance of Wood Delignification

Lignocellulosic biomass, such as wood, represents a renewable feedstock of biopolymers, *viz.* cellulose, hemicellulose and lignin. Exploitation of these biopolymers has been limited due to both the recalcitrant nature of biomass and society's shift towards petroleum-based feedstock from the 1940s onwards.[6] With the increasing depletion of fossil resources, we are rediscovering the importance of biomass for the production of chemicals, fuels, and energy. Biomass-derived energy did not only recently surpass hydroelectric energy, as the largest domestic source of renewable energy in the United States, but it also constitutes the largest share of renewable energy produced in the European Union, outweighing the total combined contribution from wind, hydro, geothermal, and solar energy.[222]

Some governments are gradually reacting, passing legislation to increase the use of renewable resources for the production of energy and chemicals. The European Union aims to derive 10 % of its transportation fuels and 20 % of its consumed energy from renewable resources by 2020, and the United States have set targets to derive 20 % of transportation fuels and 25 % of chemical commodities from renewable resources by 2030.[222–224] Biomass will certainly play a considerable role in achieving these targets.

The worldwide biomass availability and production capacity is immense. More than 370 million dry tons of forestry biomass and 1 billion dry tons of agricultural biomass are available in the United States every year.[222,224] Biomass production capacities in the European Union are already in place to produce 190 million tons of oil equivalent (Mtoe) of biomass by today, with possible increases of up to 300 Mtoe by 2030.[222,225] It is estimated that the potential production capacities are sufficient to supply all of the raw materials that are now required by the chemical industry.[222,226]

Although lignin represents a main constituent of lignocellulosic biomass—(15 to 30) % by mass and 40 % by energy—it has not received as much

attention as cellulose, and it is still considered a low value product. Worldwide, the pulp and paper industry produces 50 million tons of lignin annually but only 0.02 mass fraction of it is used commercially (e.g. as dispersing or binding agents), the remainder is burned as a low value fuel.[222,227] However, with its high degree or aromaticity, lignin represents a potential future feedstock for the sustainable production of fuels and bulk chemicals.[4,228] In fact, lignin can be regarded as the major renewable source for aromatics on the planet.[222] Its potential to transform into a desirable high-value product in the near future is obvious.

The challenge in unlocking the full potential of lignocellulosic biopolymers is their efficient separation from each other, using environmentally-benign methods without decrease in product quality.[229] Traditional methods to access these materials are expensive and chemically wasteful.[6] For example, the 120 year old Kraft process dominates commercial wood delignification, but it is an energy-intensive process—due to its high operating pressures and temperatures—with many sequential processing steps, requiring many chemicals and large amounts of water. Moreover, its capital-intensive equipment requires large plant sizes, creating additional issues with respect to transporting the low-density biomass feedstock.[5,230] Several other pulping methods—based on the use of organic solvents to dissolve lignin and hemicellulose—have been developed in order to counteract the prevailing difficulties, but all of the so-called organosolv methods suffer their own particular problems and none of them was able to replace the Kraft pulping process.[6] Consequently, an environmentally friendly method for the extraction of wood lignin, without compromising the excellent mechanical properties of native cellulosics, is desirable as it would have the potential to revolutionise cellulose-biocomposite processing, affecting a number of products ranging from simple paper sheets to high-strength and low-mass automobile parts.[231]

## 4.2 Literature Study

### 4.2.1 Lignin

Lignin is a natural, highly branched and amorphous, polymer of high molecular weight, acting as the essential glue that gives plants their structural integrity, and representing the second most abundant natural polymer on earth.[232] As an integral part of the secondary cell wall of plants, and due to its hydrophobic character, it plays an important role in transporting water in plant stems. Lignin lacks a clearly defined secondary or tertiary order and its variable composition depends on the plant source.[233,234] In a simplified way, lignin can be regarded as the polymerised product of three fundamental phenylpropane units, commonly known as monolignols: *p*-coumaryl alcohol, coniferyl alcohol and sinapyl alcohol. In the lignin macromolecule, these monolignols are incorporated in the form of phenylpropanoids: *p*-hydroxyphenyl (H), guaiacyl (G) and syringyl (S) (Figure 36).[233]

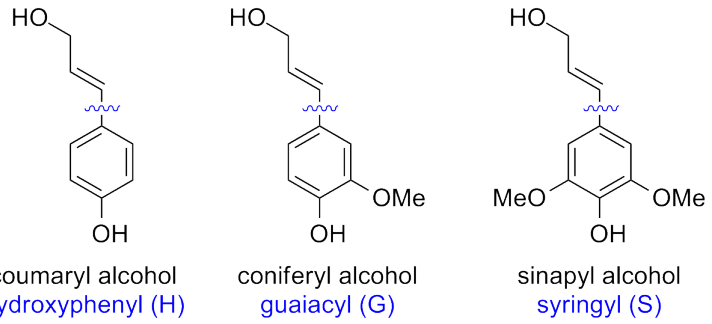


**Figure 36.** Three fundamental monolignols (and their respective phenylpropanoids): *p*-coumaryl alcohol (*p*-hydroxyphenyl), coniferyl alcohol (guaiacyl) and sinapyl alcohol (syringyl).

These monomeric units differ only in their number of substituted methoxy groups and—although representing the majority of repeating units in the lignin macropolymer—other lignols may be present in smaller quantities.

As mentioned before, the composition of lignin varies depending on the wood species and plant type; hardwoods tend to have slightly higher lignin contents than softwoods (Table 6). Softwood lignin, predominantly found in coniferous trees, consists primarily of coniferyl alcohol units, while hardwood lignin contains both coniferyl and large amounts of sinapyl units. The least substituted monolignol—*p*-coumaryl alcohol—is scarcely present in wood and is more common in grasses.[233] Of industrial importance is the classification of lignin into two different types: acid-soluble lignin and acid-insoluble (or Klason) lignin.[233] It is still under debate whether covalent bonds between lignin and wood carbohydrates exist, but many studies indicate the presence of such a lignin–carbohydrate complex (LCC).[232,235,236]

**Table 6. Total Lignin Content of Plants and Monolignol Composition of the Respective Lignins.**

| | Total Lignin | *p*-Coumaryl | Coniferyl | Sinapyl |
|---|---|---|---|---|
| | 100 *w* | | 100 *w* | |
| Softwood[94,233] | 25–31 | < 5 | > 95 | trace amounts |
| Hardwood[94,233] | 20–28 | 0–8 | 25–50 | 46–75 |
| Grasses[233,237,238] | 15–22 | 5–33 | 33–80 | 20–54 |

The biopolymerisation of lignin involves the coupling of radical species, with the the highest portion of inter-phenylpropanoid bonds arising due to coupling of the $\beta$ carbon of phenolic radicals with the methoxy group at position C-4 of another monolignol unit (Figure 37). The resulting $\beta$–O–4 linkage, an alkyl-aryl ether, is predominant in both softwoods and hardwoods. Its sensitivity towards nucleophilic attack is exploited in traditional pulping methods.[233]

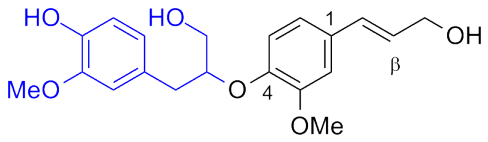


**Figure 37.** The $\beta$–O–4 linkage between monolignols dominates in both softwood and hardwood. Shown are two polymerised coniferyl alcohol units.

### 4.2.2 Lignin Extraction with Ionic Liquids

To date, it is still impossible to study naturally occurring lignin in its unaltered form, because all known isolation procedures result in chemical modification of its three dimensional network.[103,233] After the first report in 2002 that some ILs can dissolve cellulose, wood scientists were gradually becoming aware of the immense potential of ILs for their research.[107] In 2007, Kilpelainen et al. reported the complete dissolution of wood in ILs.[103] The possibility to dissolve lignin in ILs triggered investigations on both the nature and the chemical behaviour of IL-derived lignin,[239–242] and also includes studies on the depolymerisation of the IL-dissolved biopolymer.[234,243–246]

Pu et al. investigated a range of imidazolium ILs for their ability to dissolve Kraft lignin. In their study, up to 0.2 mass fraction of lignin could be dissolved in ILs containing triflate or methylsulfate anions, and it was suggested that the IL anion dominates the dissolution behaviour. Imidazolium chlorides and bromides were less potent to dissolve Kraft lignin, compared to sulfur containing anions, and both tetrafluoroborates and hexafluorophosphates did not dissolve the polymer.[247] However, the chemical nature of Kraft lignin—containing sulfur residues from the pulping process—cannot be compared with that of native wood lignin, and caution is required when interpreting these observations.[230]

Most ILs with cellulose-dissolving ability do also dissolve lignin to a certain degree. This behaviour is exploited to reduce the recalcitrance of lignocellulosic biomass towards enzymatic hydrolysis. Especially the IL 1-ethyl-3-

methylimidazolium acetate ([EMIM]Ac) has been studied to reduce both the lignin content and the crystallinity of biomass prior to its hydrolysis.[119,248]

Only few reports are available that describe efforts to extract lignin with ILs. Sun et al. completely dissolved wood in [EMIM]Ac, isolating up to 0.3 mass fraction of the initial wood lignin by precipitation in a mixture of acetone and water. Major drawbacks were long dissolution times (48 h) and a considerable loss of carbohydrates (0.4 mass fraction).[9] In subsequent studies, Sun et al. used polyoxymetalate (POM) catalysts to both reduce the long dissolution times and increase the pulping efficiency. Unfortunately, a number of problems did arise, including (i) the loss or degradation of both lignins and carbohydrates, and (ii) the instability of the POM catalyst during recycling.[249]

Inspired by the effectiveness of sodium xylenesulfonate as pulping agent in a process known as *hydrotropic* pulping, Tan et al. studied the use of 1-ethyl-3-methylimidazolium alkylbenzsulfonates ([EMIM]ABS) to dissolve lignin from sugarcane bagasse. Remarkable lignin extraction yields of up to 0.93 mass fraction were achieved, but at the expense of considerable carbohydrate losses (0.55 mass fraction). More drawbacks include (i) comparatively high extraction temperatures (463 K), (ii) the necessity to pre-treat the biomass with steam, and (iii) difficulties in the recovery of the IL.[250]

### 4.2.3 Ionic Liquid Acesulfamates

Several reports of ILs containing the acesulfamate ($[Ace]^-$) anion exist in the literature, including imidazolium, ammonium, and phosphonium cations.[251–255] Studies on these ILs include their: antimicrobial behaviour,[252,256] toxicity,[257–261] biodegradability,[259,262] thermodynamic phase behaviour,[263] pharmaceutical activity,[264] and their ability to dissolve $CO_2$[265] or carbohydrate sugars.[266] Only few of these studies deal with the 1-butyl-3-methylimidazolium

cation ([BMIM]$^+$),[251,260,261] and no reports are available on 1-ethyl-3-methylimidazolium acesulfamate ([EMIM]Ace). To the best of the author's knowledge, no reports on studies with regard to the interaction of [BMIM]Ace with either cellulose, lignin, or wood are available at present.

## 4.3 Results and Discussion

To extract wood lignin without degradation or loss of cellulosics, one is looking for a gentle extraction procedure combined with a solvent that does not interact with the cellulosic material. Ideally, this solvent is nontoxic, noncorrosive, nonhazardous, thermally stable, of low viscosity, and easy to recycle. The decision to study imidazolium acesulfamate ILs, *viz.* 1-ethyl-3-methylimidazolium acesulfamate ([EMIM]Ace) and 1-butyl-3-methylimidazolium acesulfamate ([BMIM]Ace), for the extraction of wood lignin was made for three reasons: (i) both ILs can be synthesised from acesulfamate potassium, which is a commercial sugar that is of low cost and nontoxic because it is an approved food additive; (ii) previous studies suggest that large and bulky IL anions with delocalised charge, such as [Ace]$^-$, do not dissolve cellulose (see 3.3 on page 48); and (iii) both IL ions are expected to interact with lignin due to their aromatic character.

### 4.3.1 Synthesis and Properties of Imidazolium Acesulfamate Ionic Liquids

Imidazolium acesulfamate ILs, referred to as Ace ILs, can be readily synthesised from the sugar acesulfamate potassium, also known as Ace K, Sunnett, Sweet One or as the food additive E950. Ace K is available at low cost, and cation metathesis with imidazolium halides yields the corresponding ILs (Figure 38). Traces of halide impurities remain in the ILs after synthesis (see 4.4.2 on page 123). It was decided not to remove the residual halides due

to (i) practical reasons and (ii) the author's opinion that traces of residual halide ions do not have a negative impact on the lignin extraction efficiencies of the studied ILs (4.3.3 on page 95). The presence of impurities, however, needs to be kept in mind when physical properties of ILs are discussed.

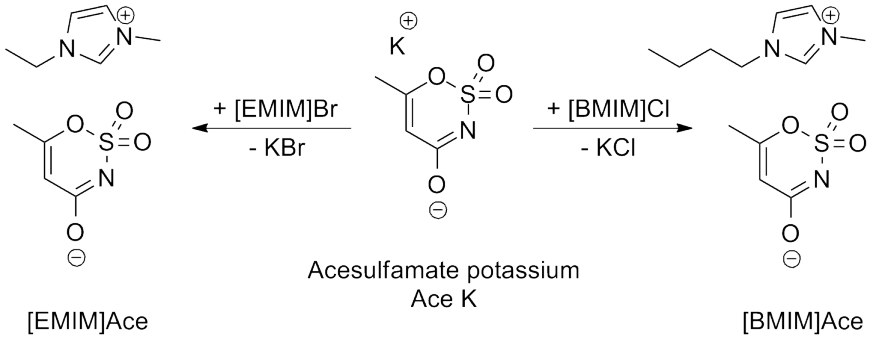


**Figure 38.** Imidazolium acesulfamate ionic liquids are readily synthesised from the commercial sweetener Ace K by cation metathesis with the corresponding imidazolium halides. Two cations, 1-ethyl-3-methylimidazolium ($EMIM]^+$) and 1-butyl-3-methylimidazolium ($[BMIM]^+$), were studied in this work.

Table 7 shows selected physical properties of the studied Ace ILs in comparison to 1-ethyl-3-methylimidazolium acetate ([EMIM]Ac). Although both ILs [EMIM]Ace and [BMIM]Ace have melting temperatures above ambient temperature, they presented themselves as supercooled melts most of the time. Due to the nature of the anion, the studied Ace ILs display greater thermal stabilities and increased viscosities compared to the IL acetate. However, the difference in viscosity rapidly decreases at elevated temperatures. Both Ace ILs have lower electrical conductivities—reflecting their more viscous behaviour—and higher densities than [EMIM]Ac.

The most intriguing property of the studied Ace ILs is a combination of both: (i) their inability to dissolve crystalline cellulose, and (ii) their ability to dissolve wood lignin (see 4.4.2 on page 124). No signs of dispersion or dissolution of microcrystalline cellulose (MCC) could be observed after mixing 0.005 mass fraction of dried MCC with any of the studied Ace ILs at 493 K

**Table 7. Selected Physical Properties of 1-Ethyl-3-methylimidazolium Acesulfamate [EMIM]Ace and 1-Butyl-3-methylimidazolium Acesulfamate [EMIM]Ace Compared to 1-Ethyl-3-methylimidazolium Acetate [EMIM]Ac: Melting Temperature $T_{fus}$, Thermal Decomposition Temperature $T_D$, Viscosity $\eta$, Electrical Conductivity $\kappa$, and Density $\rho$.**

| | [BMIM]Ace | [EMIM]Ace | [EMIM]Ac |
|---|---|---|---|
| $T_{fus}$ / K | ≈ 313 | ≈ 317 | > 253 |
| $T_{D,1K}$ / K | 500 | 485 | 446 |
| $\eta_{293\ K}$ / mPa·s$^{-1}$ | 800 | 556 | 124 |
| $\eta_{358\ K}$ / mPa·s$^{-1}$ | 26 | 22 | 10 |
| $\kappa_{293\ K}$ / S·m$^{-1}$ | 0.05 | 0.06 | 0.38 |
| $\rho_{293\ K}$ / kg·m$^{-3}$ | 1240 | 1333 | 1109 |

for 24 h, but 0.1 mass fraction of purchased lignin could be readily dissolved in the IL at 373 K within 2 h. Consequently, Ace IL treatment of wood flour allows to extract and isolate wood lignin from the residual cellulosic material (Figure 39).

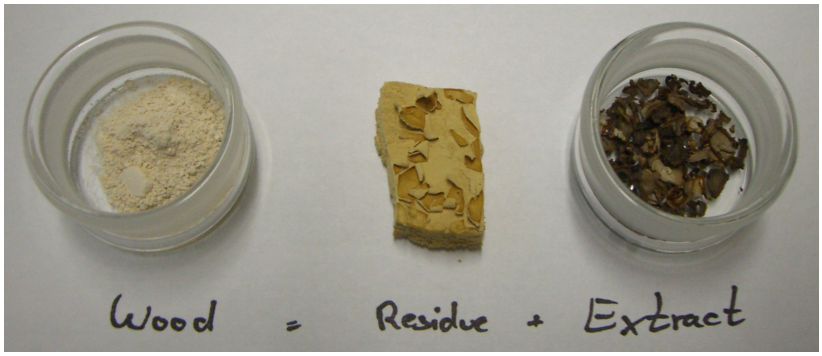


**Figure 39.** Separation of wood components with imidazolium acesulfamate ionic liquids. Treatment of wood flour with [BMIM]Ace yields a cellulosic-rich residue and extracted lignin.

### 4.3.2 Procedure for Extracting Wood Lignin

Figure 61 in Appendix E provides an overview about the IL extraction procedure for wood lignin (see section 4.4.2 on page 125 for experimental details). To give a simplified synopsis: (i) wood flour was added to pre-heated IL and the mixture was stirred at the desired conditions; (ii) the dissolved lignin was separated from the insoluble residues and precipitated upon addition of acetone (Figure 40); and (iii) the white precipitate was separated by filtration and the IL was recycled.

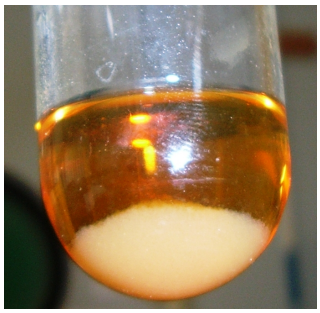

**Figure 40.** Precipitated lignin in an imidazolium acesulfamate ionic liquid. After extraction with [BMIM]Ace, wood lignin can be regenerated upon addition of acetone.

### 4.3.3 Extraction Conditions and their Effect on the Extraction Efficiency

The influence of selected experimental parameters on the lignin extraction efficiency with [BMIM]Ace was evaluated. Parameter variations include: extraction time and temperature, water content, wood load, wood particle size, wood species, type of ionic liquid cation, and IL recyclability. To maximise the extraction efficiency, the effects of both several IL treatment cycles on the same wood sample and the addition of co-solvents was investigated. Unless stated otherwise, all experiments were performed in an open atmosphere and

mass balance calculations indicated that no material was lost during the extraction experiments.

### Extraction temperature and time

Figure 41 shows the influence of both extraction time and extraction temperature on the extraction efficiency ($e = w_e/w_i$), which is defined as the mass fraction ratio of the extracted lignin ($w_e$) and the initial lignin content of the native wood sample ($w_i$). The amount of lignin present in the native wood sample was determined according to standard procedures (see 4.4.1 on page 120). In all these experiments, $w = 0.05$ of *Pinus radiata* wood flour—with a particle size of 100 $\mu$m—was mixed with $w = 0.95$ of [BMIM]Ace in an open atmosphere. The corresponding mass fraction of wood, present in the mixture, is now defined as $w_T$. Investigated extraction temperatures are (353, 373, 393, and 416) K. For all of those temperatures, extraction times of (1, 2, and 4) h have been studied. In the case of 373 K, two additional extraction times of 8 h and 16 h were included.

Lignin extraction efficiencies range from $e = (0.32$ to $0.81)$ across all experiments, showing an obvious trend towards higher extraction efficiencies with both elevated temperatures and longer extraction times. Increasing the extraction time from (1 to 4) h increases the extraction efficiencies from $e = (0.05$ to $0.07)$, if the temperature was kept at or below 393 K. Doubling the extraction time from (2 to 4) h—at a temperature of 416 K–increased the extraction efficiency by $e = 0.25$, representing a significantly larger amount of isolated extract compared to lower extraction temperatures. The increasing mass of the extract was not accompanied with a decreasing mass of the residue, resulting in an incorrect mass balance that indicated a mass gain during the extraction procedure. The same phenomena could be observed in additional experiments, which were performed at a lower extraction temperature (373 K) but with longer extraction times (8 h and 16 h). Analysis of the extract

showed that the mass gain was due to associated IL ions. A detailed discussion will follow later in this work (see 4.3.4 on page 106).

At most extraction temperatures, only a marginal increase in extraction efficiency ($e = 0.01$) could be observed upon doubling the extraction time from (1 to 2) h. This was different for extractions at 373 K, with efficiencies increasing from $e = (0.33$ to $0.38)$ under otherwise identical conditions. Considering the benefits of gentle extraction conditions—not only to avoid potential IL ion incorporation into the extract but also because of energy saving aspects—it was consequently decided to investigate all other parameter variations at $T = 373$ K and $t = 2$ h, providing a reference value of $e = 0.38$ for the extraction efficiency.

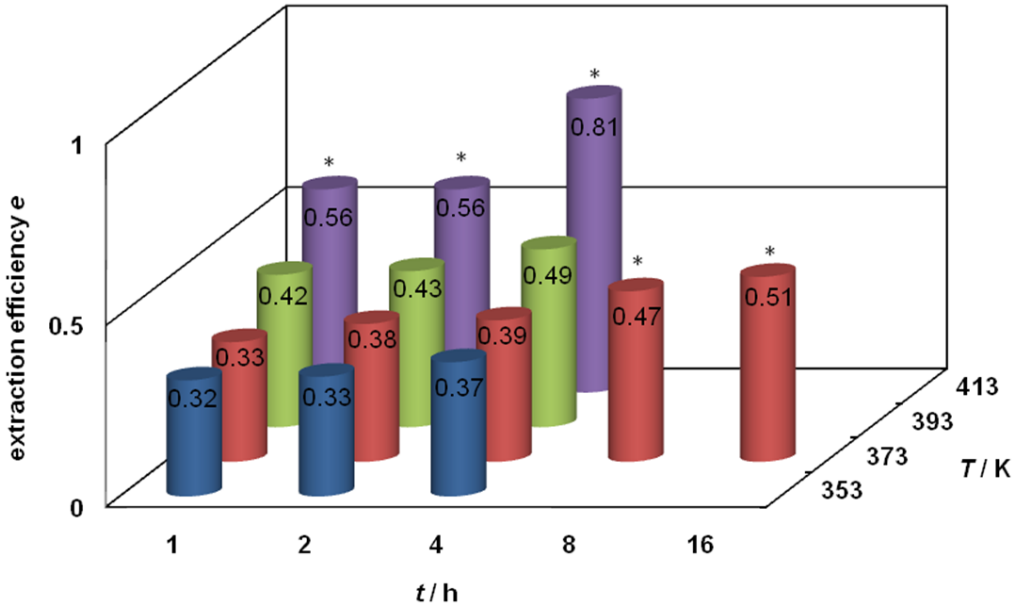


**Figure 41.** Extraction efficiency $e$ for extracting wood lignin at varying extraction temperatures and times. In all experiments, $w_T = 0.05$ of *Pinus radiata* wood flour, with a particle size of 100 $\mu$m, was treated with [BMIM]Ace in an open atmosphere ($*$ indicates an incorrect mass balance for wood components).

### Water content

Figure 42 shows how the IL water content affects the lignin extraction efficiency. Six experiments were conducted, studying "dry" ($w_{H_2O} = 5{\cdot}10^{-4}$), "ambient" ($w_{H_2O} = 5{\cdot}10^{-3}$) and "wet" atmospheres during treatment of $w_T = 0.05$ of *Pinus radiata* wood flour, with a particle size of 100 $\mu$m, in [BMIM]Ace at 373 K for 2 h. The initial water content of the IL was equal in each experiment. "Dry" conditions refer to a dry inert gas atmosphere during the extraction procedure at 373 K, while "ambient" experiments were performed in an open atmosphere, allowing the IL to absorb moisture from the environment at all times. Four extractions were investigated under "wet" conditions, deliberately adding $w = (0.01, 0.05, 0.10, \text{or } 0.15)$ of water to the IL prior to the experiment, which were conducted in an open atmosphere.

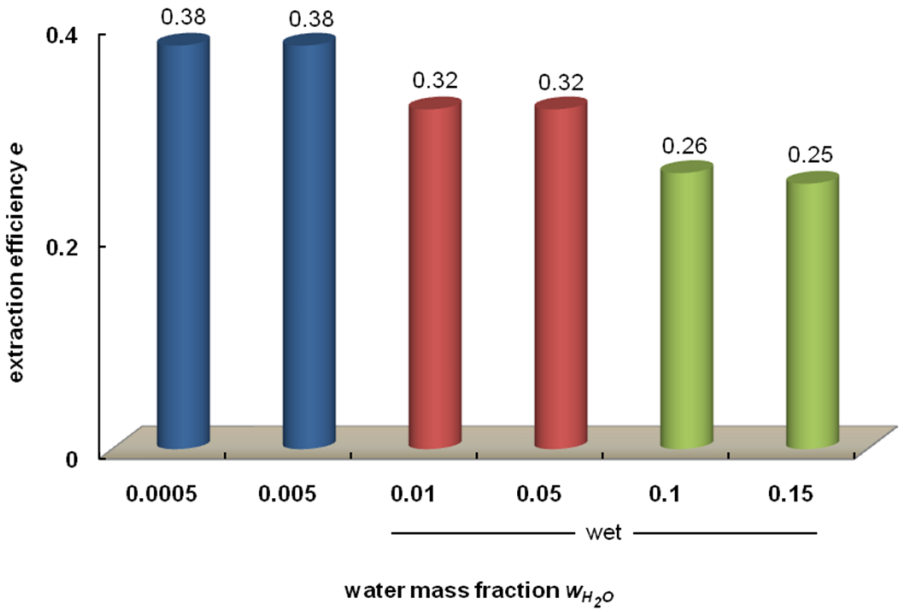


**Figure 42.** Extraction efficiency $e$ for extracting wood lignin with an ionic liquid that contains a varying mass fraction of water $w_{H_2O}$. In all experiments, $w_T = 0.05$ of *Pinus radiata* wood flour, with a particle size of 100 $\mu$m, was treated with [BMIM]Ace at 373 K for 2 h.

No difference in extraction efficiency could be observed under "dry" or "ambient" conditions, but $w_{H_2O} = 0.01$ decreases the extraction efficiency $e$ from (0.38 to 0.32), further decreasing to $e = 0.25$ if the water mass fraction was increased to $w_{H_2O} = 0.15$. However, the decrease in efficiency with increasing water content does not follow an obvious pattern. It is concluded that small amounts of water ($w_{H_2O} < 5{\cdot}10^{-3}$) in the IL does not have a negative impact on the extraction efficiency, and that Ace IL lignin extraction can be performed conveniently in an open atmosphere. The importance of small amounts of water for the extraction of lignin has already been mentioned by others, and will be discussed later (see 4.3.4 on page 107).[250]

### Wood load, wood particle size and wood species

Figure 43 shows the effect of the wood load on the lignin extraction efficiency. A mass fraction $w_T$ = (0.05, 0.10, or 0.20) of *Pinus radiata* wood flour, with a particle size of 100 $\mu$m, has been treated with [BMIM]Ace at 373 K for 2 h in an open atmosphere. No difference in extraction efficiency $e$ was observed between $0.05 < w_T < 0.10$, but $e$ decreased by more than 20 % to $e = 0.29$ as soon as the wood load $w_T$ was doubled from 0.10 to 0.20. Two factors can potentially account for this observation. First, the increased viscosity of the wood+IL mixture at increased wood loads results in a decrease in IL ion mobility. Low ion mobility results in decreased interactions between IL and wood, similar to the effect of the IL viscosity on the dissolution of cellulose. Second, an increased wood load results in more lignin available for extraction. Considering that the total IL dissolution capacity for wood lignin is not known, the lignin extraction efficiency can potentially be limited by the total dissolution capacity of the IL at increased wood loads.

Figure 44 shows how the wood particle size can influence the lignin extraction efficiency. *Pinus radiata* wood flour ($w_T = 0.05$) with a particle diameter of either (100 or 500) $\mu$m was treated with [BMIM]Ace at 373 K for 2 h in

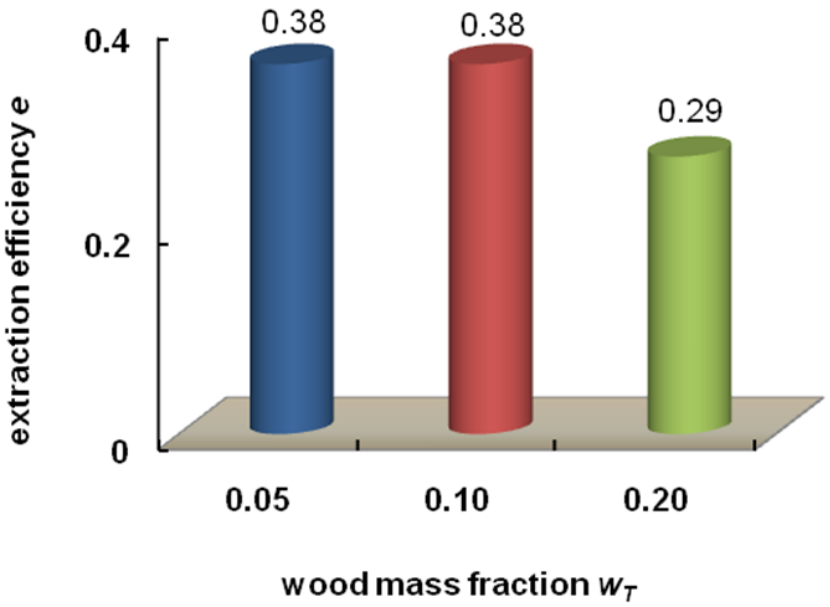


**Figure 43.** Extraction efficiency $e$ for extracting wood lignin with varying wood load $w_{\mathrm{T}}$. In all experiments, *radiata Pinus* wood flour, with a particle size of 100 $\mu$m, was treated with [BMIM]Ace at 373 K for 2 h in an open atmosphere.

an open atmosphere. The results differ considerably. An increase in wood particle diameter from (100 to 500) $\mu$m results in a decrease of extraction efficiency of more than 50 %, dropping from $e = 0.38$ to $e = 0.16$. A possible explanation for this observation is based on the disability of the studied ILs to dissolve crystalline cellulose. Larger wood particle sizes require advanced penetration of the IL into the particles in order to obtain similar extraction efficiencies compared to smaller particles. Because of the tight and interwoven polymeric network of lignocellulosic biomass, the penetration of ILs without the ability to dissolve the cellulosics—or to loosen the cellulosic network—is hindered. Adding appropriate co-solvents can potentially assist the IL in penetrating the cellulosic network to improve extraction efficiencies. This option will be discussed later (see 4.4.2 on page 126).

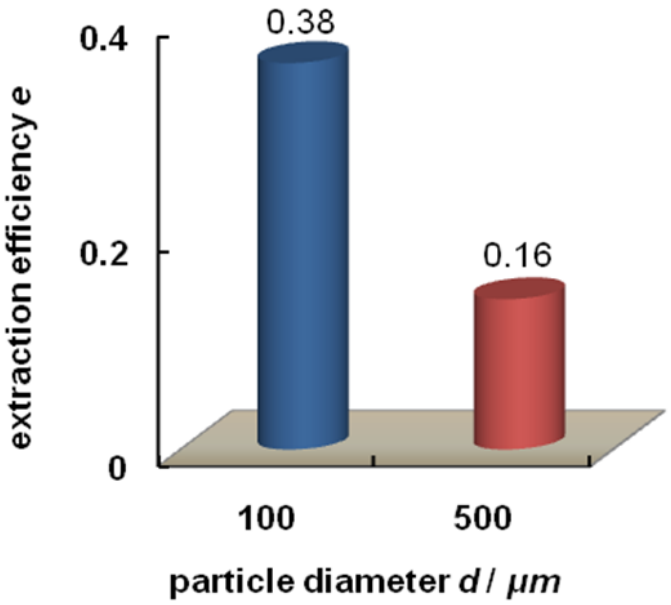


**Figure 44.** Extraction efficiency $e$ for extracting wood lignin with varying wood particle diameter $d$. In all experiments, $w_T = 0.05$ of *Pinus radiata* wood flour was treated with [BMIM]Ace at 373 K for 2 h in an open atmosphere.

The composition of lignocellulosic biomass is dependent on its origin, resulting in a variation of both the amount and the type of lignin present.[233] Figure 45 shows how the wood species affects the ability of the IL to extract lignin. Wood flour ($w_T = 0.05$) of two different wood species, *Pinus radiata* and *Eucalyptus nitens*, with a particle size of 100 $\mu$m was treated with [BMIM]Ace at 373 K for 2 h in an open atmosphere. Radiata pine is classified as softwood while Eucalyptus represents a hardwood species. Both the structure and the total lignin content is different in the two wood samples (see Table 6 on page 81 and 4.4.1 on page 120). The IL was able to extract $e = 0.38$ of lignin from both wood species under the same conditions, indicating that all lignin structures are equally favoured for dissolution in [BMIM]Ace.

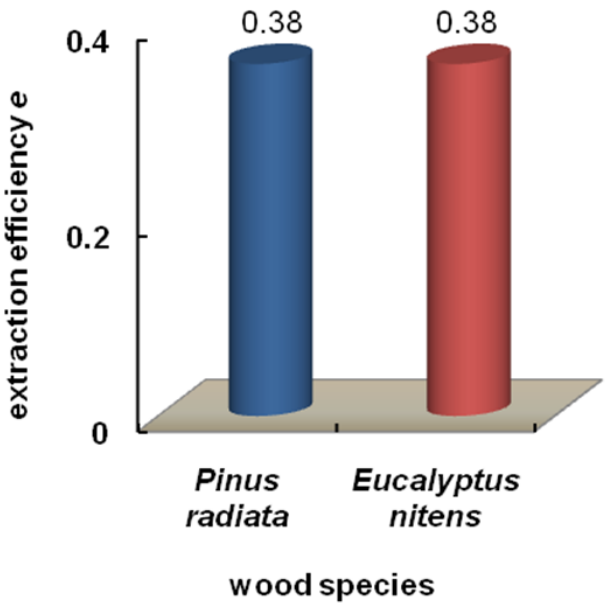


**Figure 45.** Extraction efficiency $e$ for extracting wood lignin from different wood species. Wood flour ($w_T = 0.05$) of both *Pinus radiata* and *Eucalyptus nitens*, with a particle size of 100 $\mu$m, was treated with [BMIM]Ace at 373 K for 2 h in an open atmosphere.

### Type of ionic liquid cation

The physical properties of ILs are governed by the nature of their ions. Of particular interest, with respect to solvents for biomass processing, are the toxicity and the viscosity (see 4.3 on page 84). Shorter alkyl substituents on the imidazolium cation can reduce both the viscosity and the toxicity of the IL (see 4.4.2 onpage 123).[267,268] Consequently, the lignin extraction efficiency of [EMIM]Ace—containing a shorter alkyl substituent at the cation compared to [BMIM]Ace—was examined for the treatment of $w_T = 0.05$ of *Pinus radiata* wood flour, with a particle size of 100 $\mu$m, at 373 K for 2 h in an open atmosphere (Figure 46). The extraction efficiency $e$ for [EMIM]Ace is 0.43. This equals an increase of 13 % in extraction efficiency compared to [BMIM]Ace with $e = 0.38$. One possible reason for the superior extraction

efficiency of [EMIM]Ace is the IL's lower viscosity, compared to [BMIM]Ace, resulting in increased ion mobility which favours the interaction between IL and biomass. Extrapolation of available viscosity data, however, suggests that both ILs differ only by 1 $mPa{\cdot}s^{-1}$ in their viscosity at 373 K. Another possible explanation for the different extraction efficiencies, is the increased amount of halide impurities in [EMIM]Ace with respect to [BMIM]Ace (see 4.4.2 on page 123). Halide ions are known to interact with wood cellulosics, and both the amount and type of halide ions present in the IL can influence its ability to penetrate the lignocellulosic biomass, resulting in enhanced interaction between the IL and the lignin.[152,187]

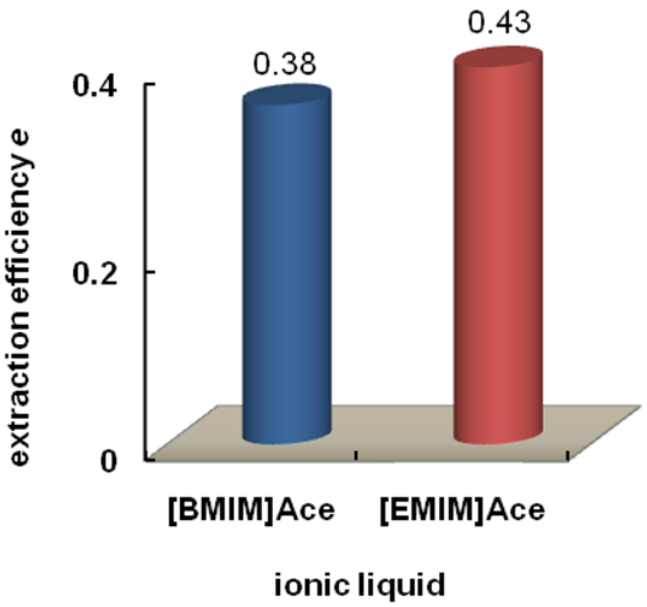


**Figure 46.** Extraction efficiency $e$ for extracting wood lignin with different ionic liquid cations. [BMIM]Ace and [EMIM]Ace have been used to extract lignin from *Pinus radiata* wood flour ($w_T = 0.05$), with a particle size of 100 $\mu$m, at 373 K for 2 h in an open atmosphere.

### Effect of ionic liquid recycling

To achieve environmentally friendly biomass processing, the extracting solvent needs to be completely recyclable without loosing its extraction efficiency. Figure 47 shows the effect of IL recycling on its extraction efficiency for wood lignin. The same sample of [BMIM]Ace was recycled up to six times, after extracting lignin from $w_T = 0.05$ of *Pinus radiata* wood flour, with a particle size of 100 $\mu$m, at 373 K for 2 h in an open atmosphere. No systematic decrease in extraction efficiency could be observed, with an average extraction efficiency of 0.383 and a standard deviation of 0.014. The mass fraction of recovered IL was $> 0.99$. IL losses are attributed to filtration and washing procedures.

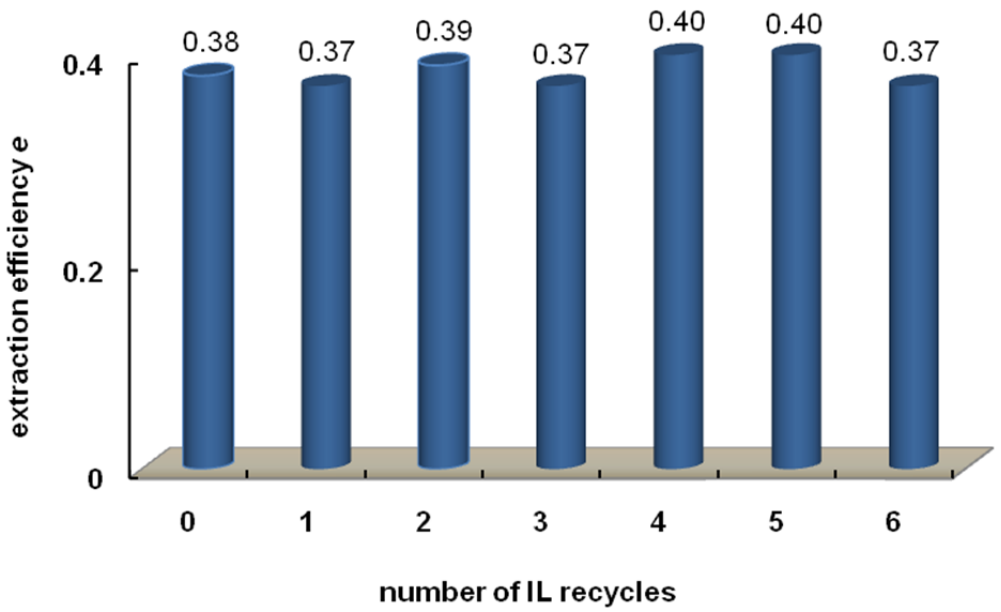


**Figure 47.** Extraction efficiency $e$ for extracting wood lignin with neat and recycled ionic liquid. [BMIM]Ace was used to extract lignin from $w_T = 0.05$ of *Pinus radiata* wood flour, with a particle size of 100 $\mu$m, at 373 K for 2 h in an open atmosphere. The same ionic liquid sample was recycled up to six times.

Figure 48 shows a photograph of neat and recycled [BMIM]Ace. An obvious observation is the colour change of the IL sample from yellow to brown, getting darker after each extraction procedure. To check the IL's purity, $^{1}$H NMR spectra of the IL were obtained after each recycling step (Figure 49). No signs of IL degradation could be detected. The colouration of the IL upon exposure to elevated temperatures, without affecting its $^{1}$H NMR spectra, is well known amongst IL researchers. Studies of Liebner et al. suggest the 1-alkyl-3-methylimidazolium cation to be responsible for traces of thermal degradation products—*viz.* imidazole, *N*-alkylimidazole and imidazole dimers—which are bases with high boiling temperatures.[269] Interaction of those bases with biomass components cannot be ruled out, although their impact will depend on both their amount and the nature of their interactions. Stoichiometric interaction of these impurities with biomass would only have a minor effect, considering the quantities present, but catalytic activity of the impurities can potentially influence biomass products at a larger scale. However, those impurities can be removed by extraction with acid-free chloroform if required.[269]


**Figure 48.** Photograph of [BMIM]Ace samples after each recycling step. The neat ionic liquid (at the left) was recycled up to six times after lignin extractions at 373 K for 2 h. The numbers indicate the number of IL recycles.

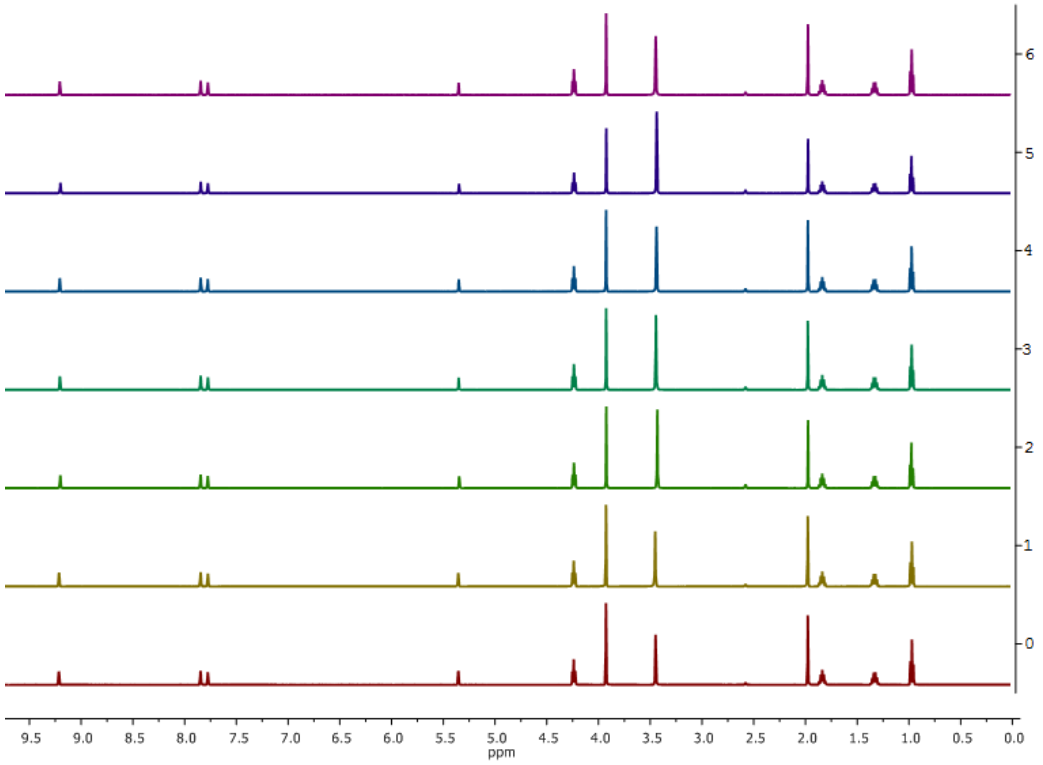


**Figure 49.** $^{1}$H NMR spectra of recycled [BMIM]Ace in DMSO-$d_6$. The ordinate denotes the number of the lignin extraction cycle for this ionic liquid. Each extraction was performed at 373 K for 2 h. The peak at 3.47 ppm is due to residual water.

### Increasing the extraction efficiency: multi-step treatment and use of co-solvents

An important aspect for all industrial processes is the efficiency of the applied method, in this case the extraction of wood lignin. One way to increase the IL extraction efficiency for wood lignin is to increase the extraction temperature and/or the extraction time (see Figure 41 on page 89). Gentle extraction procedures, however, are favoured due to potential lignin side-reactions and in order to save energy.

Another option to increase the extraction efficiency is to re-apply the same extraction process a number of times to the same wood sample. Figure 50 shows the effect of up to three IL extraction cycles on the total extraction efficiency, with regard to the same wood sample. For each experiment, a fresh sample of [BMIM]Ace was used to extract lignin from *Pinus radiata* wood flour ($w_T = 0.05$), with a particle size of 100 $\mu$m, at 373 K for 2 h in an open atmosphere. The particular extraction efficiency of each subsequent treatment step was decreasing from $e = 0.38$ in the first extraction cycle, to $e = 0.13$ in the second cycle, to $e = 0.09$ in the third extraction step. This equals a total extraction efficiency of $e = 0.6$ after three subsequent IL treatments, with a total treatment time of 6 h at 373 K. After two extraction cycles, equalling a treatment time of 4 h, $e = 0.51$ of lignin was extracted. This is an increase in extraction efficiency of $\approx 30$ %, compared to one extraction step at 373 K for 4 h under otherwise equal conditions (see Figure 41 on page 89). These results suggest that the ability of this IL to extract lignin decreases with increasing mass fraction of dissolved lignin. The IL's ability to dissolve lignin potentially depends on its total dissolution capacity and its current lignin content.

An additional way to increase the lignin extraction efficiency of the studied ILs is to enhance their penetration into the lignocellulosic framework of the wood particles. As mentioned earlier, the presence of halide ions impurities in the IL is potentially helpful for the extraction of lignin, due to their tendency to penetrate and swell the cellulosic framework (see 4.3.3 on page 95). Similarly, the presence of small amounts of a co-solvent with the ability to swell cellulose without dissolving it, such as DMSO,[203] can prove beneficial for the overall extraction efficiency. Figure 51 compares the lignin extraction efficiency of pure [BMIM]Ace against a mixture of $w = 0.9$ of [BMIM]Ace and $w = 0.1$ of DMSO. *Pinus radiata* wood flour ($w_T = 0.05$), with a particle size of 100 $\mu$m, was treated at 373 K for 2 h in an open atmosphere. The results show that the addition of DMSO is indeed beneficial for the extraction of wood lignin,

increasing the extraction efficiency from $e$ = (0.38 to 0.56) by almost 50 %, while still maintaining a gentle extraction temperature (373 K) and a short extraction time (2 h). This significantly improved extraction yield, in the presence of DMSO, is potentially due to two factors: (i) loosening the tight H–bond network of wood cellulosics, and (ii) decreasing the overall viscosity of the mixture. The combination of the two effects is believed to enhance both the penetration and the interaction of wood with the IL.

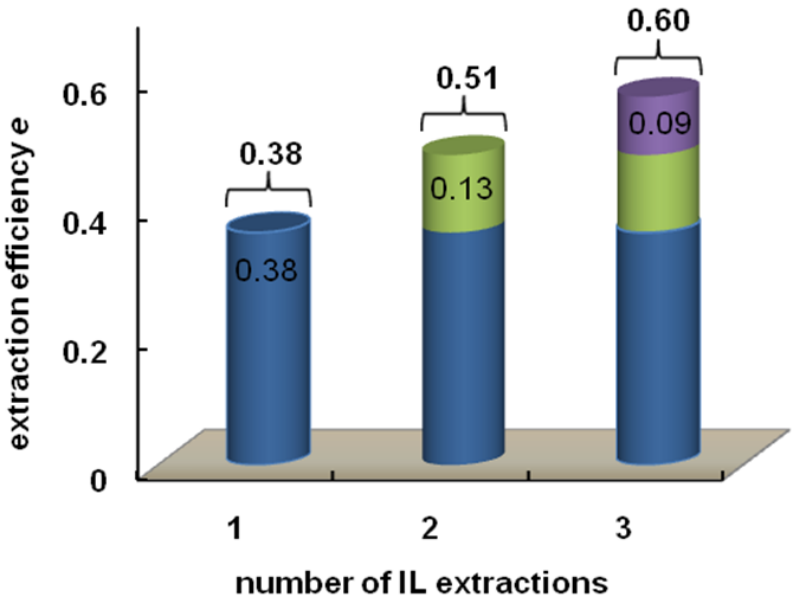


**Figure 50.** Total extraction efficiency $e$ after multi-step extraction of lignin from the same wood sample for three times with neat IL. Fresh samples of [BMIM]Ace were used to extract lignin from *Pinus radiata* wood flour ($w_T$ = 0.05), with a particle size of 100 $\mu$m, at 373 K for 2 h in an open atmosphere.

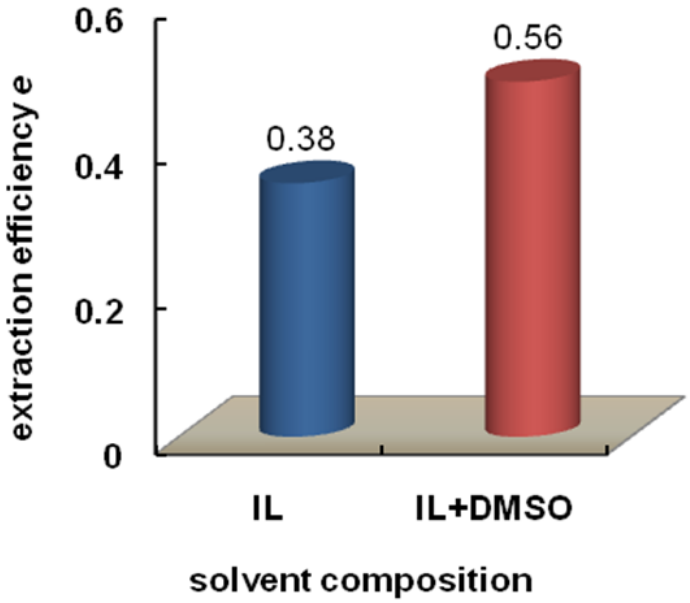


**Figure 51.** Extraction efficiency $e$ for extracting wood lignin with either pure IL or a mixture of ($w_{\mathrm{IL}} = 0.9$) IL and ($w_{\mathrm{DMSO}} = 0.1$) DMSO. [BMIM]Ace was used as IL, and *Pinus radiata* wood flour ($w_{\mathrm{T}} = 0.05$), with a particle size of 100 $\mu$m, was treated at 373 K for 2 h in an open atmosphere.

### 4.3.4 Characterising the Extracted Lignins and the Cellulosic-rich Residues

All lignins that are isolated from native biomass are believed to undergo some sort of chemical modification, either because of the cleavage of intramolecular ether bonds—those between monolignols—or through cleaving lignin–carbohydrate complexes (LCC). Each extraction method will affect the separated biomass components in a slightly different way. The following section characterises both the extracted wood lignins and the cellulosic-rich residues obtained from [BMIM]Ace treatment of $w_{\mathrm{T}} = 0.05$ of *Pinus radiata* wood flour, with a particle size of 100 $\mu$m, for 2 h in an open atmosphere at temperatures of (353, 373, 393, and 413) K. The results from extraction

experiments with *Eucalyptus nitens* at 373 K will be included in the discussion. The separated wood fractions were characterised *via* fourier transform infrared (FT-IR) spectroscopy, nuclear magnetic resonance (NMR) spectroscopy, elemental analysis (EA), thermogravimetric analysis (TGA), differential scanning calorimetry (DSC), X-ray diffraction (XRD) crystallography, and gel permeation chromatography (GPC).

### Identification and chemical composition

Figure 52 shows samples of both the cellulosic-rich residues and the extracted lignins obtained by treating $w_T = 0.05$ of *Pinus radiata* wood flour, with a particle size of 100 $\mu$m, with [BMIM]Ace for 2 h in an open atmosphere at (353, 373, 393, and 413) K. The colour intensity of the residues increases with increasing extraction temperature, from beige at 353 K to brown at 416 K. Their morphology changes as well, from powdery at 353 K to brittle at 416 K.

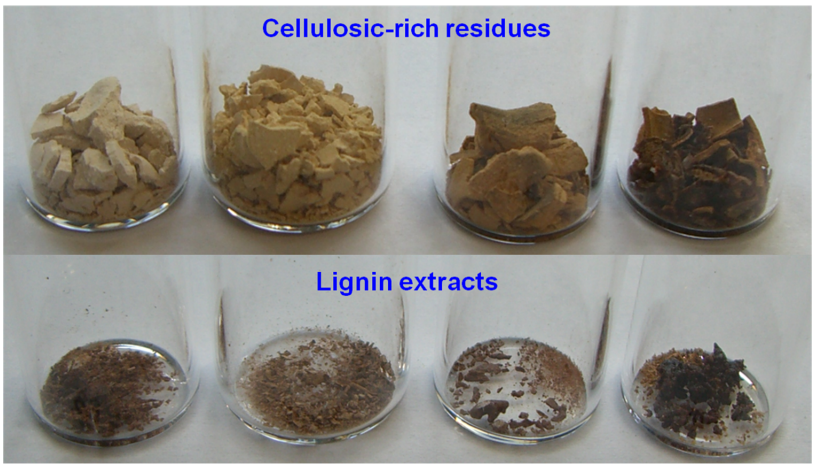


**Figure 52.** Photograph of cellulosic-rich residues and lignin extracts obtained at after treating *Pinus radiata* wood flour with [BMIM]Ace at different extraction temperatures (from left to right): 353 K, 373 K, 393 K, and 413 K.

All the extracted lignin samples, from (353 to 393) K, are very similar both in their brown colour and in their morphology. The exception is the extract

obtained at the highest extraction temperature of 413 K, showing both a darker colour and a more gluey, resin-like morphology.

**Infrared spectroscopy** To identify the isolated extracts as lignin, the IR spectra of the extracts obtained at 373 K from *Pinus radiata* and *Eucalyptus nitens* were compared with SA lignin (Figure 53). Analysis of the spectra confirms both extracts as lignin, agreeing with other published data,[250] but the results also suggest that there are structural differences between all three lignin samples, which is attributed to both the different lignin sources and the different extraction methods.[222] All three spectra show a broad absorption band at (3500 to 3200) $cm^{-1}$ due to aliphatic and phenolic OH–groups. Other peaks are assigned to alkene C–H stretching (3100 to 3000) $cm^{-1}$, alkane C–H stretching (3000 to 2850) $cm^{-1}$, C=O stretching (1760 to 1655) $cm^{-1}$, C=C stretching (1680 to 1640, and 1510) $cm^{-1}$, C–O stretching (1300 to 1000) $cm^{-1}$, and C–C stretching (1260 to 1210) $cm^{-1}$. A more detailed assignment of IR spectral bands for lignin and biomass can be found in the literature.[270] The presence of both C=C and C=O stretching bands in the extracts can only arise from aromatic lignin fractions, but the potential presence of hemicellulosic material—incorporated due to reactive hemicellulose breakdown products—cannot be excluded at this stage.[250] Further studies are required to explore this possibility.

Comparing the range of *Pinus radiata* lignins, extracted at different temperatures, shows that the intensity of the peak at 1130 $cm^{-1}$ varies and that a sharp peak at 620 $cm^{-1}$ is shared by all spectra (Figure 54). Both peaks indicate the presence of sulfur, which was potentially incorporated in the form of the $[Ace]^-$ anion. The band at 1130 $cm^{-1}$ can be assigned to symmetric $SO_2$ stretching and the band at 620 $cm^{-1}$ to C–S stretching.[250] The different appearance of the band at different extraction temperatures can be explained by a varying nature of the $SO_2$–group in the macromolecule, possibly arising from different bonding partners or chemical environments.

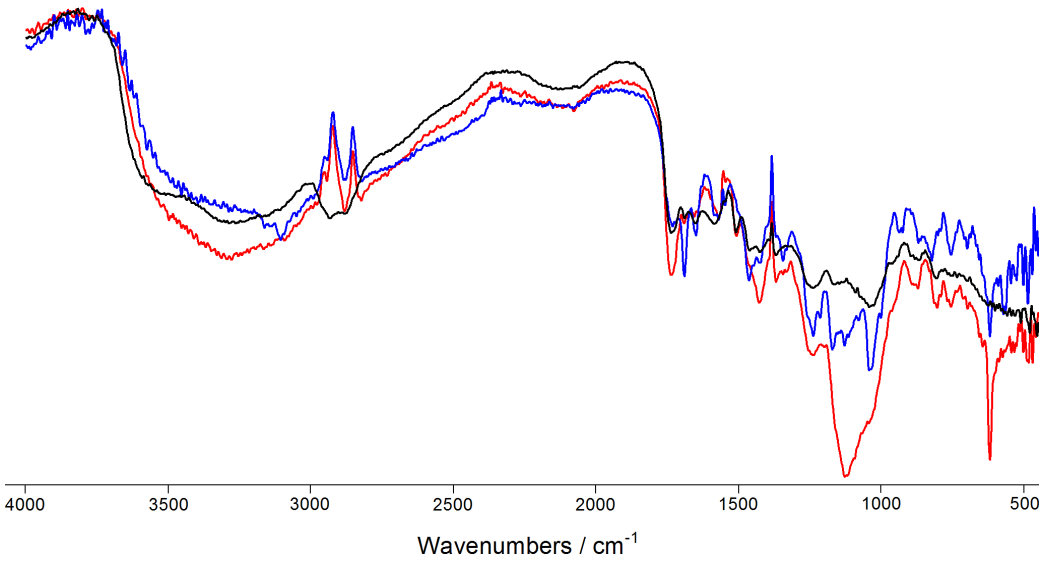


**Figure 53.** Infrared spectra of lignin extracts obtained at 373 K from *Pinus radiata* (red) and from *Eucalyptus nitens* (blue) in comparison to purchased Sigma Aldrich lignin (black).

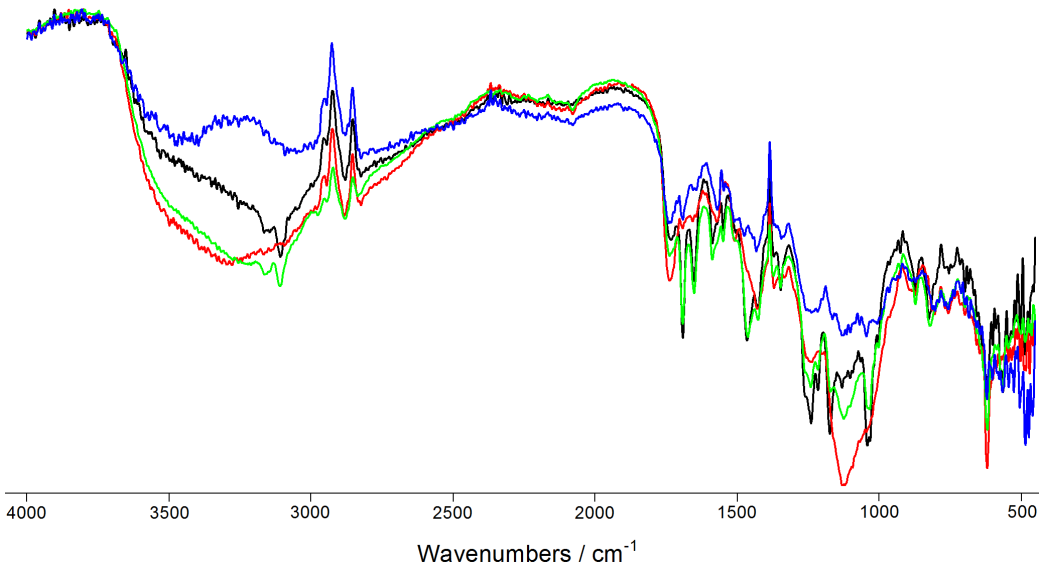


**Figure 54.** Infrared spectra of lignin extracts obtained from *Pinus radiata* at different extraction temperatures: black = 353 K, red = 373 K, green = 393 K, and blue = 413 K.

Another observation is the decreased intensity of the broad absorption band at (3500 to 3200) $cm^{-1}$, which is only present in the extract obtained at 413 K. This suggest a decreasing number of OH–groups, which—considering the distinguished optical appearance and resin-like character of this extract—may be explained by the formation of oxygen radicals and subsequent coupling reactions at elevated extraction temperatures.

Figure 55 compares both native *Pinus radiata* wood and its extract—obtained at 373 K—with microcrystalline cellulose (MCC). The separated cellulose-rich residues still show bands in the region from (1740 to 1590) $cm^{-1}$, characteristic for the presence of C=O and C=C bonds and indicating the presence of residual lignin. Those bands are absent in crystalline cellulose, with the remainder of the spectral bands being very similar to those of the cellulosic-rich residues. Equivalent IR spectra, comparing *Eucalyptus nitens* samples with MCC, show the same characteristics (see Appendix F).

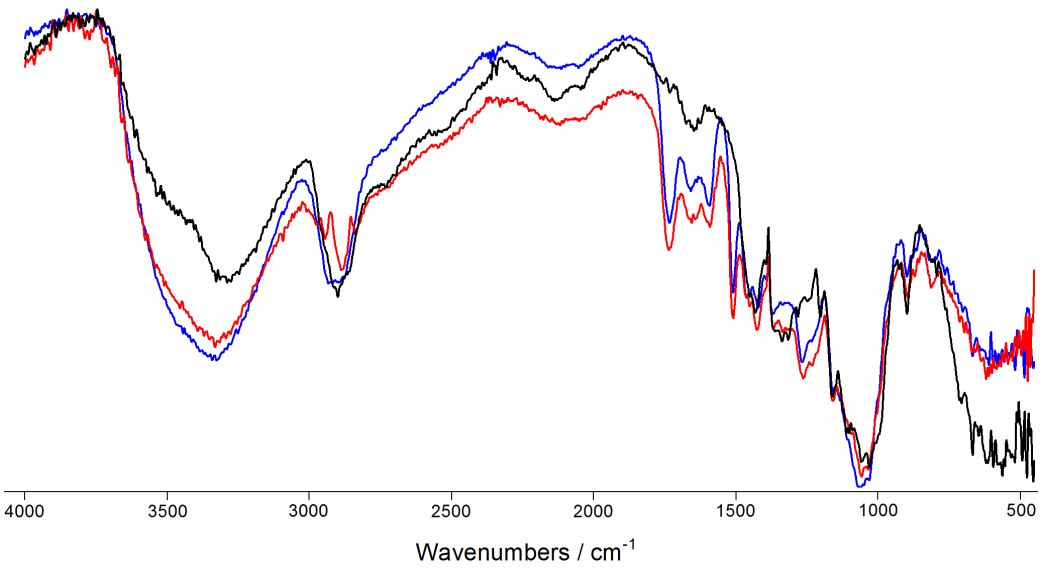


**Figure 55.** Infrared spectra of cellulosic-rich residue obtained at 373 K from *Pinus radiata* (red), native *Pinus radiata* wood (blue) and microcrystalline cellulose (black).

Figure 56 compares all four cellulosic-rich residues obtained from *Pinus radiata* at the different temperatures. Increasing treatment temperatures result in a reduced intensity for a number of bands that are associated with aromatic and ether-containing structures: phenolic OH–groups (3500 to 3200, and 2890) $cm^{-1}$, aromatic C=C and =C–H stretching (1510) $cm^{-1}$, C–H deformation of $–O–CH_3$, aryl–O–alkyl stretching (1260) $cm^{-1}$, and C–O stretching of cyclic diaryl ethers (1060) $cm^{-1}$. All those peaks are also present in the lignin extracts (see Figure 54 on page 104), indicating an increasing degree of wood delignification with increasing extraction temperatures.

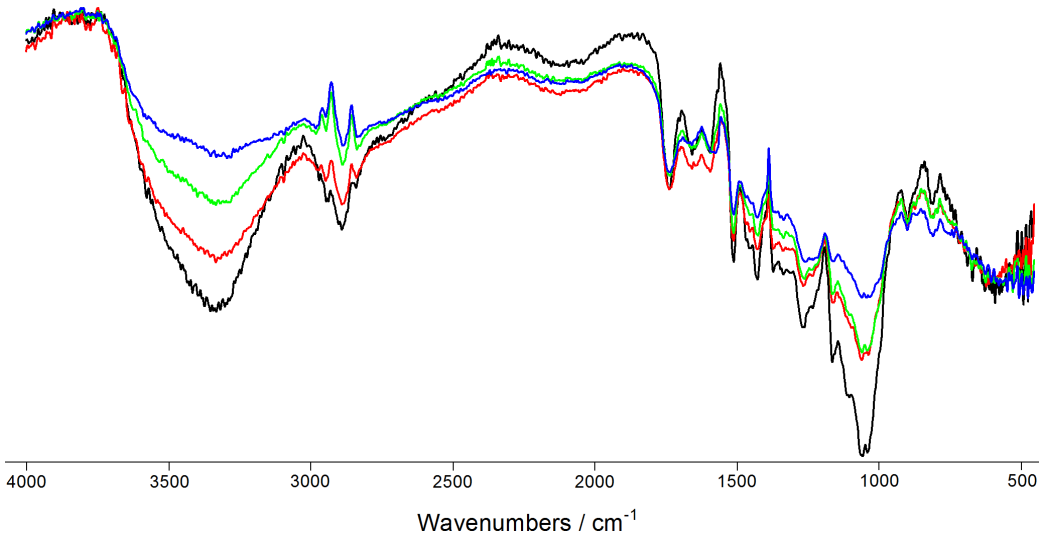


**Figure 56.** Infrared spectra of cellulosic-rich residues obtained from *Pinus radiata* at different extraction temperatures: black = 353 K, red = 373 K, green = 393 K, and blue = 413 K.

**Elemental analysis** Information about the purity and the chemical composition of the separated wood fractions can be derived from elemental analysis (EA). Based on EA results, Table 8 suggests the empirical formula and the molecular mass for the monomeric units of both the extracted lignins and the cellulosic-rich residues, obtained from [BMIM]Ace treatment of $w_T = 0.05$ of

either *Pinus radiata* or *Eucalyptus nitens* for 2 h in an open atmosphere at selected temperatures.

All analysed lignin extracts contain significant amounts of sulfur, suggesting that the [Ace]$^-$ anion got incorporated into the extract. The [Ace]$^-$ anion contains one sulfur and one nitrogen atom, while the imidazolium cation contains no sulfur and two nitrogen atoms. Assuming that wood does not contain significant amounts of nitrogen, one would expect a sulfur to nitrogen ratio of either 1:1, if only the anion is included, or 1:3 if both IL ions are present in the extract. Closest match to this expectation are the radiata extract at 416 K, being close to a 1:3 ratio, and the Eucalyptus extract at 373 K, roughly displaying a 1:1 ratio. All other lignins show a sulfur to nitrogen ration of approximately 1:2. Considering the inconsistency of these ratios across all lignins, these EA results do not allow to conclude on the presence of the IL cation in the extract. One can only speculate about the reasons for the observed ratios between sulfur and nitrogen, and one potential explanation is that the [Ace]$^-$ anion undergoes decomposition prior to—or even after—reacting with the lignin.

Cox et al. studied the degradation of lignin model compounds in acidic ILs, suggesting a pathway for the degradation which involves the IL anion, but only in a catalytic manner.[246] Figure 57 proposes another possible cleavage mechanism for the $\beta$–O–4 ether bond between two guaiacyl units (see 36 on page 80), allowing the incorporation of the IL anion into the degradation product. The required proton can potentially be sourced from residual water, and the resulting hydroxyl anion can cleave additional ether bonds, analogous to the mechanism proposed for the IL anion. With an phenolic hydroxyl at the 4-position of the aromatic ring, and assuming an hydroxyl (or alkoxy) group at the $\alpha$-position, it would also be possible to introduce the IL anion at the labile $\alpha$-position upon formation of the quinone methide intermediate.

Softwoods usually contain more lignin than hardwoods (Table 9), and more than 95 % of softwood lignin is composed of coniferyl monolignols (see

**Table 8. Suggested Empirical Formula and Molar Mass $M_w$ of the Monomeric Units of the Extracted Lignins and the Cellulosic-rich Residues Obtained from [BMIM]Ace Treatment of $w_T = 0.05$ of either *Pinus Radiata* or *Eucalyptus Nitens* for 2 h in an Open Atmosphere at Selected Temperatures $T$.**

| Wood fraction | Wood species | $T$ / K | Empirical formula | $M_w$ / g·mol$^{-1}$ |
|---|---|---|---|---|
| lignin extract | *Pinus radiata* | 353 | $C_{10.0}H_{18.6}O_{9.3}N_{1.1}S_{0.6}$ | 322.6 |
| lignin extract | *Pinus radiata* | 373 | $C_{10.0}H_{17.8}O_{9.1}N_{1.2}S_{0.6}$ | 317.5 |
| lignin extract | *Pinus radiata* | 393 | $C_{10.0}H_{17.4}O_{8.0}N_{1.3}S_{0.6}$ | 301.0 |
| lignin extract | *Pinus radiata* | 413 | $C_{10.0}H_{17.8}O_{6.3}N_{1.8}S_{0.7}$ | 285.4 |
| lignin extract | *Eucalyptus nitens* | 373 | $C_{10.0}H_{17.7}O_{23.5}N_{1.5}S_{1.7}$ | 591.4 |
| cellulosic-rich residue | *Pinus radiata* | 353 | $C_{6.0}H_{9.3}O_{4.4}$ | 152.1 |
| cellulosic-rich residue | *Pinus radiata* | 373 | $C_{6.0}H_{9.8}O_{4.2}N_{0.1}$ | 151.5 |
| cellulosic-rich residue | *Pinus radiata* | 393 | $C_{6.0}H_{9.4}O_{4.2}N_{0.1}$ | 151.2 |
| cellulosic-rich residue | *Pinus radiata* | 413 | $C_{6.0}H_{9.5}O_{4.1}N_{0.2}S_{0.1}$ | 152.7 |
| cellulosic-rich residue | *Eucalyptus nitens* | 373 | $C_{6.0}H_{9.2}O_{4.3}N_{0.1}$ | 152.2 |

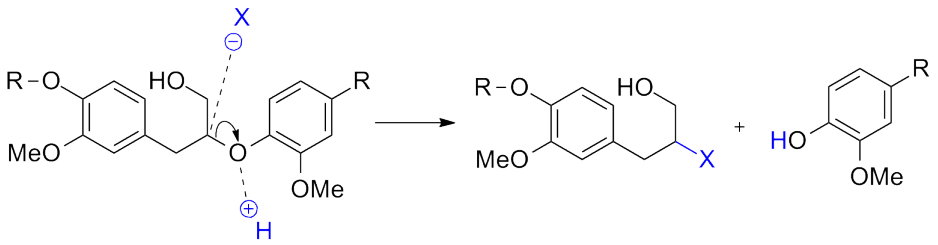


**Figure 57.** Suggested ether scissoring and integration of the ionic liquid anion $X^-$ during the extraction of wood lignin. A proton source, such as water, is required for the suggested reaction.

Figure 36 on page 80). Coniferyl alcohol has a molecular mass of 180.2 g·mol$^{-1}$ and a empirical formula of $C_{10}H_{12}O_3$. The monomeric units of all lignins that were isolated from the softwood *Pinus radiata* have much greater contents of both hydrogen and oxygen than coniferyl alcohol, and their molecular mass decreases with increasing extraction temperature. Possible reasons for

this discrepancy are (i) partial lignin oxidation during IL extraction, (ii) residual water content in the extract, (iii) chemical addition of water (in the form of protons and OH–groups) to the lignin during IL extraction at elevated temperatures, (iv) potential presence of hemicellulose fractions in the extracts, and (v) incorporation of the IL anion or its degradation products. Whatever the reason, the extraction temperature seems to influence the chemical composition of the extracted lignins. Eucalyptus-derived lignin is possibly prone to oxidation, because it shows a significantly increased oxygen content compared to the other extracts.

**Table 9. Typical Composition of Softwood and Hardwood.**

| | Softwood | Hardwood |
|---|---|---|
| | 100 *w* | 100 *w* |
| Cellulose | 40–44 | 42–46 |
| Hemicellulose | 25–29 | 23–33 |
| Lignin | 25–31 | 20–28 |
| Extractives | 1–5 | 1–7 |

The chemical composition of the cellulosic-rich residues is difficult to interpret, due to both the varying amount of residual wood lignin and the presence of hemicelluloses. The residue obtained at 416 K contains traces of sulfur, probably due to the formation of reactive IL anion species at elevated temperatures. All other residues do not have an increased sulfur content. The ratio of the amount of sulfur compared to nitrogen is also 1:2, making it difficult to comment on the presence of the IL cation in the residue.

In general, the chemical composition of the residues is much more consistent than those of the lignins, with an average molecular mass of 152 g·mol$^{-1}$. Cellulose consists solely of anhydrous glucose units with the empirical formula $C_6H_{10}O_5$, and a molecular mass of 162.16 g·mol$^{-1}$. Hemicellulose is composed of a number of hexose and pentose sugars, and both the amount and nature

of hemicellulose present in wood depends on its origin. For simplification, let's assume that hemicellulose consists only of anhydrous and nonsubstituted xylose with the empirical formula $C_5H_8O_4$ and a molecular mass of 132.13 g·mol$^{-1}$. The average molecular mass of the cellulosic-rich residues is in-between the values from cellulose and hemicellulose, with a tendency towards the molecular mass of anhydrous cellulose. This is in good agreement with the typical composition of wood, shown in Table 9, containing more cellulose than hemicellulose.[94]

### Thermal stability and phase transitions

To further study the separated wood fractions, their thermal stabilities and heat capacity characteristics were evaluated *via* thermogravimetric analysis (TGA) and differential scanning calorimetry (DSC). Table 10 shows the onset decomposition temperatures—at a fractional mass loss of 0.1—and the phase transition temperatures, both obtained at a heating rate of 1 K·min$^{-1}$, of both the extracted lignins and the cellulosic-rich residues from [BMIM]Ace treatment of $w_T = 0.05$ of either *Pinus radiata* or *Eucalyptus nitens* for 2 h in an open atmosphere at selected temperatures. Data from the native wood samples, SA lignin and MCC are included for comparison.

Two phase transitions were observed for each of the native wood samples, and none for the crystalline cellulose. All other samples showed one phase transition prior to decomposing at higher temperatures. Both native wood samples—*Pinus radiata* and *Eucalyptus nitens*—start degrading at around 562 K, but both phase transitions of the eucalyptus sample (371 K, 407 K) occur at slightly higher temperatures compared to radiata pine (368 K, 396 K). The extracted eucalyptus lignin starts decomposing at slightly higher temperatures (521 K) compared to the corresponding radiata sample ( 495 K), but the phase transition temperatures of both samples are similar (377 K and 379 K). The cellulosic-rich residue of *Eucalyptus nitens* (561 K) is less

thermally stable compared to *Pinus radiata* (570 K), but the phase transition temperature of the eucalyptus residue (414 K) is still higher compared to the softwood (396 K).

**Table 10. Onset Decomposition Temperatures $T_{D,1K}$ and Phase Transition Temperatures $T_{PT,1K}$ of Extracted Lignins and Cellulosic-rich Residues obtained after [BMIM]Ace Treatment of $w_T = 0.05$ of either *Pinus Radiata* or *Eucalyptus Nitens* for 2 h in an Open Atmosphere at Selected Temperatures $T$. Native Wood Samples, Sigma Aldrich Lignin, and Microcrystalline Cellulose are Included for Comparison.**

| Sample | Origin | $T$ | $T_{D,1K}$ | $T_{PT,1K}$ |
|---|---|---|---|---|
| | | K | K | K |
| lignin | Sigma Aldrich | | 544 | 383 |
| lignin extract | *Pinus radiata* | 353 | 515 | 368 |
| lignin extract | *Pinus radiata* | 373 | 495 | 379 |
| lignin extract | *Pinus radiata* | 393 | 518 | 363 |
| lignin extract | *Pinus radiata* | 413 | 522 | 385 |
| crystalline cellulose | Merck | | 598 | |
| native wood | *Pinus radiata* | | 563 | 368, 396 |
| cellulosic-rich residue | *Pinus radiata* | 353 | 585 | 384 |
| cellulosic-rich residue | *Pinus radiata* | 373 | 570 | 396 |
| cellulosic-rich residue | *Pinus radiata* | 393 | 540 | 404 |
| cellulosic-rich residue | *Pinus radiata* | 413 | 500 | 382 |
| native wood | *Eucalyptus nitens* | | 562 | 371, 407 |
| lignin extract | *Eucalyptus nitens* | 373 | 521 | 377 |
| cellulosic-rich residue | *Eucalyptus nitens* | 373 | 561 | 414 |

All extracted lignins show a lower degradation temperature than Sigma Aldrich lignin, but their thermal stability tends to increase with their extraction temperatures. Their phase transition temperatures appear to be random. The observed differences in their thermal stabilities can be inversely correlated to their extraction temperatures. This can be explained by assuming that (i) the partial degradation of native wood lignin already takes place during

IL treatment, and (ii) the degree of degradation increases with increasing extraction temperatures, suggesting that a more native-like lignin extract can be obtained at gentle extraction temperatures.

Different to the extracts, the thermal stability of the cellulosic-rich residues decreases with increasing extraction temperatures. The two residues resulting from treatment at (353 and 373) K display even higher decomposition temperatures (585 K and 570 K) than the native wood species (563 K). This observation can be explained by considering the good thermal stability of crystalline cellulose (598 K). Gentle removal of lignin at reduced temperatures increases the overall degree of crystalline components in the residues, resulting in an increased thermal stability. At elevated extraction temperatures ($>$ 393 K), the thermal degradation of cellulosic material start to dominate, resulting in a decrease of the overall thermal stability of the residues.

The phase transition temperatures of the residues follow a similar pattern. They tend to increase with increasing extraction temperature, reflecting an associated increase in the amount of lignin removed. The outlier value observed at an extraction temperature of 413 K can be attributed to the degradation of cellulosics.

### Crystallinity of the cellulosic-rich residue

X-ray diffraction (XRD) measurements can provide information about the crystalline structure of the cellulosic components in biomass. This information is especially important to estimate the relative amount of crystalline material present in the sample, which allows eventually to speculate on its mechanical characteristics. A number of different methods exist to calculate the crystallinity index (CrI) from XRD data, and the results can vary depending on the applied method.[271,272] In this study, the degree of crystallinity was calculated according to the peak height method,[273] which is the most popular and useful method to compare relative differences in the CrI of cellulose.[272]

Figure 58 shows the XRD pattern of native *Pinus radiata* wood flour, with a particle size of 100 $\mu$m, compared to its cellulosic-rich residues after treatment with [BMIM]Ace for 2 h in an open atmosphere. Both the lowest (353 K) and the highest (413 K) extraction temperature was investigated. Both XRD patterns show the presence of cellulose I, which is the native form of cellulose, and no signs of cellulose II were found (see 3.1.1 on page 19).[274] The main peak at $\approx$ 22 ° is indicative of the distance between the H–bonded sheets in cellulose I, and its position depends on both the crystallite size and the moisture content.[275–277] The second peak at $\approx$ 16 ° is a composite peak, resulting from the two cellulose allomorphs $I_\alpha$ and $I_\beta$.[275] The XRD pattern of the cellulosic-rich residue, obtained at gentle extraction conditions (353 K), does not show significant differences compared to the native wood sample. This contrasts the XRD pattern of the residue that was obtained at 413 K. In this case, the main peak broadens and slightly shifts to lower $2\Theta$, while the second peak starts to disappear. These results are indicative for changes in the CrI of the cellulosic material.

Table 11 summarises the calculated CrI of native wood and selected cellulosic-rich residues obtained from treatment with either neat [BMIM]Ace or with a mixture of $w_{\mathrm{IL}} = 0.9$ of [BMIM]Ace and $w_{\mathrm{DMSO}} = 0.1$ of DMSO (see 51 on page 101). Native *Pinus radiata* wood is calculated to have a CrI of 60, agreeing with literature data.[275] The CrI does not change if the wood is treated with neat [BMIM]Ace for 2 h at a gentle temperature of 353 K. More elevated extraction temperatures ($>$ 413 K) result in a decrease of the crystallinity of the cellulosic residue. Interesting are the results obtained from wood treatment with a mixture of IL and DMSO at a moderate temperature of 373 K, showing a slight increase in the calculated CrI. Further studies are required to investigate this phenomena, but the observed increase in the CrI value can potentially be attributed to the combined uncertainty of the XRD measurement and the CrI evaluation method.

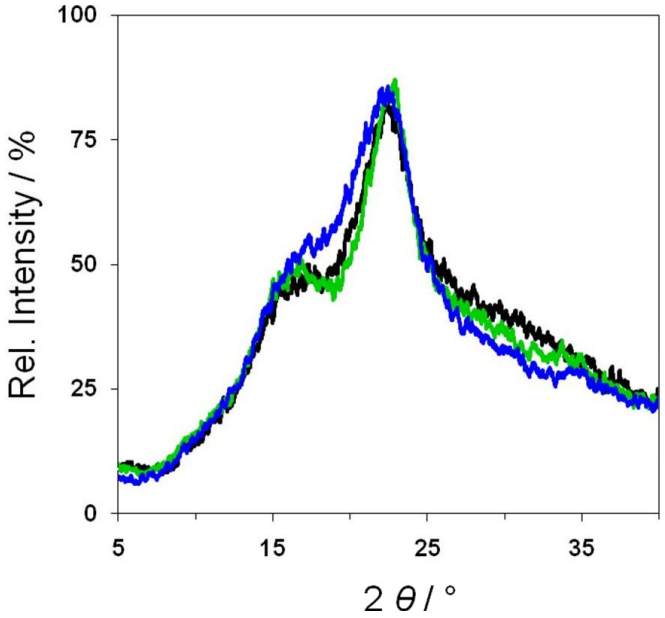


**Figure 58.** X-ray diffraction pattern of native radiata pine (black) and the cellulosic-rich residues obtained from [BMIM]Ace treatment at either 353 K (green) or 413 K (blue). *Pinus radiata* wood flour ($w_T = 0.05$), with a particle size of 100 $\mu$m, was treated for 2 h in an open atmosphere.

Figure 59 compares the XRD pattern of untreated wood with the cellulosic-rich residue that was obtained after treatment at 373 K for 2 h with the IL+DMSO mixture. Similar to the residue that was obtained from wood treatment with neat IL at 353 K, the XRD pattern of the residue obtained from the solvent mixture agrees with the pattern of native wood (a). One difference, however, is the appearance of a small peak at $\approx$ 34.5 ° in the residue pattern (b). This peak is indicative of the length of the cellobiose unit and arises due to its ordering along the fibre direction.[275] Based on this observation, one can further speculate on the increased CrI that was observed in the residue obtained from the solvent mixture. The combination of a solvent that only swells cellulose (DMSO) with another solvent that dissolves lignin (Ace IL) can potentially enhance an increased ordering of

**Table 11. Calculated Crystallinity Index CrI of Native Wood and Cellulosic-rich Residues Obtained from Treatment of $w_T = 0.05$ of *Pinus Radiata* Wood Flour, With a Particle Size of 100 $\mu$m, for 2 h in an Open Atmosphere at Selected Temperatures $T$. Extraction Solvents Were Either Neat [BMIM]Ace or a Mixture of ($w_{IL} = 0.9$) [BMIM]Ace and ($w_{DMSO} = 0.1$) DMSO.**

| Sample | Solvent | $T$ | CrI |
|---|---|---|---|
| | | K | % |
| native wood | [BMIM]Ace | | 60 |
| cellulosic-rich residue | [BMIM]Ace | 353 | 60 |
| cellulosic-rich residue | [BMIM]Ace | 413 | 57 |
| cellulosic-rich residue | [BMIM]Ace + DMSO | 373 | 63 |

the cellulosics after partial lignin removal, resulting in an increased CrI of the residue. Further studies are required to conclude on this possibility, but the presence of DMSO as co-solvent does not decrease the overall degree of crystallinity in the studied residue.

### Molecular mass distribution of the extracted lignin

Gel permeation chromatography (GPC) is a common method to determine the molecular mass of polymers. Usually, the polymer needs to be acetylated to increase its solubility in THF, which is used as eluent in the size exclusion chromatography. Three characteristics of the polymer mix are of particular interest: (i) the number average molecular mass $\bar{M}_n$, (ii) the mass average molecular mass $\bar{M}_w$, and (iii) the polydispersity index (DPI). $\bar{M}_n$ is the average mass of each polymer with respect to number fractions, while $\bar{M}_w$ describes the average mass of each polymer with respect to mass fractions. The ration of both numbers ($\bar{M}_w/\bar{M}_n$) is called PDI and describes the distribution of molecular mass in the sample.

Table 12 summarises $\bar{M}_w$, $\bar{M}_n$, and PDI for the lignins that were separated

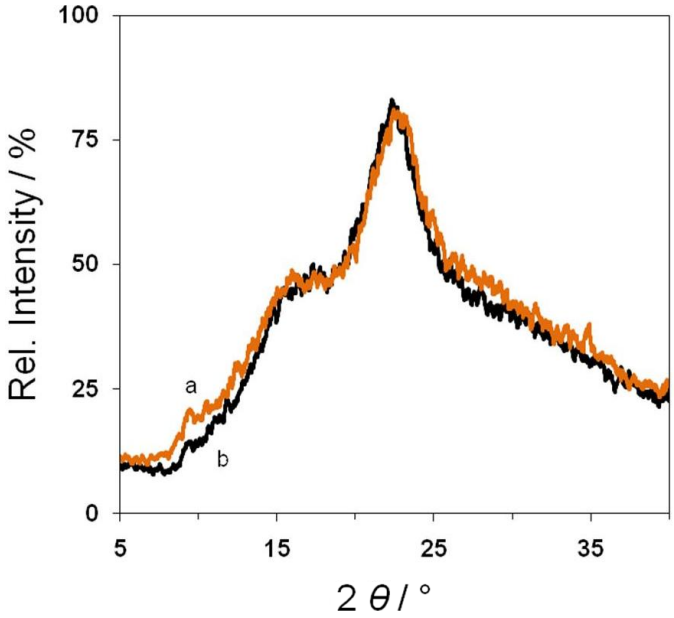


**Figure 59.** X-ray diffraction pattern of **(a)** native radiata pine and **(b)** the cellulosic-rich residue obtained after lignin extraction with a mixture of ($w_{\mathrm{IL}} = 0.9$) [BMIM]Ace and ($w_{\mathrm{DMSO}} = 0.1$) DMSO. *Pinus radiata* wood flour ($w_{\mathrm{T}} = 0.05$), with a particle size of 100 $\mu$m, was treated at 373 K for 2 h in an open atmosphere.

from both *Pinus radiata* and *Eucalyptus nitens*. The wood flour, with a particle size of 100 $\mu$m, was treated with [BMIM]Ace at 373 K for 2 h in an open atmosphere. Literature data of two commercial softwood lignins, Indulin AT and Organocell, is also included for comparison.[278] Indulin AT lignin was extracted from pine wood with the Kraft method, while ethanol was used to extract Organocell lignin from spruce wood. The lignins that were extracted with Ace ILs have significantly greater $\bar{M}_{\mathrm{n}}$ values and considerably smaller PDI values, than lignins that were extracted by traditional methods (see Table 12) or with other ILs.[250,278]

This suggests a more uniform—and maybe more native—character of the lignins obtained from gentle IL extraction with [BMIM]Ace. It is known that lignins obtained from sulfite pulping, for example, can contain $\bar{M}_{\mathrm{w}}$ values

in the range from (5 to 400) $10^3$ g·mol$^{-1}$, due to excessive incorporation of sulfonate groups.[233] As a consequence, the partially incorporated IL anion is potentially responsible for the greater molecular mass values observed in Ace IL extracted lignins. Interestingly, all Ace IL extracted lignins show the presence of a second polymer species in the GPC analysis. The average of its $\bar{M}_n$ values is 287.5 g·mol$^{-1}$ with an averaged PDI of 1.05, roughly equalling the mass of the [Ace]$^-$ anion with one nitrogen atom subtracted. One possible explanation is that the associated [Ace]$^-$ anions gets detached from the lignin polymer during its acetylation. This assumption is supported by the low PDI value observed for this molecule, suggesting a rather uniform molecular mass distribution. Further studies are necessary to identify this byproduct.

**Table 12. Mass Average Molecular Mass $\bar{M}_w$, Number Average Molecular Mass $\bar{M}_n$ and Polydispersity Index (DPI) of [BMIM]Ace Extracted Lignin. Either *Pinus Radiata* or *Eucalyptus Nitens* Wood Flour, With a Particle Size of 100 $\mu$m, was treated at 373 K for 2 h in an Open Atmosphere. Literature Values of Other Softwood Lignins are Included for Comparison.**

| Sample | $\bar{M}_w$ | $\bar{M}_n$ | PDI |
|---|---|---|---|
| | $10^{-3}$ g·mol$^{-1}$ | $10^{-3}$ g·mol$^{-1}$ | % |
| Pinus extract | 25.6 | 18.9 | 1.4 |
| Eucalyptus extract | 53.9 | 32.9 | 1.6 |
| Indulin AT lignin[278] | 19.8 | 2.2 | 9.0 |
| Organocell lignin[278] | 10.8 | 2.3 | 4.7 |

## 4.4 Experimental

### 4.4.1 Materials and Instruments

#### Materials

Acesulfame potassium (Ace K) was purchased from Absolute Ingredients Ltd, Auckland, New Zealand. 1-Butyl-3-methylimidazolium chloride ([BMIM]Cl), 1-ethyl-3-methylimidazolium acetate ([EMIM]Ac), dimethylsulfoxide (DMSO), 1-methylimidazole, 1-bromoethane, acetic anhydride and molecular sieve type 4A were purchased from Fluka. Microcrystalline cellulose (MCC) and chemicals for Karl Fischer titrations were obtained from Merck, and acetone was from Allied Petroleum, Christchurch, New Zealand. HPLC grade tetrahydrofuran (THF), anhydrous pyridine, toluene, methanol, 1-methylimidazole and 1-bromoethane were from Sigma Aldrich. Unless otherwise stated, all reagents were used without further purification. Distilled acetone, DMSO, acetic anhydride, pyridine, toluene and methanol were dried with molecular sieve prior to use. All ILs were dried at 353 K for 48 h prior to both their use in cellulose dissolution experiments and for the measuring their physical properties. The reference ionic liquid 1-hexyl-3-methylimidazolium bis(trifluoromethylsulfonyl) amide ([HMIM]$Tf_2N$) was prepared according to literature methods,[279] and it contained a final water mass fraction of $2{\cdot}10^{-5}$. Water was deionised with a Millipore Elix 5 to a final resistivity of 15 M$\Omega$·cm. MCC, with a particle size of (20 to 160) $\mu$m and a degree of polymerisation (DP) of 163[138], was dried at 353 K for 72 h to reduce the initial water content by 90 % to a final water mass fraction of $2.9{\cdot}10^{-3}$. Lignin, alkali with a low sulfonate content, was purchased from Sigma Aldrich. Wood samples, of the species *Pinus radiata*, were collected from a local sawmill in Kaiapoi, New Zealand. Samples of the species *Eucalyptus nitens* were kindly provided by the Forestry School of the University of Canterbury. Vacuum drying at 353 K and 10 Pa for 24 h, and subsequent knife milling, yielded wood sawdust with

an average particle diameter of 100 $\mu$m and with a final water mass fraction of 6.9 $\cdot 10^{-3}$. Hardened Microanalytix Advantec filter paper 4A was used for the lignin extraction experiments.

### Instruments

Fourier transform infrared (FT-IR) spectra were recorded on a Perkin–Elmer Spectrum One FT-IR spectrometer over a range of (4000 to 450) $cm^{-1}$. A total of 20 scans at a resolution of 4 $cm^{-1}$ was taken for each sample. Liquid samples were sandwiched between two polished KBr plates, and solid samples were pelleted with KBr containing a sample mass fraction of 0.01. Nuclear magnetic resonance (NMR) spectra were recorded on a Varian INOVA 500 spectrometer (500 MHz and 125 MHz for $^{1}H$ and $^{13}C$, respectively), using the signals of the residual solvent protons and the solvent carbons as internal references ($\delta_H$ 2.6 ppm and $\delta_C$ 39.6 ppm for DMSO-$d_6$). Water content was determined with a Radiometer Analytical TIM550 Volumetric Karl Fischer Titrator using Karl Fischer Reagent 5. The titrant was calibrated with a 0.01 % Apura® water standard. Thermogravimetric analysis (TGA) was conducted on a SDT Q600 from TA Instruments by heating (5 to 10) mg of sample in a platinum pan under a nitrogen atmosphere ($N_2$ flow rate 100 ml·$min^{-1}$). The decomposition temperatures $T_D$ were determined at a fractional mass loss of 0.1 at two different heating rates $\dot{T}_{1K} = 1$ K·$min^{-1}$ and $\dot{T}_{10K} = 10$ K·$min^{-1}$. Differential scanning calorimetry (DSC) was conducted on a Perkin Elmer DSC 8000, with (5 to 10) mg of sample contained in closed aluminium pans, at a heating rate of $\dot{T}_{1K} = 1$ K·$min^{-1}$. Electrospray ionisation mass spectra (ESI-MS) were recorded on a Bruker maXis 3G mass spectrometer, and microscopy was performed with an Olympus PX60 microscope. Elemental analysis (EA) was carried out by Campbell Microanalysis Laboratory, Department of Chemistry, University of Otago, Dunedin, New Zealand. All samples were dried prior to analysis. Wood

sample analysis, according to TAPPI standards T 222om-88 and UM 250, was carried out by Veritec, Rotorua, New Zealand. Results are expressed in mass fraction: (i) *Pinus radiata*: 0.2980 acid insoluble lignin, 0.0071 acid soluble lignin, 0.0315 extractives, and 0.6634 cellulosics; (ii) *Eucalyptus nitens*: 0.2754 acid insoluble lignin, 0.0459 acid soluble lignin, 0.0056 extractives, and 0.6731 cellulosics. X-ray diffraction (XRD) experiments were recorded on a Philips PW1729 diffractometer operating at 50 kV and 40 mA. The diffractometer was equipped with a PW1820/00 goniometer, a PW1752/00 monochromator, a PW1710 diffractometer control unit, and a PW1711/10 proportional detector probe with a sealed Xe detector. Cu $K_\alpha$ radiation was used for the diffraction experiments. The scan range was (3 to 40)° of $2\theta$, at a step seize of 0.01° of $2\theta$ and with a scan rate of 1° of $2\theta$ per minute. Gel permeation chromatography (GPC) was carried out by the School of Chemistry, Monash University, Melbourne, Australia, on an Agilent 1200 HPLC with a Sedex 55 evaporative light scattering detector. The columns, Waters Ultrastyragel 100 Å, Waters Ultrastyragel 500 Å and Agilent PLgel 10 $\mu$m were used. Calibration was performed on polystyrene standards. Lignin samples were acetylated according to literature methods[236] and dissolved in THF prior to molecular mass analysis.

## 4.4.2 Methods

### Physical property measurements

The studied ILs—[BMIM]Ace, [EMIM]Ace and [EMIM]Ac—were degassed at room temperature at a pressure of less than 100 Pa for at least 12 h prior to measurement. To minimise water uptake from the environment, all samples were kept under inert gas atmosphere ($N_2$) at all times. Prior to measurement, the instrument sample chambers were cleaned with (i) purified water from a Millipore Elix 5 with a final resistivity of 15 MΩ·cm, and (ii) distilled acetone. Subsequently, the sample chambers were flushed with ambient air overnight to

ensure complete solvent removal. All instrument sample chambers were then flushed with dry nitrogen gas prior to sample injection. IL sample volumes of 1 mL were required for each instrument.

**Density** Densities were measured with an Anton Paar DMA 602 H vibrating tube densimeter. Prior to measurement, the densimeter was calibrated with purified water and air over a temperature range from (278.15 to 358.15) K. For this purpose, the water was degassed and deionised, and its calculated density values were retrieved from the NIST Chemistry WebBook.[280] Ambient air with a relative humidity of 44.3 %, at a temperature of 295.05 K and a pressure of 1.013 bar, was used for calibration, and the density values of the moist air were calculated with consideration of its water content.[281] The calibration was verified with the IUPAC reference ionic liquid [HMIM]$Tf_2N$.[282] The combined expanded ($k = 2$) relative uncertainty of the density measurements was estimated to be 0.3 %.

**Viscosity** Viscosities were measured with a cone and plate Brookfield DV-II+Pro viscometer (model LVDV-11) with a CPE-40 cone spindle. Prior to measurement, the viscometer was calibrated over a temperature range from (278.15 to 333.15) K with reference oils (Canon S20 and S60, and Paragon N10, N100 and N1000) covering a viscosity range from (6 to 865) mPa·s. The calibration was verified with the IUPAC reference ionic liquid [HMIM]$Tf_2N$.[282] Only viscosities of less than 1 Pa·s were measurable, and the resulting combined expanded ($k = 2$) relative uncertainty of the viscosity measurements was estimated to be 3.0 %.

**Electrical conductivity** Electrical conductivities were measured with a conductivity flow cell (LKB model 5312 A), made from borosilicate glass with two platinum black electrodes.[283] The maximum operating temperature of the conductivity cell was 348.15 K, due to restrictions imposed by its plastic

framework. The resistance *R(f)* of the cell was determined with a Fluke PM 6306 RCL meter at a frequency $f$ of 1 kHz, and the electrical conductivity $\kappa$ was calculated according to

$$\kappa = \frac{K}{R}$$

with a cell constant $K$ of 90.1 $m^{-1}$.[283] Prior to measurement, the accuracy of the instrument was checked over a temperature range from (278.15 to 323.15) K with the IUPAC reference ionic liquid [HMIM]$Tf_2N$.[282] The combined expanded ($k = 2$) relative uncertainty of the measurements was estimated to be 2.0 %. Previously, Kandil *et al.* determined the frequency dependency for the IUPAC reference ionic liquid [HMIM]$Tf_2N$ from (0.5 to 10) kHz, and the extrapolation from 1 kHz to infinite frequency as $f^{-1}$ gave an additional relative uncertainty of less than 0.5 %.[283]

The temperature of the densimeter was measured with an industrial grade platinum resistance thermometer of nominal resistance 100 Ω that had been calibrated against a standard platinum thermometer of nominal resistance 25 Ω, which itself had been calibrated on ITS-90. The temperature of the conductivity cell was measured with the 25 Ω thermometer. The uncertainty in temperature for the density measurements were estimated to be ± 0.02 K, while the uncertainty in temperature for the electrical conductivity measurements was estimated to be ± 0.01 K. The temperature of the viscometer was determined with its built-in resistance temperature detector, with a stated uncertainty of ± 1.0 K.

### Synthesis and characterisation of ionic liquids

**Synthesis** Both ILs 1-butyl-3-methylimidazolium acesulfamate ([BMIM]Ace) and 1-ethyl-3-methylimidazolium acesulfamate ([EMIM]Ace) were synthesised according to the literature.[250] [BMIM]Ace was prepared from a stoichiometric ratio between Ace K and [BMIM]Cl. 25 g of Ace K was dissolved in 100 mL of hot water and added to 21.66 g of [BMIM]Cl. The mixture was stirred at

353 K for at least 24 h. The water was removed under vacuum and 150 mL of dry acetone was added. Insoluble potassium chloride was removed by filtration. Vacuum distillation was used to remove the acetone prior to IL vacuum drying at 353 K for 12 h. The IL was redissolved in 250 mL of dry acetone and refrigerated overnight. Residual precipitations of potassium chloride were filtered off and acetone was removed under vacuum. The IL was dried at 353 K and 10 Pa for 12 h. [EMIM]Ace was synthesised correspondingly with [EMIM]Br as starting material, which was prepared according to the literature.[279] The residual water content of the ILs was determined with Karl-Fischer titration, and elemental analysis was used to examine halide impurities.

**Characterisation** See Figure 60 for atom numbering in the NMR assignments. 1-Butyl-3-methylimidazolium acesulfamate, [BMIM]Ace (CASRN 697248-66-1). $^{1}$H NMR (DMSO-$d_6$, $\delta$/ppm): 9.21 (s, 1H, H-a), 7.87 & 7.80 (2s, 2H, H-b/H-b'), 5.36 (s, 1H, H-7), 4.26 (t, J = 7.0 Hz, 2H, H-1), 3.94 (s, 3H, H-1'), 2.00 (s, 3H, H-5), 1.86 (m, 2H, H-2), 1.36 (m, 2H, H-3), 1.00 (m, 3H, H-4). $^{13}$C NMR (DMSO-$d_6$, $\delta$/ppm): 167.88 (C-8), 159.74 (C-6), 136.62 (C-a), 123.71 (C-b), 123.36 (C-b'), 102.18 (C-7), 48.59 (C-1), 35.84 (C-1'), 31.45 (C-2), 19.51 (C-3), 18.87 (C-5), 13.38 (C-4). ES-MS: MS$^{+}$ $m/z$ 139.1240 [BMIM]$^{+}$ (calcd for $C_8H_{15}N_2$ 139.1230). ES-MS: MS$^{-}$ $m/z$ 162.0135 [Ace]$^{-}$ (calcd for $C_4H_4NO_4S$ 161.9867). FT-IR (KBr, $\nu_{max}$/cm$^{-1}$: 3414, 3152, 3110, 2963, 2875, 1651, 1575, 1466, 1430, 1388, 1353, 1316, 1173, 1059, 1015, 939, 855, 748, 718, 647, 623. Melting temperature ($T_{fus}$/K): $\approx$ 313; Water mass fraction 4.9 $\cdot 10^{-4}$; Residual halide mass fraction $3.8 \cdot 10^{-3}$; Thermal decomposition temperatures ($T_{D,1K}$/K, $T_{D,10K}$/K): 500, 537; Viscosity ($\eta_{293\ K}$/mPa·s$^{-1}$, $\eta_{358\ K}$/mPa·s$^{-1}$): 800, 26; Density ($\rho_{293\ K}$/kg·m$^{-3}$): 1240. Electrical conductivity ($\kappa_{293\ K}$/S·m$^{-1}$): 0.05. 1-Ethyl-3-methylimidazolium acesulfamate, [EMIM]Ace (no CASRN). $^{1}$H NMR (DMSO-$d_6$, $\delta$/ppm): 9.23 (s, 1H, H-a), 7.88 & 7.80 (2s, 2H, H-b/H-b'), 5.36 (s, 1H, H-7), 4.28 (t, J = 7.0

Hz, 2H, H-1), 3.94 (s, 3H, H-1'), 2.00 (s, 3H, H-5), 1.51 (t, J = 7.0 Hz, 3H, H-2). $^{13}$C NMR (DMSO-$d_6$, $\delta$/ppm): 167.81 (C-8), 159.68 (C-6), 123.63 (C-a), 122.13 (C-b), 102.20 (C-b'), 81.64 (C-7), 44.21 (C-1), 35.80 (C-1'), 19.51 (C-5), 15.22 (C-2). ES-MS: $MS^+$ $m/z$ 111.0922 $[EMIM]^+$ (calcd for $C_6H_{11}N_2$ 111.0917). ES-MS: $MS^-$ $m/z$ 162.0135 $[Ace]^-$ (calcd for $C_4H_4NO_4S$ 161.9867). FT-IR (KBr, $\nu_{max}$/cm$^{-1}$: 3419, 3151, 3095, 2987, 2474, 2092, 1913, 1652, 1575, 1431, 1388, 1351, 1314, 1266, 1172, 1059, 1017, 939, 855, 750, 719, 647, 622, 598, 560, 545, 519, 496, 483, 476, 453. Melting temperature ($T_{fus}$/K): $\approx$ 317; Water mass fraction 3.7 $\cdot 10^{-4}$; Residual halide mass fraction 4.9$\cdot 10^{-2}$; Thermal decomposition temperatures ($T_{D,1K}$/K, $T_{D,10K}$/K): 485, 526; Viscosity ($\eta_{293\ K}$/mPa$\cdot$s$^{-1}$, $\eta_{358\ K}$/mPa$\cdot$s$^{-1}$): 556, 22; Density ($\rho_{293\ K}$/kg$\cdot$m$^{-3}$): 1333. Electrical conductivity ($\kappa_{293\ K}$/S$\cdot$m$^{-1}$): 0.06.

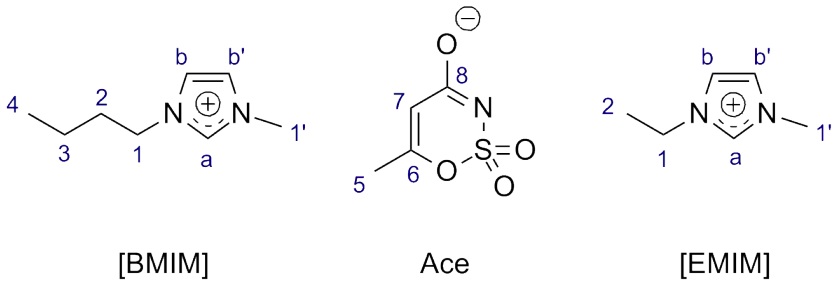


**Figure 60.** Numbering of imidazolium acesulfamate ILs for NMR assignment.

### Solubility studies with cellulose and lignin

All experiments were conducted in a dry $N_2$ atmosphere, and were performed with both ILs [EMIM]Ace and [BMIM]Ace.

**Solubility of cellulose** Five grams of dried IL was transferred to a moisture-free 25 mL flask. 0.005 mass fraction of dried MCC was added to the IL and mixed with a magnetic stirrer at 473 K for 24 h, and subsequently at 493 K for another 24 h. No signs of dispersion or dissolution of the cellulose

could be observed. Upon addition of water and after thorough stirring, the IL+water supernatant was analysed with an Olympus PX 60 microscope (magnifications of 10×, 50×, and 100×) for the existence of regenerated cellulose. No regenerated cellulose could be detected.

**Solubility of lignin** Up to 0.1 mass fraction of Sigma Aldrich lignin could be readily dissolved in the IL at 373 K within 2 h in an open atmosphere.

### Extraction of wood lignin

**Neat IL extraction** All experiments were conducted in an open atmosphere. Five to ten grams of dried IL was transferred to a 25 mL flask, equipped with a magnetic stirring bar and lacking a stopper. The IL was heated to 473 K, and 0.05 mass fraction of wood was added and stirred at constant temperature for 2 h. Afterwards, the undissolved wood particles were separated from the IL by gentle vacuum filtration, from the hot mixture, with pre-dried and weighed filter paper. The residue was washed with excess of hot water to ensure complete removal of the IL. Subsequently, the residue was dried to a constant mass at 353 K and 10 Pa. The water was removed from the filtrate by vacuum distillation. White flocs precipitated from the filtrate upon the addition of 200 mL of dry acetone. The mixture was refrigerated overnight at 278 K to ensure complete precipitation. The precipitate was separated by filtration, washed with excess of dried acetone to ensure complete IL removal, and finally dried to a constant mass at 353 K and 10 Pa. The resulting IL+acetone mixture was refrigerated overnight one more time to check for additional precipitates, but none were observed. The acetone was now removed from the IL by vacuum distillation and the IL was recovered. After drying, both the mass of the IL and its water mass fraction were determined. Finally, the mass of the separated wood fractions (residue and extract) was compared against the mass of the initial wood sample to ensure that no wood components,

such as hemicellulose, were lost. If not mentioned otherwise, the mass of the untreated wood sample agreed within at least 0.1 mg with the combined mass of both the extracted lignin and the cellulosic-rich residues.

**IL+DMSO extraction** The extraction of wood lignin with a mixture of IL+DMSO was performed in the same manner as the lignin extraction with the pure IL. The only difference was the extraction solvent, now a mixture of 0.9 mass fraction of [BMIM]Ace and 0.1 mass fraction of dried DMSO.

## 4.5 Conclusions

In summary, two imidazolium ILs have been presented with the ability to dissolve lignin without dissolving cellulose. These ILs are based on the acesulfamate anion, which is the main component of a sweetener (Ace K) used in the food industry. Ace K is of low cost and non-toxic to the environment. The IL synthesis is straightforward, and the studied ILs are non-corrosive, thermally stable and easy to handle at elevated temperatures. Lignin from both softwood and hardwood, with a particle size of 100 $\mu$m, can be isolated with an extraction efficiency $e$ of up to 0.38 within 2 h at 373 K in an open atmosphere. IL recycling works efficiently and it does not decrease the lignin extraction efficiency of these ILs. Multi-step treatment of the same wood sample—for three times—with fresh IL increases the total lignin extraction efficiency to $e = 0.6$, indicating that the ability of Ace ILs to extract lignin decreases with increasing mass fraction of dissolved lignin. Alternatively, a mixture of [BMIM]Ac ($w_{\mathrm{IL}} = 0.9$) and DMSO ($w_{\mathrm{DMSO}} = 0.1$) can be used to yield $e = 0.56$ of lignin in one extraction cycle of 2 h at 373 K.

No loss of biomass was observed during the extraction process, but indications suggest that traces of the IL anion get incorporated into the extract with either elevated extraction temperatures ($> 393$ K) or longer extraction times ($> 4$ h). Observations from analysing the molecular mass of the extract

suggest that the IL anion can be removed again from the extract. No decrease in the crystallinity of the cellulosic-rich wood residue was observed after 2 h treatment at 353 K with neat IL, or after 2 h treatment at 373 K with the IL+DMSO mixture. X-ray diffraction experiments suggest the possibility of a cellulosic-rich wood residue with an increased degree of crystallinity—compared to the native wood—if the lignin was extracted with the solvent mixture.

The IL extracted lignins have a higher molecular mass—and a much more uniform molecular mass distribution—compared to lignins obtained with traditional methods. The experimental results do not allow to conclude on the presence, or absence, of hemicellulose in the extract. Further studies are required in this respect.

In conclusion, IL extraction of wood lignin holds promising potential for being a low-cost and environmental benign method to obtain both uniform lignins—a potential feedstock for aromatic bio-derived chemicals—and cellulosic-rich wood residues with a high degree of crystallinity, which can be used for the manufacturing of biocomposites with superior mechanical properties.

# 5 Summary and Outlook

## 5.1 Assessment and Summary

The objective of this work was to (i) develop a concept that offers an explanation for the fact that only specific ionic liquids (ILs) have an ability to dissolve cellulose, and (ii) investigate the use of ionic liquids for the extraction of wood lignin.

The first part of this thesis combined an extensive literature study with the results derived from cellulose dissolution experiments to conclude a dissolution mechanism that can explain why only certain IL ion combinations are able to dissolve cellulose. It was postulated that all successful cellulose solvents are able to position their dipoles in a favourable geometry, which allows them to form H–bonds with cellulose that are of enhanced stability. Both the IL cation and the IL anion play an important role in the dissolution process. IL cation characteristics that are expected to enhance cellulose dissolution are (i) an aromatic heterocycle with the ability to sufficiently delocalise the positive charge, and (ii) a second heteroatom in the aromatic ring that results in a dipolar character of the cation. IL anion characteristics that are expected to enhance cellulose dissolution are (i) being an H–bond acceptor of small size, (ii) having substituents that are neither bulky nor hydrophobic, and (iii) possessing the ability to offer several H–bond acceptor sites. Proposed alternatives for cellulose-dissolving IL ions include oxazolium, 1,3-oxaphospholium,

dimethylcarbamate, phosphate, nitrate, and nitrite. However, one needs to keep in mind that the cellulose-dissolving ability is not the only aspect to consider while searching for superior cellulose solvents. Other physical properties, such as viscosity or toxicity for example, are of equal importance. In addition, the ability of the studied AAILs to finely disperse the cellulose is potentially very useful for various applications, which do not require the dissolution of the biopolymer.

The overall objective of this particular work is primarily to provide guidance for the development of highly efficient IL cellulose solvents. Further studies are required to confirm, reject, or refine the postulates of this work. It was almost a decade ago when the solubility of cellulose in some ILs was first reported, but the dissolution mechanism is still unknown. Understanding this mechanism is a major factor for the development of superior cellulose solvents that combine enhanced biopolymer solubility with desirable physical properties. Such solvents are crucial for the biomass industry to accelerate its progress in order to ensure a rapid transformation of our society towards full sustainability.

In the second part of this thesis, it was discovered that imidazolium acesulfamate ILs have the ability to dissolve wood lignin without dissolving cellulose. In particular 1-ethyl-3-methylimidazolium acesulfamate exhibits physical properties that are desirable in industrial processing. Gentle extraction conditions of 373 K are sufficient to give a lignin extraction efficiency $e$ of 0.43 within 2 h. Multi-step treatment of the same wood sample with fresh IL can further enhance lignin removal—up to $e = 0.6$ after three consecutive steps—and a mixture of IL and DMSO allows a lignin extraction efficiency $e$ of 0.56 after only one step at the same conditions. Loss of cellulosic material was not observed, and gentle extraction temperatures did not decrease the crystallinity of the wood cellulosics during IL treatment. The extracted lignins possess both a larger average molecular mass and a more uniform molecular

mass distribution compared to lignin obtained from the Kraft process, which is the dominating process for the extraction of lignin in the pulp and paper industry.

These results represent a significant progress towards the development of superior methods for the environmentally benign extraction of wood lignin that still allows to exploit the desirable mechanical properties of crystalline cellulose for the production of advanced biocomposites. Viewed from a different perspective, it allows to transform native wood into a lignin-deficient material with an increased cellulose content, but without compromising its crystallinity. IL lignin removal has numerous advantages, compared to prevailing methods, representing an opportunity for future biorefineries—producing renewable feedstock material for aromatic biochemicals and cellulosic biocomposites—with the potential to transform current industries such as the pulp and paper industry.

However, it is equally important to acknowledge the current limits and drawbacks of the studied IL lignin extractions. Although the incorporation of the IL anion into the extracted lignin was only observed at elevated extraction temperatures or with increased extraction times, this does not imply a nonreactive IL anion in general. Both the wood load and the wood particle size, used in the experiments, are far below the requirements of the wood industry, and the results obtained cannot quite simply be compared to those of large scale processes. Moreover, the wood samples were extensively dried prior to use in the IL extraction experiments. Although it has been shown that small amounts a residual water do not negatively impact the lignin extraction efficiency, it is very likely that the water content of natural biomass material exceeds this tolerance. In addition, the presence of hemicellulose in the wood extract cannot be excluded based on the experimental data available. Preliminary Klason lignin analysis of the wood extracts indicate $w$=0.05 of acid soluble material in the Radiata extract, and $w$=0.025 of acid soluble material in the Eucalyptus extract. This could be either acid soluble

lignin or associated hemicellulose. Due to the impact of the earthquakes on the University infrastructure it was not possible to continue these experiments. Additional studies, which would have included HPLC oligosaccharide analysis and NMR analysis of the lignin extracts, could not be undertaken. A number of additional studies are required to address these drawbacks. Still, the concept of IL lignin removal is of great merit, and—considering the tremendous progress of IL research within the last decade—significant improvements are to be expected in the near future.

## 5.2 Future Work

A number of questions remain unanswered after discussing the results of this work, and a number of further studies are possible. The first part of this thesis concluded on a hypothetical dissolution mechanism for cellulose in ILs. Additional studies require further refinement of the hypothesis, including both experimental validation of the proposed IL cellulose solvents and consideration of novel literature data.

The second part of this thesis investigated the extraction of wood lignin with Ace ILs. Numerous possibilities for further work exist. First of all, it can be determined whether any hemicellulosic material is associated with the extracted lignin. This can be achieved by acid hydrolysis of the extracts and subsequent HPLC analysis for the presence of hemicellulose sugars.

Second, it can be investigated whether traces of IL anions are generally associated with the extract, regardless of extraction temperature or extraction time, and whether this can be avoided. Possible approaches are to (i) apply a more sensitive method, such as energy-dispersive X-ray spectroscopy, for analysing the sulfur content of the extracted lignin, and (ii) investigate the use of IL additives that react favourably with wood lignin, competing with

the IL anion. Such additives must be easily removable from the lignin after extraction. An idea along that line would be to test the use of polyoxymetalate catalysts in ILs that do not dissolve cellulose, expecting more favourable results compared to studies with cellulose-dissolving ILs.[249]

Third, more investigations on the effect of IL co-solvents are possible, investigating both DMSO and other co-solvents. The effects of the IL+co-solvent mixing ratio on a number of aspects are of interest, such as the lignin extraction efficiency, the solvent recyclability, or the crystallinity of the cellulosic residue. In addition, experiments investigating the effect of solvent mixtures on (i) different wood particle sizes, or (ii) multi-step treatments of wood—particularly with respect to determine the optimal conditions for multiple extraction—are of interest.

Fourth, the extracted lignins can potentially be investigated with further methods to determine whether their uniform molecular mass distribution can be exploited. The extracted lignins will be of particular interest if they can be obtained as a defined substance in a reproducible fashion.[233]

Fifth, the extraction efficiency of other IL cations for wood lignin can be explored, with phosphonium cations being a potential alternative because of their low toxicity and low cost. Additional ideas for further research include scaled-up experiments—maybe in the form of a continuous flow reactor—and studies on different biomass materials, such as grass or sugarcane. Possibilities for further studies in this area seem endless, demonstrating the great potential of IL chemistry for superior biomass processing.

# References


(1) Hubbert, M. K. *Spring Meeting of the Southern District, Division of Production, American Petroleum Institute* San Antonio, TX, United States, March 7-9, 1956.

(2) Werpy, T.; Peterson, G. *Pacific Northwest National Laboratory and National Renewable Energy Laboratory, Department of Energy* Oak Ridge, TN, United States, August, 2004.

(3) Arioli, T.; Peng, L.; Betzner, A. S. et al. *Science* **1998**, *279*, 717–720.

(4) Alonso, D. M.; Bond, J. Q.; Dumesic, J. A. *Green Chem.* **2010**, *12*, 1493–1513.

(5) Wegner, T. H.; Jones, E. P. In *A Fundamental Review of the Relationships between Nanotechnology and Lignocellulosic Biomass*; Lucian A. Lucia, O. J. R., Ed.; The Nanoscience and Technology of Renewable Biomaterials; Wiley, West Sussex, 2009.

(6) Sun, N.; Rodriguez, H.; Rahman, M. et al. *Chem. Commun.* **2011**, *47*, 1405–1421.

(7) Remsing, R. C.; Petrik, I. D.; Liu, Z. et al. *Phys. Chem. Chem. Phys.* **2010**, *12*, 14827–14828.

(8) Zhang, J.; Zhang, H.; Wu, J. et al. *Phys. Chem. Chem. Phys.* **2010**, *12*, 14829–14830.

(9) Sun, N.; Rahman, M.; Qin, Y. et al. *Green Chem.* **2009**, *11*, 646–655.

(10) Wasserscheid, P.; Welton, T. *Ionic Liquids in Synthesis*; Wiley: Weinheim, Germany, 2007; Vol. 1.

(11) Wilkes, J. S.; Zaworotko, M. J. *Chem. Commun.* **1992**, 965–967.

(12) Ramnial, T.; Ino, D. D.; Clyburne, J. A. C. *Chem. Commun.* **2005**, 325–327.

(13) Abbott, A. P.; Capper, G.; Davies, D. L. et al. *Green Chem.* **2002**, *4*, 24–26.

(14) Bonhote, P.; Dias, A.-P.; Papageorgiou, N. et al. *Inorg. Chem.* **1996**, *35*, 1168–1178.

(15) Forsyth, S. A.; Pringle, J. M.; MacFarlane, D. R. *Aust. J. Chem.* **2004**, *57*, 113–119.

(16) Visser, A. E.; Swatloski, R. P.; Reichert, W. M. et al. *Chem. Commun.* **2001**, 135–136.

(17) Markgraf, J. H.; Sangani, P. K.; Manalansan, R. J. et al. *J. Chem Res., Synop.* **2000**, *2000*, 561–563.

(18) Heinze, T.; Dorn, S.; Schoebitz, M. et al. *Macromol. Symp.* **2008**, *262*, 8–22.

(19) Carmichael, A. J.; Deetlefs, M.; Earle, M. J. et al. *Ionic Liquids as Green Solvents: Progress and Prospects*; ACS Symposium Series; American Chemical Society: Washington, DC, 2003; Vol. 856; pp 14–31.

(20) Wasserscheid, P.; van Hal, R.; Bosmann, A. et al. *Ionic Liquids as Green Solvents: Progress and Prospects*; ACS Symposium Series; American Chemical Society: Washington, DC, 2003; Vol. 856; pp 57–69.

(21) Ren, R. X. *Ionic Liquids as Green Solvents: Progress and Prospects*; ACS Symposium Series; American Chemical Society: Washington, DC, 2003; Vol. 856; pp 70–81.

(22) Varma, R. S. *Ionic Liquids as Green Solvents: Progress and Prospects*; ACS Symposium Series; American Chemical Society: Washington, DC, 2003; Vol. 856; pp 82–92.

(23) Wasserscheid, P.; Gerhard, D.; Himmler, S. et al. *Ionic Liquids IV—Not Just Solvents Anymore*; ACS Symposium Series; American Chemical Society: Washington, DC, 2007; Vol. 231; pp 258–271.

(24) Ohno, H.; Kameda, M.; Fukumoto, K. et al. *Proc. Electrochem. Soc.* **2006**, *2004-24*, 346–352.

(25) Earle, M. J.; Esperanca, J. M. S. S.; Gilea, M. A. et al. *Nature* **2006**, *439*, 831–834.

(26) Swatloski, R. P.; Holbrey, J. D.; Rogers, R. D. *Green Chem.* **2003**, *5*, 361–363.

(27) Docherty, K. M.; Kulpa, J., Charles F. *Green Chem.* **2005**, *7*, 185–189.

(28) Baker, S. N.; McCleskey, T. M.; Baker, G. A. *Ionic Liquids IIIB: Fundamentals, Progress, Challenges, and Opportunities*; ACS Symposium Series 902; American Chemical Society: Washington, DC, 2005; pp 171–181.

(29) Park, S.; Viklund, F.; Hult, K. et al. *Ionic Liquids as Green Solvents: Progress and Prospects*; ACS Symposium Series; 2003; Vol. 856; pp 225–238.

(30) Biedron, T.; Kubisa, P. *Macromol. Rapid Commun.* **2001**, *22*, 1237–1242.

(31) Seddon, K. R.; Stark, A. *Green Chem.* **2002**, *4*, 119–123.

(32) Ohno, H. *Electrochim. Acta* **2001**, *46*, 1407–1411.

(33) Hines, J. H.; Wanigasekara, E.; Rudkevich, D. M. et al. *J. Mater. Chem.* **2008**, *18*, 4050–4055.

(34) Borra, E. F.; Seddiki, O.; Angel, R. et al. *Nature* **2007**, *447*, 979–981.

(35) Fei, Z.; Geldbach, T. J.; Zhao, D. et al. *Chem.–Eur. J.* **2006**, *12*, 2122–2130.

(36) Bara, J. E.; Gin, D. L.; Noble, R. D. *Ind. Eng. Chem. Res.* **2008**, *47*, 9919–9924.

(37) Kachoosangi, R. T.; Musameh, M. M.; Abu-Yousef, I. et al. *Anal. Chem.* **2009**, *81*, 435–442.

(38) Seddon, K. R.; Stark, A.; Torres, M.-J. *Pure Appl. Chem.* **2000**, *72*, 2275–2287.

(39) Carda-Broch, S.; Berthod, A.; Armstrong, D. W. *Anal. Bioanal. Chem.* **2003**, *375*, 191–199.

(40) Laus, G.; Bentivoglio, G.; Schottenberger, H. et al. *Lenzinger Berichte* **2005**, *84*, 71–85.

(41) Seddon, K. R. *J. Chem. Technol. Biotechnol.* **1997**, *68*, 351–356.

(42) Stegemann, H.; Rhode, A.; Reiche, A. et al. *Electrochim. Acta* **1992**, *37*, 379–383.

(43) Plechkova, N. V.; Seddon, K. R. *Chem. Soc. Rev.* **2008**, *37*, 123–150.

(44) Katritzky, A. R.; Jain, R.; Lomaka, A. et al. *J. Chem. Inf. Comput. Sci.* **2002**, *42*, 225–231.

(45) Katritzky, A. R.; Lomaka, A.; Petrukhin, R. et al. *J. Chem. Inf. Comput. Sci.* **2002**, *42*, 71–74.

(46) Abdul-Sada, A. K.; Greenway, A. M.; Hitchcock, P. B. et al. *Chem. Commun.* **1986**, 1753–1754.

(47) Wang, Y.; Li, H.; Han, S. *J. Chem. Phys.* **2006**, *124*, 044504/1–044504/8.

(48) Avent, A. G.; Chaloner, P. A.; Day, M. P. et al. *Inorg. Chem.* **1994**, 3405–3413.

(49) Ganesan, K.; Alias, Y.; Ng, S. W. *Acta Crystallogr., Sect. C* **2008**, *64*, 478–480.

(50) Holbrey, J. D.; Seddon, K. R. *Inorg. Chem.* **1999**, 2133–2140.

(51) Gordon, C. M.; Holbrey, J. D.; Kennedy, A. R. et al. *J. Mater. Chem.* **1998**, *8*, 2627–2636.

(52) Widegren, J. A.; Laesecke, A.; Magee, J. W. *Chem. Commun.* **2005**, 1610–1612.

(53) Perry, R. L.; Jones, K. M.; Scott, W. D. et al. *J. Chem. Eng. Data* **1995**, *40*, 615–619.

(54) Liao, Q.; Hussey, C. L. *J. Chem. Eng. Data* **1996**, *41*, 1126–1130.

(55) Okoturo, O. O.; VanderNoot, T. J. *J. Electroanal. Chem.* **2004**, *568*, 167–181.

(56) Baker, S. N.; Baker, G. A.; Kane, M. A. et al. *J. Phys. Chem. B* **2001**, *105*, 9663–9668.

(57) Harris, K. R.; Kanakubo, M.; Woolf, L. A. *J. Chem. Eng. Data* **2007**, *52*, 2425–2430.

(58) Harris, K. R.; Kanakubo, M.; Woolf, L. A. *J. Chem. Eng. Data* **2008**, *53*, 1230–1230.

(59) Abbott, A. P. *ChemPhysChem* **2004**, *5*, 1242–1246.

(60) Xu, W.; Angell, C. A. *Science* **2003**, *302*, 422–425.

(61) Dzyuba, S. V.; Bartsch, R. A. *ChemPhysChem* **2002**, *3*, 161–166.

(62) Chiappe, C.; Pieraccini, D. *J. Phys. Org. Chem.* **2005**, *18*, 275–297.

(63) Pringle, J. M.; Golding, J.; Baranyai, K. et al. *New J. Chem.* **2003**, *27*, 1504–1510.

(64) Law, G.; Watson, P. R. *Langmuir* **2001**, *17*, 6138–6141.

(65) Ngo, H. L.; LeCompte, K.; Hargens, L. et al. *Thermochim. Acta* **2000**, *357-358*, 97.

(66) Crosthwaite, J. M.; Muldoon, M. J.; Dixon, J. K. et al. *J. Chem. Thermodyn.* **2005**, *37*, 559–568.

(67) Baranyai, K. J.; Deacon, G. B.; MacFarlane, D. R. et al. *Aust. J. Chem.* **2004**, *57*, 145–147.

(68) Wooster, T. J.; Johanson, K. M.; Fraser, K. J. et al. *Green Chem.* **2006**, *8*, 691–696.

(69) Baker, S. N.; Baker, G. A.; Bright, F. V. *Green Chem.* **2002**, *4*, 165–169.

(70) Crowhurst, L.; Mawdsley, P. R.; Perez-Arlandis, J. M. et al. *Phys. Chem. Chem. Phys.* **2003**, *5*, 2790–2794.

(71) Huddleston, J. G.; Broker, G. A.; Willauer, H. D. et al. *Ionic Liquids–Industrial Applications for Green Chemistry*; ACS Symposium Series; American Chemical Society: Washington, DC, 2002; Vol. 818; pp 270–288.

(72) Carmichael, A. J.; Seddon, K. R. *J. Phys. Org. Chem.* **2000**, *13*, 591–595.

(73) Anderson, J. L.; Ding, J.; Welton, T. et al. *J. Am. Chem. Soc.* **2002**, *124*, 14247–14254.

(74) Weingaertner, H. *Angew. Chem., Int. Ed.* **2008**, *47*, 654–670.

(75) Huang, M.-M.; Weingaertner, H. *ChemPhysChem* **2008**, *9*, 2172–2173.

(76) Daguenet, C.; Dyson, P. J.; Krossing, I. et al. *J. Phys. Chem. B* **2006**, *110*, 12682–12688.

(77) Weingaertner, H.; Sasisanker, P.; Daguenet, C. et al. *J. Phys. Chem. B* **2007**, *111*, 4775–4780.

(78) Weingaertner, H.; Knocks, A.; Schrader, W. et al. *J. Phys. Chem. A* **2001**, *105*, 8646–8650.

(79) Wakai, C.; Oleinikova, A.; Ott, M. et al. *J. Phys. Chem. B* **2005**, *109*, 17028–17030.

(80) Schroedle, S.; Annat, G.; MacFarlane, D. R. et al. *Chem. Commun.* **2006**, 1748–1750.

(81) Weingaertner, H. *Z. Phys. Chem.* **2006**, *220*, 1395–1405.

(82) Dimitrakis, G.; Villar-Garcia, I. J.; Lester, E. et al. *Phys. Chem. Chem. Phys.* **2008**, *10*, 2947–2951.

(83) Wu, B.; Zhang, Y.; Wang, H. *J. Phys. Chem. B* **2008**, *112*, 6426–6429.

(84) Cammarata, L.; Kazarian, S. G.; Salter, P. A. et al. *Phys. Chem. Chem. Phys.* **2001**, *3*, 5192–5200.

(85) Mele, A.; Tran, C. D.; De Paoli Lacerda, S. H. *Angew. Chem.* **2003**, *42*, 4364–4366.

(86) Swatloski, R. P.; Holbrey, J. D.; Memon, S. B. et al. *Chem. Commun.* **2004**, 668–669.

(87) Jastorff, B.; Moelter, K.; Behrend, P. et al. *Green Chem.* **2005**, *7*, 362–372.

(88) Stock, F.; Hoffmann, J.; Ranke, J. et al. *Green Chem.* **2004**, *6*, 286–290.

(89) Ranke, J.; Molter, K.; Stock, F. et al. *Ecotoxicol. Environ. Saf.* **2004**, *58*, 396–404.

(90) Latala, A.; Stepnowski, P.; Nedzi, M. et al. *Aquat. Toxicol.* **2005**, *73*, 91–98.

(91) Righi, S.; Morfino, A.; Galletti, P. et al. *Green Chem.* **2011**, *13*, 367–375.

(92) Zhang, S.; Sun, N.; He, X. et al. *J. Phys. Chem. Ref. Data* **2006**, *35*, 1475–1517.

(93) Ionic Liquids Database–IL Thermo. Online database, 2011; http://ilthermo.boulder.nist.gov/ILThermo/mainmenu.uix, (accessed Feb. 2011).

(94) Walker, J. *Primary Wood Processing: Principles and Pratice,* 1st ed.; Chapman and Hall: London, 1993.

(95) Klemm, D.; Heublein, B.; Fink, H.-P. et al. *Angew. Chem.* **2005**, *44*, 3358–3398.

(96) Kraessig, H.; Schurz, J.; Steadman, R. et al. *Ullmann's Encyclopedia of Industrial Chemistry*, 5th ed.; Wiley: Weinheim, Germany, 2002.

(97) Van de Vyver, S.; Geboers, J.; Jacobs, P. A. et al. *ChemCatChem* **2011**, *3*, 82–94.

(98) Young, R. A., Rowell, R. M., Eds. *Cellulose: Structure, Modification, and Hydrolysis*, 1st ed.; Wiley-Interscience: New York, 1986.

(99) Hinterstoisser, B.; Salmen, L. *Vib. Spectrosc.* **2000**, *22*, 111–118.

(100) Gardner, K. H.; Blackwell, J. *Biopolymers* **1974**, *13*, 1975–2001.

(101) Diddens, I.; Murphy, B.; Krisch, M. et al. *Macromolecules* **2008**, *41*, 9755–9759.

(102) Fort, D. A.; Remsing, R. C.; Swatloski, R. P. et al. *Green Chem.* **2007**, *9*, 63–69.

(103) Kilpelainen, I.; Xie, H.; King, A. et al. *J. Agric. Food Chem.* **2007**, *55*, 9142–9148.

(104) Aaltonen, O.; Jauhiainen, O. *Carbohydr. Polym.* **2009**, *75*, 125–129.

(105) Heinze, T.; Schwikal, K.; Barthel, S. *Macromol. Biosci.* **2005**, *5*, 520–525.

(106) Barthel, S.; Heinze, T. *Green Chem.* **2006**, *8*, 301–306.

(107) Swatloski, R. P.; Spear, S. K.; Holbrey, J. D. et al. *J. Am. Chem. Soc.* **2002**, *124*, 4974–4975.

(108) Feng, L.; Chen, Z.-l. *J. Mol. Liq.* **2008**, *142*, 1–5.

(109) Erdmenger, T.; Haensch, C.; Hoogenboom, R. et al. *Macromol. Biosci.* **2007**, *7*, 440–445.

(110) Remsing, R. C.; Swatloski, R. P.; Rogers, R. D. et al. *Chem. Commun.* **2006**, 1271–1273.

(111) Kosan, B.; Michels, C.; Meister, F. *Cellulose* **2008**, *15*, 59–66.

(112) Zhang, H.; Wu, J.; Zhang, J. et al. *Macromolecules* **2005**, *38*, 8272–8277.

(113) Ebner, G.; Schiehser, S.; Potthast, A. et al. *Tetrahedron Lett.* **2008**, *49*, 7322–7324.

(114) Leipner, H.; Fischer, S.; Brendler, E. et al. *Macromol. Chem. Phys.* **2000**, *201*, 2041–2049.

(115) Myllymaeki, V.; Aksela, R. World Patent, WO 2005/017001 A1; 2005.

(116) Cuissinat, C.; Navard, P.; Heinze, T. *Cellulose* **2008**, *15*, 75–80.

(117) Koehler, S.; Liebert, T.; Heinze, T. *J. Polym. Sci., Part A: Polym. Chem.* **2008**, *46*, 4070–4080.

(118) Gericke, M.; Liebert, T.; Heinze, T. *Macromol. Biosci.* **2009**, *9*, 343–353.

(119) Lee, S. H.; Doherty, T. V.; Linhardt, R. J. et al. *Biotechnol. Bioeng.* **2009**, *102*, 1368–1376.

(120) El Seoud, O. A.; Koschella, A.; Fidale, L. C. et al. *Biomacromolecules* **2007**, *8*, 2629–2647.

(121) Zavrel, M.; Bross, D.; Funke, M. et al. *Bioresour. Technol.* **2009**, *100*, 2580–2587.

(122) Boerstoel, H.; Maatman, H.; Westerink, J. B. et al. *Polymer* **2001**, *42*, 7371–7379.

(123) Bicak, N. *J. Mol. Liq.* **2004**, *116*, 15–18.

(124) Honglu, X. *Holzforschung* **2006**, *50*, 509–512.

(125) Xie, H.; Li, S.; Zhang, S. *Green Chem.* **2005**, *7*, 606–608.

(126) Zhao, H.; Baker, G. A.; Song, Z. et al. *Green Chem.* **2008**, *10*, 696–705.

(127) Argyropoulos, D. S.; Xie, H. World Patent WO/2008/098037; 2008.

(128) Fukaya, Y.; Sugimoto, A.; Ohno, H. *Biomacromolecules* **2006**, *7*, 3295–3297.

(129) Vitz, J.; Erdmenger, T.; Haensch, C. et al. *Green Chem.* **2009**, *11*, 417–424.

(130) Zimmermann, J.; Ondruschka, B.; Stark, A. *Org. Process Res. Dev.* **2010**, *14*, 1102–1109.

(131) Guo, L.; Shi, T.; Li, Z. *e-Polymers* **2009**, ISSN 1618–7229.

(132) Yang, F.; Li, L.; Li, Q. et al. *Carbohydr. Poly.* **2010**, *81*, 311–316.

(133) Fukaya, Y.; Hayashi, K.; Wada, M. et al. *Green Chem.* **2008**, *10*, 44–46.

(134) Luo, H.-M.; Li, Y.-Q.; Zhou, C.-R. *Gaofenzi Cailiao Kexue Yu Gongcheng* **2005**, *21*, 233–235.

(135) Lateef, H.; Grimes, S.; Kewcharoenwong, P. et al. *J. Chem. Technol. Biotechnol.* **2009**, *84*, 1818–1827.

(136) Zhu, S.; Wu, Y.; Chen, Q. et al. *Green Chem.* **2006**, *8*, 325–327.

(137) Dadi, A. P.; Varanasi, S.; Schall, C. A. *Biotechnol. Bioeng.* **2006**, *95*, 904–910.

(138) Duchemin, B. J. C. Structure, property and processing relationships of all-cellulose composites, Ph.D. thesis, University of Canterbury, Christchurch, New Zealand, 2008.

(139) Fink, H.-P.; Weigel, P.; Purz, H. J. et al. *Prog. Polym. Sci.* **2001**, *26*, 1473–1524.

(140) Zhao, H.; Jones, C. L.; Baker, G. A. et al. *J. Biotechnol.* **2009**, *139*, 47–54.

(141) Ibbett, R. N.; Schuster, K. C.; Fasching, M. *Polymer* **2008**, *49*, 5013–5022.

(142) Li, L.; Lin, Z.; Yang, X. et al. *Chin. Sci. Bull.* **2009**, *54*, 1622–1625.

(143) Zhang, J.; Lin, L.; Sun, Y. et al. *J. Biobased Mater. Bioenergy* **2009**, *3*, 69–74.

(144) Bagheri, M.; Rodriguez, H.; Swatloski, R. P. et al. *Biomacromolecules* **2008**, *9*, 381–387.

(145) Duchemin, B. J. C.; Newman, R. H.; Staiger, M. P. *Compos. Sci. Technol.* **2009**, *69*, 1225–1230.

(146) Tsioptsias, C.; Stefopoulos, A.; Kokkinomalis, I. et al. *Green Chem.* **2008**, *10*, 965–971.

(147) Huber, G. W.; Iborra, S.; Corma, A. *Chem. Rev.* **2006**, *106*, 4044–4098.

(148) Barbosa, M. A.; Granja, P. L.; Barrias, C. C. et al. *ITBM-RBM* **2005**, *26*, 212–217.

(149) Czaja, W. K.; Young, D. J.; Kawecki, M. et al. *Biomacromolecules* **2007**, *8*, 1–12.

(150) Lee, K. Y.; Mooney, D. J. *Chem. Rev.* **2001**, *101*, 1869–1879.

(151) Ramakrishna, S.; Mayer, J.; Wintermantel, E. et al. *Compos. Sci. Technol.* **2001**, *61*, 1189–1224.

(152) Pinkert, A.; Marsh, K. N.; Pang, S. et al. *Chem. Rev.* **2009**, *109*, 6712–6728.

(153) Gabriel, S.; Weiner, J. *Ber. Dtsch. Chem. Ges.* **1888**, *21*, 2669–2679.

(154) Yuan, X.; Zhang, S.; Liu, J. et al. *Fluid Phase Equilib.* **2007**, *257*, 195–200.

(155) Hekmat, D.; Hebel, D.; Joswig, S. et al. *Biotechnol. Lett.* **2007**, *29*, 1703–1711.

(156) Yuan, X.; Zhang, S.; Liu, J. et al. *Fluid Phase Equilib.* **2007**, *257*, 195–200.

(157) Cota, I.; Gonzalez-Olmos, R.; Iglesias, M. et al. *J. Phys. Chem. B* **2007**, *111*, 12468–12477.

(158) Khodadadi-Moghaddam, M.; Habibi-Yangjeh, A.; Gholami, M. R. *J. Mol. Catal. A: Chem.* **2009**, *306*, 11–16.

(159) Mann, J. P.; McCluskey, A.; Atkin, R. *Green Chem.* **2009**, *11*, 785–792.

(160) Iglesias, M.; Torres, A.; Gonzalez-Olmos, R. et al. *J. Chem. Thermodyn.* **2008**, *40*, 119–133.

(161) Greaves, T. L.; Weerawardena, A.; Fong, C. et al. *J. Phys. Chem. B* **2006**, *110*, 22479–22487.

(162) Valderrama, J. O.; Robles, P. A. *Ind. Eng. Chem. Res.* **2007**, *46*, 1338–1344.

(163) Kurnia, K. A.; Wilfred, C. D.; Murugesan, T. *J. Chem. Thermodyn.* **2009**, *41*, 517–521.

(164) Nuthakki, B.; Greaves, T. L.; Krodkiewska, I. et al. *Aust. J. Chem.* **2007**, *60*, 21–28.

(165) Wang, J.; Li, X.; Meng, H. et al. *J. Chem. Thermodynamics* **2009**, *41*, 167–170.

(166) Yue, C.; Mao, A.; Wei, Y. et al. *Catal. Commun.* **2008**, *9*, 1571–1574.

(167) Kurnia, K. A.; Harris, F.; Wilfred, C. D. et al. *J. Chem. Thermodyn.* **2009**, *41*, 1069–1073.

(168) Greaves, T. L.; Kennedy, D. F.; Mudie, S. T. et al. *J. Phys. Chem. B* **2010**, *114*, 10022–10031.

(169) Zhao, C.; Burrell, G.; Torriero, A. A. J. et al. *J. Phys. Chem. B* **2008**, *112*, 6923–6936.

(170) Burrell, G. L.; Burgar, I. M.; Separovic, F. et al. *Phys. Chem. Chem. Phys.* **2010**, *12*, 1571–1577.

(171) Sharma, Y. O.; Degani, M. S. *Green Chem.* **2009**, *11*, 526–530.

(172) Cichy, B.; Gabarski, K.; Wojciechowski, J. Method of obtaining 1,3-dimethyl-4-(gamma -hydroxypropylamino)uracil. Polish Patent PL 162859 B1; 1994.

(173) Zhang, J. H.; Faryniarz, J. R.; Cheney, M. C. Sunscreen cosmetic compositions storage stabilized with malonate salts. World Patent WO 2003099250 A1; 2003.

(174) Faryniarz, J. R.; Miner, P. E.; Cheney, M. C. et al. Cosmetic compositions containing salts of malonic acid. World Patent WO 2003099254 A1; 2003.

(175) Subramanyan, K. K.; Faryniarz, J. R.; Zhang, J. H. Terpenoid fragrance components stabilized with malonic acid salts. World Patent WO 2004082652 A1; 2004.

(176) Faryniarz, J. R.; Cheney, M. C.; Johnson, A. W. Compositions containing malonate for prevention of in-grown hair arising from shaving. World Patent WO 2004082651 A1; 2004.

(177) Faryniarz, J. R.; Cheney, M. C.; Johnson, A. W. Methods and compositions comprising malonic acid useful to prevent in-grown hair arising from shaving. US Patent US 2005202054 A1; 2005.

(178) Brand, J. R.; Story, P. M. Titanium dioxide pigment compositions. US Patent US 4752340 A; 1988.

(179) Walker, A. J. Ionic liquids containing protonated primary, secondary or tertiary ammonium ions. British Patent GB 2412912 A; 2005.

(180) Jenny, A. L.; Curtis, J. H. Electrolyte for capacitors. German Patent DE 1918246; 1969.

(181) Suga, T.; Saito, K.; Kato, R. et al. Storage-stable residue-free solder paste. US Patent US 2004000355 A1; 2004.

(182) Yoshizawa, M.; Xu, W.; Angell, C. A. *J. Am. Chem. Soc.* **2003**, *125*, 15411–15419.

(183) Angell, C. A.; Byrne, N.; Belieres, J.-P. *Acc. Chem. Res.* **2007**, *40*, 1228–1236.

(184) MacFarlane, D. R.; Seddon, K. R. *Aust. J. Chem.* **2007**, *60*, 3–5.

(185) Pinkert, A.; Marsh, K. N.; Pang, S. et al. *Abstracts of Papers, 239th ACS National Meeting,* San Francisco, CA, United States, March 21-25, 2010.

(186) Marsh, K. N.; Pinkert, A.; Pang, S. et al. *21st IUPAC International Conference on Chemical Thermodynamics,* Tsukuba Science City, Ibaraki, Japan, August 1-6, 2010.

(187) Pinkert, A.; Marsh, K. N.; Pang, S. *Ind. Eng. Chem. Res.* **2010**, *49*, 11121–11130.

(188) Hassan, Ahmad Y. Transfer of Islamic Technology to the West, Part III, Technology Transfer in the Chemical Industries, http://www.history-science-technology.com/Articles/articles\72.htm, (accessed Nov. 2009).

(189) de Vains, A. R. British Patent GB189561; 1921.

(190) Li, Q.; He, Y.-C.; Xian, M. et al. *Biores. Technol.* **2009**, *100*, 3570–3575.

(191) Zhang, J.; Zhang, H.; Wu, J. et al. *Phys. Chem. Chem. Phys.* **2010**, *12*, 1941–1947.

(192) Liu, H.; Sale, K. L.; Holmes, B. M. et al. *J. Phys. Chem. B* **2010**, *114*, 4293–4301.

(193) Lindman, B.; Karlström, G.; Stigsson, L. *J. Mol. Liq.* **2010**, *156*, 76–81.

(194) Heinze, T.; Koschella, A. *Polímeros* **2005**, *15*, 84–90.

(195) Saalwachter, K.; Burchard, W.; Klufers, P. et al. *Macromolecules* **2000**, *33*, 4094–4107.

(196) Heinze, T. *Macromol. Chem. Phys.* **1998**, *199*, 2341–2364.

(197) Egal, M.; Budtova, T.; Navard, P. *Biomacromolecules* **2007**, *8*, 2282–2287.

(198) Lue, A.; Zhang, L.; Ruan, D. *Macromol. Chem. Phys.* **2007**, *208*, 2359–2366.

(199) Potthast, A.; Rosenau, T.; Sixta, H. et al. *Tetrahedron Lett.* **2002**, *43*, 7757–7759.

(200) Le Moigne, N.; Spinu, M.; Heinze, T. et al. *Polymer* **2010**, *51*, 447–453.

(201) Ramos, L.; Frollini, E.; Koschella, A. et al. *Cellulose* **2005**, *12*, 607–619.

(202) Rosenau, T.; Potthast, A.; Sixta, H. et al. *Prog. Polym. Sci.* **2001**, *26*, 1763–1837.

(203) Cuissinat, C.; Navard, P.; Heinze, T. *Carbohydr. Polym.* **2008**, *72*, 590–596.

(204) Kosan, B.; Schwikal, K.; Meister, F. *Cellulose* **2010**, *17*, 495–506.

(205) Remsing, R. C.; Hernandez, G.; Swatloski, R. P. et al. *J. Phys. Chem. B* **2008**, *112*, 11071–11078.

(206) Brandt, A.; Hallett, J. P.; Leak, D. J. et al. *Green Chem.* **2010**, *12*, 672–679.

(207) Xu, A.; Wang, J.; Wang, H. *Green Chem.* **2010**, *12*, 268–275.

(208) Youngs, T. G. A.; Holbrey, J. D.; Deetlefs, M. et al. *ChemPhysChem* **2006**, *7*, 2279–2281.

(209) Youngs, T. G. A.; Hardacre, C.; Holbrey, J. D. *J. Phys. Chem. B* **2007**, *111*, 13765–13774.

(210) Schöbitz, M.; Meister, F.; Heinze, T. *Macromol. Symp.* **2009**, *280*, 102–111.

(211) Koehler, S.; Liebert, T.; Schoebitz, M. et al. *Macromol. Rapid Commun.* **2007**, *28*, 2311.

(212) Pinkert, A.; Marsh, K. N.; Pang, S. *Ind. Eng. Chem. Res.* **2010**, *49*, 11809–11813.

(213) Sashina, E.; Novoselov, N. *Russ. J. Gen. Chem.* **2009**, *79*, 1057–1062.

(214) Marsh, K.; Pinkert, A.; Pang, S. et al. Presented at the 17$^{\text{th}}$ Symposium on Thermophysical Properties, Boulder, CO, 2009.

(215) Balevicius, V.; Gdaniec, Z.; Aidas, K. *Phys. Chem. Chem. Phys.* **2009**, *11*, 8592–8600.

(216) Krekeler, C.; Dommert, F.; Schmidt, J. et al. *Phys. Chem. Chem. Phys.* **2010**, *12*, 1817–1821.

(217) Spange, S.; Reuter, A.; Vilsmeier, E. et al. *J. Polym. Sci., Part A: Polym. Chem.* **1998**, *36*, 1945–1955.

(218) Östlund, A.; Lundberg, D.; Nordstierna, L. et al. *Biomacromolecules* **2009**, *10*, 2401–2407.

(219) Roder, T.; Potthast, A.; Rosenau, T. et al. *Macromol. Symp.* **2002**, *190*, 151–159.

(220) Marhoefer, R. Computersimulationen zum Loeseverhalten von Cellulose in aliphatischen Amin-N-oxiden, Ph.D. thesis, University of Technology, Darmstadt, Germany, 2004.

(221) Kosmulski, M.; Gustafsson, J.; Rosenholm, J. B. *Thermochim. Acta* **2004**, *412*, 47–53.

(222) Zakzeski, J.; Bruijnincx, P. C. A.; Jongerius, A. L. et al. *Chem. Rev.* **2010**, *110*, 3552–3599.

(223) European Parliament and the Council, Directive 2009/28/EC, 2009.

(224) Perlack, R. D.; Wright, L. L.; Turhollow, A. F. et al. *Biomass as Feedstock for a bioenergy and bioproducts industry: the technical feasibility of a billion-ton annual supply*; Oak Ridge National Laboratory, Oak Ridge, TN, United States, April, 2005.

(225) Wiesenthal, T.; Mourelatou, A.; Peterson, J.-E. et al. *How much bioenergy can Europe produce without harming the environment?*; European Environment Agency, Copenhagen, Denmark, 2006.

(226) Bozell, J. J.; Holladay, J. E.; Johnson, D. et al. *Top Value Added Candidates from Biomass, Volume II: Results of Screening for Potential Candidates from Biorefinery Lignin*; Pacific Northwest National Laboratory, Richland, WA, United States, 2007.

(227) Gosselink, R. J. A.; de Jong, E.; Guran, B. et al. *Ind. Crops Prod.* **2004**, *20*, 121–129.

(228) FitzPatrick, M.; Champagne, P.; Cunningham, M. F. et al. *Bioresour. Technol.* **2010**, *101*, 8915–8922.

(229) US Department of Energy, *Basic Energy Sciences Workshop: Catalysis for Energy*; Bethesda, MD, United States, August 6-8, 2007.

(230) Gierer, J. *Wood Sci. Technol.* **1980**, *14*, 241–266.

(231) Simonsen, J.; Habibi, Y. *Cellulose Nanocrystals in Polymer Matrices*; The Nanoscience and Technology of Renewable Biomaterials; John Wiley & Sons, Ltd, 2009.

(232) Guerra, A.; Filpponen, I.; Lucia, L. A. et al. *J. Agric. Food Chem.* **2006**, *54*, 5939–5947.

(233) Notley, S. M.; Norgren, M. *Lignin: Functional Biomaterial with Potential in Surface Chemistry and Nanoscience*; The Nanoscience and Technology of Renewable Biomaterials; John Wiley & Sons, Ltd, 2009.

(234) Stärk, K.; Taccardi, N.; Bösmann, A. et al. *ChemSusChem* **2010**, *3*, 719–723.

(235) Iversen, T. *Wood Sci. Technol.* **1985**, *19*, 243–251.

(236) Lawoko, M.; Henriksson, G.; Gellerstedt, G. *Biomacromolecules* **2005**, *6*, 3467–3473.

(237) Li, C.; Knierim, B.; Manisseri, C. et al. *Bioresour. Technol.* **2010**, *101*, 4900–4906.

(238) Mann, D.; Labbé, N.; Sykes, R. et al. *Bioenerg. Res.* **2009**, *2*, 246–256.

(239) Zoia, L.; King, A. W. T.; Argyropoulos, D. S. *J. Agric. Food Chem.* **2011**, *59*, 829–838.

(240) King, A. W. T.; Zoia, L.; Filpponen, I. et al. *J. Agric. Food Chem.* **2009**, *57*, 8236–8243.

(241) Xie, H.; King, A.; Kilpelainen, I. et al. *Biomacromolecules* **2007**, *8*, 3740–3748.

(242) Zakzeski, J.; Jongerius, A. L.; Weckhuysen, B. M. *Green Chem.* **2010**, *12*, 1225–1236.

(243) Binder, J. B.; Gray, M. J.; White, J. F. et al. *Biomass Bioenergy* **2009**, *33*, 1122–1130.

(244) Jia, S.; Cox, B. J.; Guo, X. et al. *ChemSusChem* **2010**, *3*, 1078–1084.

(245) Songyan, J.; Cox, B. J.; Xinwen, G. et al. *Holzforschung* **2010**, *64*, 577–580.

(246) Cox, B. J.; Jia, S.; Zhang, Z. C. et al. *Polym. Degrad. Stab.* **2011**, *96*, 426–431.

(247) Pu, Y.; Jiang, N.; Ragauskas, A. J. *J. Wood Chem. Technol.* **2007**, *27*, 23–33.

(248) Fu, D.; Mazza, G.; Tamaki, Y. *J. Agric. Food Chem.* **2010**, *58*, 2915–2922.

(249) Sun, N.; Jiang, X.; Maxim, M. L. et al. *ChemSusChem* **2011**, *4*, 65–73.

(250) Tan, S. S. Y.; MacFarlane, D. R.; Upfal, J. et al. *Green Chem.* **2009**, *11*, 339–345.

(251) Carter Elke, B.; Culver Stephanie, L.; Fox Phillip, A. et al. *Chem. Commun.* **2004**, 630–631.

(252) Hough-Troutman, W. L.; Smiglak, M.; Griffin, S. et al. *New J. Chem.* **2009**, *33*, 26–33.

(253) Pernak, J.; Stefaniak, F.; Węglewski, J. *Eur. J. Org. Chem.* **2005**, *2005*, 650–652.

(254) Fraser, K. J.; Izgorodina, E. I.; Forsyth, M. et al. *Chem. Commun.* **2007**, 3817–3819.

(255) Sambasivarao, S. V.; Acevedo, O. *J. Chem. Theory Comput.* **2009**, *5*, 1038–1050.

(256) Stasiewicz, M.; Fojutowski, A.; Kropacz, A. et al. *Holzforschung* **2008**, *62*, 309–317.

(257) Jodynis-Liebert, J.; Nowicki, M.; Adamska, T. et al. *Drug Chem. Toxicol.* **2009**, *32*, 395–404.

(258) Nockemann, P.; Thijs, B.; Driesen, K. et al. *J. Phys. Chem. B* **2007**, *111*, 5254–5263.

(259) Stasiewicz, M.; Mulkiewicz, E.; Tomczak-Wandzel, R. et al. *Ecotoxicol. Environ. Saf.* **2008**, *71*, 157–165.

(260) Frade, R. F.; Rosatella, A. A.; Marques, C. S. et al. *Green Chem.* **2009**, *11*, 1660–1665.

(261) Frade, R. F. M.; Matias, A.; Branco, L. C. et al. *Green Chem.* **2007**, *9*, 873–877.

(262) Coleman, D.; Gathergood, N. *Chem. Soc. Rev.* **2010**, *39*, 600–637.

(263) Domańska, U.; Żołek-Tryznowska, Z.; Królikowski, M. *J. Chem. Eng. Data* **2007**, *52*, 1872–1880.

(264) Dean, P. M.; Turanjanin, J.; Yoshizawa-Fujita, M. et al. *Cryst. Growth Des.* **2008**, *9*, 1137–1145.

(265) Muldoon, M. J.; Aki, S. N. V. K.; Anderson, J. L. et al. *J. Phys. Chem. B* **2007**, *111*, 9001–9009.

(266) Rosatella, A. A.; Branco, L. C.; Afonso, C. A. M. *Green Chem.* **2009**, *11*, 1406–1413.

(267) Yu, M.; Wang, S.-H.; Luo, Y.-R. et al. *Ecotoxicol. Environ. Saf.* **2009**, *72*, 1798–1804.

(268) Pinkert, A.; Ang, K. L.; Marsh, K. N. et al. *Phys. Chem. Chem. Phys.* **2011**, *13*, 5136 – 5143.

(269) Liebner, F.; Patel, I.; Ebner, G. et al. *Holzforschung* **2010**, *64*, 161–166.

(270) Kline, L. M.; Hayes, D. G.; Womac, A. R. et al. *BioResources* **2010**, *5*, 1366–1383.

(271) Thygesen, A.; Oddershede, J.; Lilholt, H. et al. *Cellulose* **2005**, *12*, 563–576.

(272) Park, S.; Baker, J.; Himmel, M. et al. *Biotechnol. Biofuels* **2010**, *3*, 10.

(273) Jager, G.; Wu, Z.; Garschhammer, K. et al. *Biotechnol. Biofuels* **2010**, *3*, 18.

(274) Isogai, A.; Usuda, M.; Kato, T. et al. *Macromolecules* **1989**, *22*, 3168–3172.

(275) Cheng, G.; Varanasi, P.; Li, C. et al. *Biomacromolecules* **2011**, DOI: 10.1021/bm101240z.

(276) Abe, K.; Yamamoto, H. *J. Wood Sci.* **2005**, *51*, 334–338.

(277) Newman, R. H. *Cellulose* **2008**, *15*, 769–778.

(278) Glasser, W. G.; Davé, V.; Frazier, C. E. *J. Wood Chem. Technol.* **1993**, *13*, 545–559.

(279) Widegren, J. A.; Magee, J. W. *J. Chem. Eng. Data* **2007**, *52*, 2331–2338.

(280) NIST Chemistry WebBook, http://webbook.nist.gov/chemistry/fluid/, (accessed Nov. 2009).

(281) The Engineering ToolBox, http://www.engineeringtoolbox.com/density-air-d_680.html, (accessed Nov. 2009).

(282) Marsh, K. N.; Brennecke, J. F.; Chirico, R. D. et al. *Pure Appl. Chem.* **2009**, *81*, 781–790.

(283) Kandil, M. E.; Marsh, K. N.; Goodwin, A. R. H. *J. Chem. Eng. Data* **2007**, *52*, 2382–2387.

# List of Figures

# List of Tables

# Glossary

## General abbreviations

| | |
|---|---|
| AAIL | Alkanolammonium ionic liquid |
| Ace | Acesulfamate |
| CASRN | Chemical Abstracts Service Registration Number |
| CrI | Crystallinity index |
| $CHCl_3$ | Chloroform |
| DSC | Differential scanning calorimetry |
| $d$ | Diameter |
| DMA | *N*,*N*-Dimethylacetamide |
| DMF | Dimethylformamide |
| DMSO | Dimethylsulfoxide |
| DMSO-$d_6$ | Trideuterio(trideuteriomethylsulfinyl)methane |
| DP | Degree of polymerisation |
| $e$ | Lignin extraction efficiency ($e = w_e/w_\mathrm{i}$) |
| EA | Elemental analysis |
| $EC_{50}$ | Half maximal effective concentration |
| EN | Electronegativity |
| ESI-MS | Electro-spray ionisation mass spectra |
| FRST | Foundation for Research, Science and Technology |
| $f$ | Frequency |
| FT-IR | Fourier transform infrared |
| G | Guaiacyl |
| GPC | Gel permeation chromatography |
| H | *p*-Hydroxyphenyl |
| H–bond | Hydrogen bond |
| HPLC | High-performance liquid chromatography |
| IL | Ionic liquid |
| IUPAC | International Union of Pure and Applied Chemistry |
| LiCl | Lithium chloride |
| LCC | Lignin–carbohydrate complex |

| | |
|---|---|
| $M_{\mathrm{w}}$ | Molar mass |
| $\bar{M}_{\mathrm{w}}$ | Mass average molecular mass |
| $\bar{M}_{\mathrm{n}}$ | Number average molecular mass |
| MCC | Microcrystalline cellulose |
| Mtoe | Million tons of oil equivalent |
| $N_2$ | Nitrogen gas |
| NMMO | *N*-methylmorpholine-*N*-oxide |
| NMR | Nuclear magnetic resonance |
| OH–group | Hydroxy(l) group |
| PDI | Polydispersity index |
| $\mathrm{p}K_{\mathrm{a}}$ | Negative common logarithm of the acid dissociation constant $K_{\mathrm{a}}$ |
| POM | Polyoxymetalate |
| ppm | Parts per million |
| QSPR | Quantitative structure–property relationship |
| RTIL | Room temperature ionic liquid |
| S | Syringyl |
| SA | Sigma Aldrich |
| $T$ | Thermodynamic temperature |
| $t$ | Time |
| $\dot{T}_{\mathrm{xK}}$ | Heating rate of x K·min$^{-1}$ |
| $T_{\mathrm{D}}$ | Onset thermal decomposition temperature |
| $T_{\mathrm{D,xK}}$ | Onset thermal decomposition temperature at a fractional mass loss of 0.1 at a heating rate of x K·min$^{-1}$ |
| $T_{\mathrm{PT,xK}}$ | Phase transition temperature at a heating rate of x K·min$^{-1}$ |
| $T_{\mathrm{fus}}$ | Melting temperature |
| TBAF | Tetrabutylammonium fluoride |
| TGA | Thermogravimetric analysis |
| THF | Tetrahydrofuran |
| TSIL | Task specific ionic liquid |
| $w$ | Mass fraction |
| $w_{\mathrm{e}}$ | Mass fraction of extracted wood lignin |
| $w_{\mathrm{H_2O}}$ | Mass fraction of water |
| $w_{\mathrm{i}}$ | Mass fraction of lignin in native wood |
| $w_{\mathrm{T}}$ | Mass fraction of wood |
| XRD | X-ray diffraction crystallography |

## Ionic liquid cations

| | |
|---|---|
| [AMIM] | 1-Allyl-3-methylimidazolium |
| [BMIM] | 1-Butyl-3-methylimidazolium |
| [BuMePy] | 1-Butyl-1-methylpyridinium |
| [BMPyr] | 1-Butyl-1-methylpyrrolidinium |
| [BPy] | 1-Butylpyridinium |
| [$C_n$MIM] | 1-Alkyl-3-methylimidazolium |
| [DAA] | Diallylammonium |
| [DEA] | Bis(2-hydroxyethyl)ammonium |
| [EMIM] | 1-Ethyl-3-methylimidazolium |
| [HEA] | 2-Hydroxyethylammonium |
| [HPA] | 3-Hydroxypropylammonium |
| [IM] | Imidazolium |
| [MIM] | 1-Methylimidazolium |
| [$NR_4$] | Tetraalkylammonium |
| [$PR_4$] | Tetraalkylphosphonium |
| [$P_{666n}$] | Alkyl-trihexylphosphonium |
| [$P_{666n}$] | Tetraalkylphosphonium |
| [RPy] | 1-Alkylpyridinium |
| [$R_1R_2$IM] | 1,3-Dialkylimidazolium |
| [TEA] | Tris(2-hydroxyethyl)ammonium |

## Ionic liquid anions

| | |
|---|---|
| ABS | Alkylbenzsulfonates |
| Ac | Acetate |
| Ace | Acesulfamate |
| Br | Bromide |
| $BF_4$ | Tetrafluoroborate |
| $CH_3CO_2$ | = Ac |
| $CH_3SO_3$ | Methanesulfonate (mesylate) |
| $CH_3SO_4$ | Methylsulfate |
| $CF_3SO_3$ | Trifluoromethanesulfonate (triflate) |
| Cl | Chloride |
| $EtOSO_3$ | Ethylsulfate |

| | |
|---|---|
| Fmt | Formate |
| I | Iodide |
| $Ms_2N$ | Bis-(methanesulfonyl)amide |
| Mal | Malonate |
| $NO_3$ | Nitrate |
| $PF_6$ | Hexafluorophosphate |
| $R_1R_2PO_4$ | Dialkylphosphate |
| $Tf_2N$ | Bis-(trifluoromethanesulfonyl)amide, also known as Bis-(triflyl)amide |
| TsO | *p*-Toluenesulfonate, also known as Tosylate |

## Greek letters

| | |
|---|---|
| $\epsilon_s$ | Relative dielectric permittivity, also known as dielectric constant |
| $\eta$ | Viscosity |
| $\kappa$ | Electrical conductivity |
| $\nu$ | Wavenumber |
| $\rho$ | Density |

# Appendices

## Appendix A – Author statement

***Author Statement***

The purpose of this statement is to:

(i) outline the contribution of the main author (André Pinkert) with regard to the publications listed below;

(ii) ensure that all co-authors give permission to the main author to incorporate the content of these publications in his PhD thesis.

List of publications:

1. **Pinkert, A.;** Goeke, D. F.; Marsh, K. N.; Pang, S. Food additive-based ionic liquids for the selective extraction of wood lignin, *(Journal still to be decided)*, **2011**, (in preparation).
2. **Pinkert, A.**; Keng, A. L.; Marsh, K. N.; Pang, S. Density, viscosity and electrical conductivity of alkanolammonium ionic liquids, *Phys. Chem. Chem. Phys.*, **2011**, *13 (11)*, 5136-5143.
3. **Pinkert, A.**; Marsh, K. N.; Pang, S. Reflections on the solubility of cellulose, *Ind. Eng. Chem. Res.*, **2010**, *49*, 1121–11130.
4. **Pinkert, A.**; Marsh, K. N.; Pang, S. Alkanolamine ionic liquids and their inability to dissolve crystalline cellulose, *Ind. Eng. Chem. Res.*, **2010**, *49*, 11809–11813.
5. **Pinkert, A.**; Marsh, K. N.; Pang, S; Staiger, M. P. Ionic liquids and their interaction with cellulose, *Chem. Rev.*, **2009**, *109*, 6712-6728.

Author contribution:

- **André Pinkert**: Main author; contributed at least 90 % of each of the following: (i) intellectual concepts, (ii) analysis of the results & their interpretation, and (iii) preparation of the manuscripts for publication.
- **Kenneth N. Marsh**: Provided guidance and advice for parts (i), (ii) and (iii), as defined above. Main mentor.
- **Shusheng Pang**: Provided guidance and advice for parts (i), and (iii), as defined above.
- **Mark P. Staiger**: Contributed to the editing of the relevant manuscript.
- **Ang L. Keng**: Contributed to the practical work of the relevant manuscript.
- **Dagmar F. Goeke**: Contributed to the practical work of the relevant manuscript.

Disclaimer:

In signing below, the co-authors confirm their agreement with this statement. Furthermore, the co-authors give permission to the main author (André Pinkert) to use any part of these publications for the preparation of his PhD thesis.

Kenneth N. Marsh 21 March 2011

Shusheng Pang 25/03/2011

Keng L. Ang 27/3/2011

Dagmar F. Goeke 27/03/2011

Mark P. Staiger 30/3/11

# Appendix B – Copyright licences

**AMERICAN CHEMICAL SOCIETY LICENSE**
**TERMS AND CONDITIONS**

Feb 02, 2011

This is a License Agreement between André Pinkert ("You") and American Chemical Society ("American Chemical Society") provided by Copyright Clearance Center ("CCC"). The license consists of your order details, the terms and conditions provided by American Chemical Society, and the payment terms and conditions.

**All payments must be made in full to CCC. For payment instructions, please see information listed at the bottom of this form.**

| | |
|---|---|
| License Number | 2600950062928 |
| License Date | Feb 02, 2011 |
| Licensed content publisher | American Chemical Society |
| Licensed content publication | Chemical Reviews |
| Licensed content title | Ionic Liquids and Their Interaction with Cellulose |
| Licensed content author | André Pinkert et al. |
| Licensed content date | Dec 1, 2009 |
| Volume number | 109 |
| Issue number | 12 |
| Type of Use | Thesis/Dissertation |
| Requestor type | Not specified |
| Format | Print and Electronic |
| Portion | 50% or more of original article |
| Author of this ACS article | Yes |
| Order reference number | |
| Title of the thesis / dissertation | Investigations on the use of ionic liquids for superior biomass processing |
| Expected completion date | May 2011 |
| Estimated size(pages) | 300 |
| Billing Type | Invoice |
| Billing Address | University of Canterbury<br><br>Christchurch, other 8041<br>New Zealand |
| Customer reference info | |
| Total | 0.00 USD |

**AMERICAN CHEMICAL SOCIETY LICENSE TERMS AND CONDITIONS**

Feb 02, 2011

This is a License Agreement between André Pinkert ("You") and American Chemical Society ("American Chemical Society") provided by Copyright Clearance Center ("CCC"). The license consists of your order details, the terms and conditions provided by American Chemical Society, and the payment terms and conditions.

**All payments must be made in full to CCC. For payment instructions, please see information listed at the bottom of this form.**

| | |
|---|---|
| License Number | 2600950363377 |
| License Date | Feb 02, 2011 |
| Licensed content publisher | American Chemical Society |
| Licensed content publication | Industrial & Engineering Chemistry Research |
| Licensed content title | Reflections on the Solubility of Cellulose |
| Licensed content author | André Pinkert et al. |
| Licensed content date | Nov 1, 2010 |
| Volume number | 49 |
| Issue number | 22 |
| Type of Use | Thesis/Dissertation |
| Requestor type | Not specified |
| Format | Print and Electronic |
| Portion | 50% or more of original article |
| Author of this ACS article | Yes |
| Order reference number | |
| Title of the thesis / dissertation | Investigations on the use of ionic liquids for superior biomass processing |
| Expected completion date | May 2011 |
| Estimated size(pages) | 300 |
| Billing Type | Invoice |
| Billing Address | University of Canterbury<br><br>Christchurch, other 8041<br>New Zealand |
| Customer reference info | |
| Total | 0.00 USD |

**AMERICAN CHEMICAL SOCIETY LICENSE TERMS AND CONDITIONS**

Feb 02, 2011

This is a License Agreement between André Pinkert ("You") and American Chemical Society ("American Chemical Society") provided by Copyright Clearance Center ("CCC"). The license consists of your order details, the terms and conditions provided by American Chemical Society, and the payment terms and conditions.

**All payments must be made in full to CCC. For payment instructions, please see information listed at the bottom of this form.**

| | |
|---|---|
| License Number | 2600950251441 |
| License Date | Feb 02, 2011 |
| Licensed content publisher | American Chemical Society |
| Licensed content publication | Industrial & Engineering Chemistry Research |
| Licensed content title | Alkanolamine Ionic Liquids and Their Inability To Dissolve Crystalline Cellulose |
| Licensed content author | André Pinkert et al. |
| Licensed content date | Nov 1, 2010 |
| Volume number | 49 |
| Issue number | 22 |
| Type of Use | Thesis/Dissertation |
| Requestor type | Not specified |
| Format | Print and Electronic |
| Portion | 50% or more of original article |
| Author of this ACS article | Yes |
| Order reference number | |
| Title of the thesis / dissertation | Investigations on the use of ionic liquids for superior biomass processing |
| Expected completion date | May 2011 |
| Estimated size(pages) | 300 |
| Billing Type | Invoice |
| Billing Address | University of Canterbury<br><br>Christchurch, other 8041<br>New Zealand |
| Customer reference info | |
| Total | 0.00 USD |

**From:** CONTRACTS-COPYRIGHT (shared)
**To:** Andre Pinkert;
**Subject:** [SPAM: 8.000] RE: Website Email: PhD thesis
**Date:** Tuesday, 8 February 2011 9:01:56 p.m.

---

Dear André

The Royal Society of Chemistry (RSC) hereby grants permission for the use of your paper(s) specified below in the printed and microfilm version of your thesis. You may also make available the PDF version of your paper(s) that the RSC sent to the corresponding author(s) of your paper(s) upon publication of the paper (s) in the following ways: in your thesis via any website that your university may have for the deposition of theses, via your university's Intranet or via your own personal website. We are however unable to grant you permission to include the PDF version of the paper(s) on its own in your institutional repository. The Royal Society of Chemistry is a signatory to the STM Guidelines on Permissions (available on request).

Please note that if the material specified below or any part of it appears with credit or acknowledgement to a third party then you must also secure permission from that third party before reproducing that material.

Please ensure that the thesis states the following:

*Reproduced by permission of the PCCP Owner Societies*

and include a link to the paper on the Royal Society of Chemistry's website.

Please ensure that your co-authors are aware that you are including the paper in your thesis.

Best wishes

Gill

Gill Cockhead (Mrs), Contracts & Copyright Executive
Royal Society of Chemistry, Thomas Graham House
Science Park, Milton Road, Cambridge CB4 0WF, UK
Tel +44 (0) 1223 432134, Fax +44 (0) 1223 423623
http://www.rsc.org

# Appendix C – Density, viscosity and electrical conductivity of protic alkanolammonium ionic liquids

The following article has been published by the Royal Society of Chemistry in the journal *Physical Chemistry Chemical Physics* (see http://dx.doi.org/10.1039/c0cp02222e), and is reproduced by permission of the PCCP Owner Societies (see Appendix B). The associated supplementary material is deposited at the University of Canterbury online repository (see http://ir.canterbury.ac.nz/handle/10092/5095).

PCCP

Dynamic Article Links

Cite this: *Phys. Chem. Chem. Phys.*, 2011, **13**, 5136–5143

www.rsc.org/pccp

**PAPER**

# Density, viscosity and electrical conductivity of protic alkanolammonium ionic liquids†

**André Pinkert, Keng L. Ang, Kenneth N. Marsh* and Shusheng Pang**

***Received 20th October 2010, Accepted 16th December 2010***
**DOI: 10.1039/c0cp02222e**

Ionic liquids are molten salts with melting temperatures below the boiling point of water, and their qualification for applications in potential industrial processes does depend on their fundamental physical properties such as density, viscosity and electrical conductivity. This study aims to investigate the structure–property relationship of 15 ILs that are primarily composed of alkanolammonium cations and organic acid anions. The influence of both the nature and number of alkanol substituents on the cation and the nature of the anion on the densities, viscosities and electrical conductivities at ambient and elevated temperatures are discussed. Walden rule plots are used to estimate the ionic nature of these ionic liquids, and comparison with other studies reveals that most of the investigated ionic liquids show Walden rule values similar to many non-protic ionic liquids containing imidazolium, pyrrolidinium, tetraalkylammonium, or tetraalkylphosphonium cations. Comparison of literature data reveals major disagreements in the reported properties for the investigated ionic liquids. A detailed analysis of the reported experimental procedures suggests that inappropriate drying methods can account for some of the discrepancies. Furthermore, an example for the improved presentation of experimental data in scientific literature is presented.

## Introduction

Clean energy production ranks highly amongst several human challenges that need to be resolved in order to secure our future. Fossil fuel combustion is still our dominating method to generate electric power. This results in emitting large amounts of $CO_2$, which is considered to be a major contributor to anthropogenic global warming. Power that is generated from renewable resources, such as wind and solar, is the most promising alternative to produce sustainable energy, but a major drawback is its intermittency. However, it has been shown that $CO_2$ can be converted into methanol, or maybe even isopropanol, in solar driven photoelectrochemical cells.[1,2] This approach, referred to as "chemical carbon mitigation", has the potential to solve two problems at once: (i) it can sequestrate $CO_2$, and (ii) it does provide an alternative for storing renewable energy. In order to successfully perform chemical carbon mitigation it requires improved technologies for the efficient, reversible and economic capture of $CO_2$.

Aqueous alkanolamines are widely used for the removal of $CO_2$ from industrial flue gas.[3] Advantages of monoethanolamine for example are low cost, reasonable thermal stability, low thermal degradation rate, high reactivity towards $CO_2$, and a low molecular weight resulting in a favorable absorption capacity on a mass basis.[4] However, monoethanolamine, and other alkanolamine, solutions are far from being ideal due to drawbacks with regard to corrosion, recovery, regeneration, and losses because of their relatively high vapor pressure.[4–8]

Room temperature ionic liquids (RTILs) offer many opportunities to reassess and improve existing technologies and processes.[9–11] RTILs are salts that exhibit melting temperatures at or below room temperature. Their unique chemistry is responsible for many advantages compared to molecular solvents, which can be exploited in chemical engineering applications such as gas separations.[3] The high solubility of $CO_2$ in many RTILs offers the possibility to exploit them in different media, such as aqueous or non-aqueous solutions, membranes or as pure solvents, for $CO_2$ trapping.[8,12–17] In that respect, particular attention has been devoted to ionic liquids (ILs) that mimic alkanolamine chemistry.[7,18–22] However, in the end it will be the physical properties, such as viscosity and in particular thermal stability, of these ILs that will decide on their suitability for possible industrial applications.

*Department of Chemical and Process Engineering, University of Canterbury, Christchurch, New Zealand. E-mail: ken@kbmarsh.com; Fax: +64 3364 2063; Tel: +1 480 802 8911*

† Electronic supplementary information (ESI) available: (1) Thermal decomposition temperatures of investigated AAILs; (2) tabulated summary of relevant experimental information reported in the literature on the measurements of the density, viscosity and electrical conductivity of the investigated AAILs; and (3) tabulated presentation of the experimental results of the density, viscosity and electrical conductivity of the investigated AAILs, including information on instrument calibration, sample purity, error analysis, and comparison with literature data. See DOI: 10.1039/c0cp02222e

The general properties of protic alkanolammonium ionic liquids (AAILs) have been the subject of many studies. Investigations include their role as catalysts in chemical reactions,[23–25] the thermophysical behavior of binary mixtures of AAILs with water or short chain alcohols,[26,27] the ability of AAILs to stabilize enzymes and to promote their activity,[28] their ionic nature and suitability to act as electrolytes in fuel cells,[29,30] their nanostructure,[31] their electrochemical properties,[32] and their ability to dissolve gases such as $CO_2$[21,22] and $SO_2$.[33] Recently, our group investigated the influence of both the cation structure (ethanolammonium, diethanolammonium, triethanolammonium, propan-1-olammonium, diallylammonium) and the nature of the anion (formate, acetate, malonate) of protic ILs on their ability to dissolve crystalline cellulose.[34] Although physicochemical properties such as density, viscosity or electrical conductivity of some of those AAILs have been reported previously,[23,30–33,35–37] it is not possible to derive a common structure–property relationship for these types of ILs mainly because of the inconsistency, variability and lack of data. The majority of these studies focused on two AAILs, *viz.* ethanolammonium formate and ethanolammonium acetate,[21–24,26–29,31,33,35–41] but only two groups reported measurements covering temperature ranges.[23,37] Little data are available on ILs containing the diethanolammonium and triethanolammonium cation,[21–23,25,26,30–32,42] and just a few patents have been published on alkanolammonium malonates or ILs containing the diallylammonium or the propan-1-olammonium cation.[43–52] In addition, the nomenclature of AAILs in the literature varies significantly resulting in incorrect novelty claims and confusion about the correct structure of the studied ILs.[23,27,35] Therefore, we believe that a comprehensive evaluation of the physicochemical properties of these ILs, including a detailed comparison with literature data, is necessary and of value for future research in this field.

The aim of this study is (i) to measure the density, viscosity, and the electrical conductivity of 15 AAILs with varying cations and anions in order to establish structure–property relationships; (ii) to provide an estimate of the ionic nature of these ILs by applying Walden's rule; (iii) to compare our results with literature data; and (iv) to gather information about the experimental conditions in other studies in order to suggest an explanation for the significant variations in the property data reported.

## Results and discussion

The investigated AAILs were prepared *via* proton exchange reactions between amines and organic acids (Fig. 1). Their synthesis and characterization is described elsewhere.[34] Fig. 2 shows the particular starting materials that were used for the

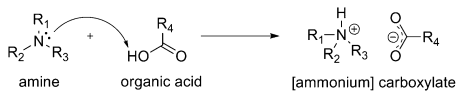


**Fig. 1** Synthesis of alkanolammonium ionic liquids: proton exchange reactions between organic acids and amines result in ammonium carboxylates.

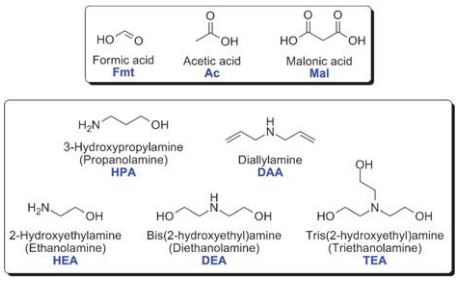


**Fig. 2** Organic acids and amines used for the synthesis of alkanolammonium ionic liquids.

IL synthesis. Five different amines (mainly ethanolamines) were used to study the effect of the cation structure on selected properties of the resulting ILs. Table 1 summarizes the acronyms of all ILs and amines that are compared in this study. Structural variations on the cation include (i) the number of carbon atoms between the hydroxy group and the nitrogen atom (HEA < HPA), (ii) the number of alkanol substituents on the nitrogen atom (HEA < DEA < TEA), and (iii) the replacement of alkanol substituents with allyl groups (DAA). The anions vary in both their number of $–CO_2H$ groups (Fmt = Ac < Mal) and their number of α-carbons (Fmt < Ac = Mal).

The purity of the ILs was evaluated *via* $^1$H Nuclear Magnetic Resonance (NMR) spectroscopy.[34] Apart from negligible traces of condensation by-products in the case of [DEA] and [TEA] malonates, all but one of the investigated ILs were confirmed to be pure. The exception was [DAA]Fmt, with $^1$H NMR and pH studies questioning the purity of the final compound.[34] However, we decided to include [DAA]Fmt in our studies and to include its purity issues in the discussion. An important note is our observation that conventional drying techniques are not suitable for the studied ILs, probably due to both their protic nature and the volatility of some of the starting materials. However, molecular sieves can be used to gently reduce the IL's water content to a minimum without promoting decomposition.[34]

In order to evaluate the effect of the cation structure on the investigated properties, the studied ILs have been categorized

**Table 1** Acronyms for ionic liquid ions and ethanolamines

| Acronym | Explanation |
|---|---|
| [HEA] | 2-Hydroxyethylammonium |
| [HPA] | 3-Hydroxypropylammonium |
| [DEA] | Bis(2-hydroxyethyl)ammonium |
| [TEA] | Tris(2-hydroxyethyl)ammonium |
| [DAA] | Diallylammonium |
| [EMIM] | 1-Ethyl-3-methylimidazolium |
| [BMIM] | 1-Butyl-3-methylimidazolium |
| HEA | Ethanolamine |
| DEA | Diethanolamine |
| TEA | Triethanolamine |
| Fmt | Formate |
| Ac | Acetate |
| Mal | Malonate |

into three groups according to their type of anion: formate, acetate and malonate. Additionally, two common imidazolium ILs 1-ethyl-3-methylimidazolium acetate ([EMIM]Ac) and 1-butyl-3-methylimidazolium acetate ([BMIM]Ac) were included in the discussion in order to put the results of the alkanolammonium ILs into perspective. Furthermore, the measurements are compared to property data of three ethanolamines (mono-, di- and tri-) which served as starting materials for some of the investigated ILs.[53] All literature data on the relevant properties of the investigated ILs are included, but they will be discussed separately. Another aspect to consider are the limited thermal stabilities of some AAILs,[34] particularly the diallylammonium ILs (see ESI 1†). Consequently, the results obtained from measurements at elevated temperatures need to be treated with reservation. However, it is assumed that the property data obtained at elevated temperatures can be representative for the pure ILs if the results did not show unexpected deviations at these temperatures.

### Density

The densities of the ILs were measured at temperatures from (278 to 348) K, and the results cover a density range from (910 to 1347) kg·m$^{-3}$, decreasing linearly with increasing temperature (Fig. 3). The diallylammonium ILs display significantly lower densities than the other AAILs due to the lack of hydroxy groups which are strong hydrogen bond participants.[6] Larger numbers of hydroxy groups on the cation ([DAA] < [HEA] = [HPA] < [DEA] < [TEA]) result in more interionic hydrogen bonds and consequently in higher densities. In the case of AAIL formates and acetates, AAILs with three cationic hydroxy groups do not display much greater density values compared to cations with two hydroxy groups. This is in contrast to the malonates where all AAILs exhibit similar densities, apart from the two extremes [DAA]Mal and [TEA]Mal that contain either none or three cationic hydroxy groups. In general, AAIL acetates show lower densities than the formates with the exception of [HEA]Ac and [DAA]Ac. The corresponding malonates display the highest density values due to the increased size of the anion. Increasing the number of carbon atoms between the cationic hydroxy group and the nitrogen atom from two to three ([HEA] < [HPA]) does not significantly affect the AAIL density. This excludes the exception [HEA]Ac, as mentioned before (*vide supra*). As expected, all ethanolammonium ILs ([HEA], [DEA], [TEA]) present higher densities than their ethanolamine starting materials (HEA, DEA, TEA). All AAILs with cationic hydroxy groups show higher densities than the investigated imidazolium acetates without OH-groups ([EMIM] < [BMIM]), only [HPA]Ac and [DAA]Mal exhibit densities comparable to [EMIM]Ac. To summarize, two factors govern the AAIL density: (i) the ion size and (ii) the presence of hydroxy groups on both cations and anions. Larger ions result in less denser ILs, whereas an increasing number of hydroxy groups on both ions results in increased densities. Amongst all investigated AAILs the acetates show the lowest densities, with the exception of the ethanolammonium cation ([HEA]Ac > [HEA]Fmt).

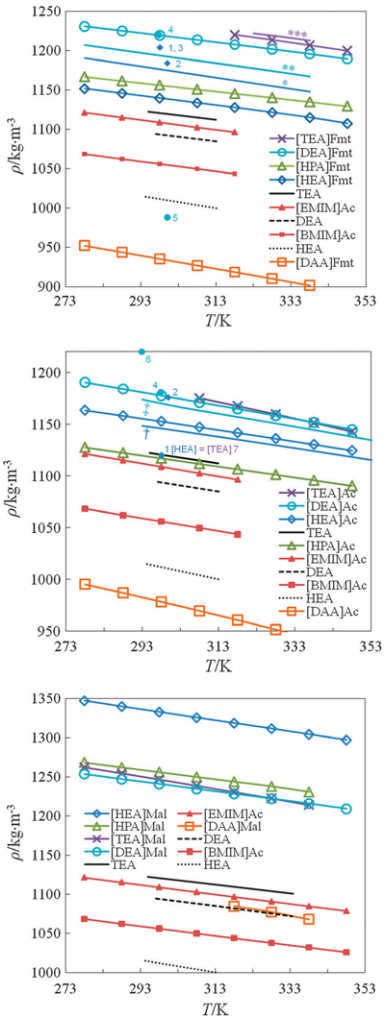


**Fig. 3** Densities of AAILs at temperatures from (278 to 348) K grouped by their anions. The densities of three alkanolamines (HEA, DEA, TEA),[53] two imidazolium acetate ILs ([EMIM]Ac, [BMIM]Ac) and available literature data on the investigated AAILs are included for the purpose of comparison. [HEA]: *,[23] †,[37] 1,[33] 2,[36] 3;[35] [DEA]: **,[23] ‡,[37] 4,[30] 5,[31] 6;[32] [TEA]: ***,[23] 7.[33] See Table 1 for acronym explanation.

### Viscosity

The viscosities of the ILs were measured at temperatures from (278 to 358) K, and the results cover a viscosity range from (3 to 833) mPa·s, with viscosities decreasing with increasing temperature (Fig. 4). With regard to the AAIL formates it is the cation that dictates the viscosity of the IL, resulting in higher viscosity values with both increasing ion size and

 

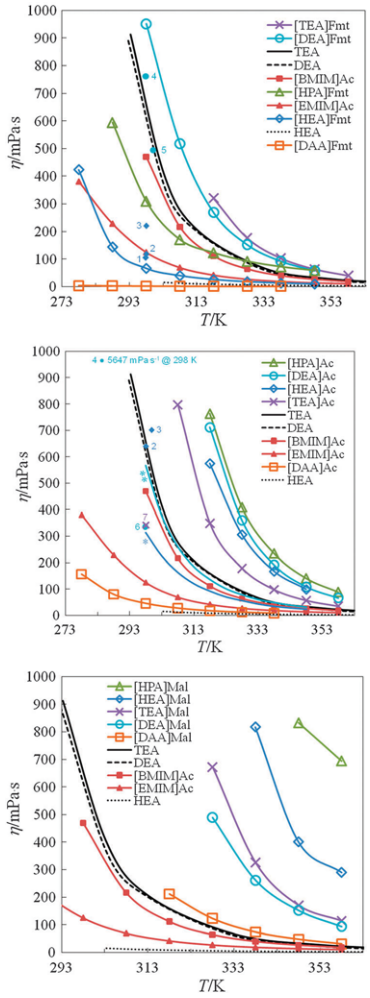


**Fig. 4** Viscosities of AAILs at temperatures from (278 to 358) K grouped by their anions. The viscosities of three alkanolamines (HEA, DEA, TEA),[53] two imidazolium acetate ILs ([EMIM]Ac, [BMIM]Ac) and available literature data on the investigated AAILs are included for the purpose of comparison. [HEA]: *,[37] 1,[35] 2,[33] 3;[36] [DEA]: **,[37] 4,[30] 5,[31] 6;[32] [TEA]: 7.[33] See Table 1 for acronym explanation.

increasing number of cationic hydroxy groups present ([DAA] < [HEA] < [HPA] < [DEA] < [TEA]). The lack of hydroxy groups on the diallylammonium cation [DAA]Fmt explains its significantly lower viscosities compared to the other AAIL formates. AAIL acetates generally show greater viscosities compared to their formates. The anionic viscosity effect is most obvious if no cationic hydroxy groups are present ([DAA]Ac), resulting in significantly higher viscosity compared to the corresponding formate ([DAA]Fmt < [DAA]Ac). However, the effect of the anion on the viscosities of AAILs is not obvious. To give an example, the viscosities of [TEA]Ac and [TEA]Fmt differ marginally with respect to the increase in viscosity observed with other AAILs. This results in [TEA]Ac being the ethanolammonium acetate with the lowest viscosities, as compared to its formate derivative ([TEA]Fmt) which showed the highest viscosities of all studied AAIL formates. Furthermore, the fact that propan-1-olammonium acetate displays higher viscosities than diethanolammonium acetate ([DEA]Ac < [HPA]Ac) also demonstrates the influence of the anion on the AAIL viscosities. Amongst the ILs studied, the AAIL malonates show the highest viscosities due to the size of the anion and the number of hydroxy groups. It is probably because of the increased number of hydroxy groups of the anion that an increased number of cationic hydroxy groups does not result in higher viscosities of the AAIL malonates. All AAIL malonates with cationic hydroxy groups display higher viscosities than the diallylammonium malonate, but both monoalcohol ILs exhibit higher viscosities than their multi-alcohol derivatives ([DEA] < [TEA] < [HEA] < [HPA]). In fact, [DEA]Mal and [TEA]Mal show significantly lower viscosities than the monoethanolammonium IL [HEA]Mal. The highest viscosities are displayed by propan-1-olammonium malonate ([HPA]Mal), however it is questionable whether this high value can be attributed to the longer alkyl chain on the cation as it was shown before (*vide supra*) that the cation size does not govern the viscosity behavior of the AAIL malonates. As expected, due to their ionic nature, the viscosities of the ethanolammonium ILs are always higher than those of their ethanolamine starting materials. Only the AAIL formates display viscosities comparable to the selected imidazolium acetate ILs, *viz*. [HPA]Fmt ≈ [BMIM]Ac and [HEA]Fmt ≈ [EMIM]Ac. All AA acetates and malonates show higher viscosities than the studied imidazolium acetates, with the exception of diallylammonium acetate, and the viscosities of the studied imidazolium ILs are governed by their ion size ([DAA]Ac < [EMIM]Ac < [BMIM]Ac). To summarize, the viscosities of AAIL formates are governed by both ion size and attractive interionic interactions, *viz*. hydrogen bonds. This observation is not valid for the corresponding acetates and malonates where the effect of the anion is more substantial, resulting in viscosity trends that are problematic to anticipate.

### Electrical conductivity

The electrical conductivities of the studied ILs were measured at temperatures from (278 to 348) K, and the results cover a conductivity range from ($4.8 \times 10^{-4}$ to 2.3) $S \cdot m^{-1}$, increasing with increasing temperature (Fig. 5). The conductivity pattern of the AAIL formates is governed by their ion mobility, similar to their viscosity behavior (*vide supra*). Small ions with little interionic interactions should result in high conductivities and *vice versa*, however the diallylammonium formate does not follow this trend, displaying electrical conductivities in the range from ($0.5$ to $1.1$) $\times 10^{-3}$ $S \cdot m^{-1}$ ([DAA] < [TEA] < [DEA] < [HPA] < [HEA]). Several conductivity measurements with different [DAA]Fmt samples confirmed

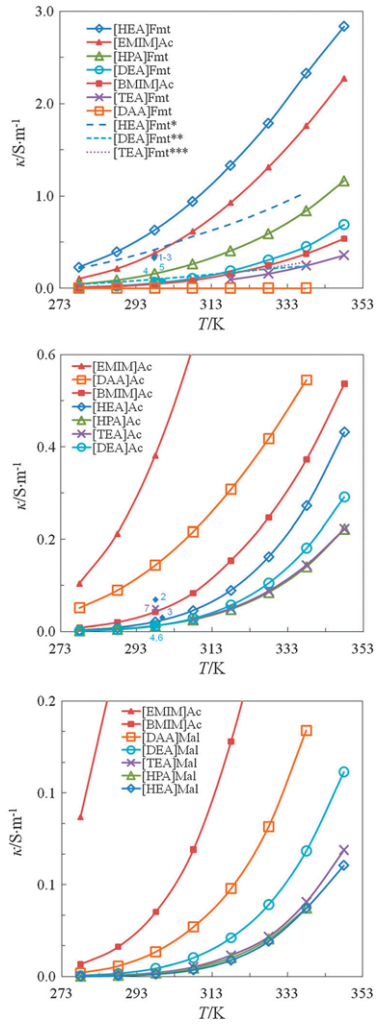


**Fig. 5** Electrical conductivities of AAILs at temperatures from (278 to 348) K grouped by their anions. The electrical conductivities of two imidazolium acetate ILs ([EMIM]Ac, [BMIM]Ac) and available literature data on the investigated AAILs are included for the purpose of comparison. [HEA]: *,[23] 1,[35] 2,[33] 3;[36] [DEA]: **,[23] 4,[30] 5,[31] 6;[32] [TEA]: ***,[23] 7.[33] See Table 1 for acronym explanation.

these results, indicating that the ion mobility in [DAA]Fmt was very low. These findings support the assumption, based upon $^1$H NMR studies of [DAA]Fmt,[34] that the diallylamine did not react successfully with the formic acid. As anticipated, the AAIL acetates show lower conductivities than the formates, with the diallylammonium cation ([DAA]Ac) displaying the highest and the triethanolammonium cation ([TEA]Ac) displaying the lowest values. The decrease of conductivity from the AAIL formates to the acetates depends on the nature of the cation. Compared to the AAIL formates, the corresponding acetates with mobile cations, such as [HEA], show a more significant decrease in electrical conductivity than cations with lower mobility, such as [TEA]. To give an example, the electrical conductivity at 298 K decreases from [HEA]Fmt to [HEA]Ac from (2.83 to 0.43) S·m$^{-1}$, whereas the decrease in conductivity from [TEA]Fmt to [TEA]Ac is from (0.36 to 0.22) S·m$^{-1}$. Consequently, [HPA]Ac and [TEA]Ac show very similar conductivity values although the two cations differ significantly in size and number of hydroxy groups ([HPA]Ac ≈ [TEA]Ac). Furthermore, diethanolammonium acetate exhibits higher conductivities than propan-1-olammonium acetate ([HPA]Ac < [DEA]Ac). The AAIL malonates show the lowest electrical conductivities of the ILs studied, with [DAA]Mal being the most conductive with 0.16 S·m$^{-1}$ at 338 K. The effect of the malonate anion dominates the conductive behavior of the studied monoalcohol and trialcohol ILs ([HEA]Mal ≈ [HPA]Mal ≈ [TEA]Mal). Only diethanolammonium malonate ([DEA]Mal) shows higher conductivity values, but still lower when compared to diallylammonium malonate ([DEA]Mal < [DAA]Mal). The conductivities of the AAIL formates are in the same range as the conductivities of the imidazolium acetates, with [EMIM]Ac showing slightly lower conductivities than [HEA]Fmt and with [BMIM]Ac showing slightly lower conductivities than [DEA]Fmt. With regard to the AAIL acetates, only [DAA]Ac exhibits conductivity values similar to the two imidazolium ILs ([BMIM]Ac < [DAA]Ac < [EMIM]Ac). All AAIL malonates have lower conductivities than the compared imidazolium ILs. To summarize, the electrical conductivities of most AAIL formates are governed by their cation mobility, whereas the corresponding malonates are dominated by the mobility of their anions ([AA]Mal < [AA]Ac < [AA]Fmt). [HPA]Ac displays conductivities that are both lower than expected and similar to [TEA]Mal. The conductivity of [DAA]Fmt is unexpectedly low, confirming our doubts regarding its molecular state.

### Walden rule

The tendency of ILs to form independent, non-associated ions is of significant importance to a wide range of applications and can be described with the Walden equation.[54] The Walden rule relates the mobility of ions to the fluidity of their surrounding medium according to:

$$\Lambda\eta = k \qquad (1)$$

where $\Lambda$ is the molar conductivity and $\eta$ is the viscosity; $k$ is a temperature dependent constant. On a logarithmic plot of the molar conductivity $\Lambda$, representing the ion mobility, *vs.* the fluidity $\phi$ ($\phi = \eta^{-1}$) one can compare the tendency to form ions of non-aqueous electrolyte solutions, molten salts and ionic liquids.[54–56] An "ideal" reference line, established by using dilute aqueous KCl solutions, is representative for independent ions without any interionic interactions.[57] The proximity of the plotted values to the KCl reference line is an indicator of the interionic interactions between IL anions and

 

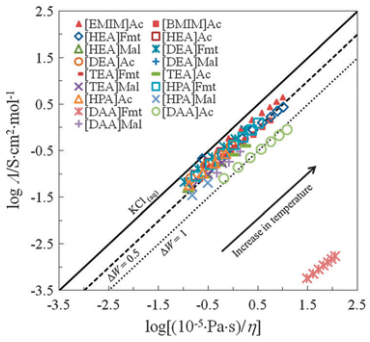


**Fig. 6** Walden plot for alkanolammonium ILs and two imidazolium acetate ILs at temperatures from (278 to 358) K. $\Delta W$ denotes the vertical distance to the KCl line. See Table 1 for acronym explanation.

cations. Walden plot values above the reference line are typical for highly ionic solutions such as concentrated mineral acids.[56] ILs with high tendency to form ions are located close to the reference line, while ILs with low tendency to form ions are situated further away. $\Delta W$ denotes the vertical distance to the KCl line and it is used to define the extent to which a fluid is ionic. A $\Delta W$ value of 0.5, for example, means that an IL displays 31.6 % of the ionic conductivity compared to the KCl line, and a $\Delta W$ value of 1 corresponds to 10 % of the reference conductivity.

Fig. 6 shows a Walden plot for the ILs investigated in this study. All but one of the ILs are found to be within the $\Delta W = 1$ region, with many of the ILs even being closer than $\Delta W = 0.5$ to the KCl line. Consequently, the estimated ionicities of most AAILs in this study are similar to those of many non-protic ILs that contain imidazolium, pyrrolidinium, tetraalkylammonium, or tetraalkylphosphonium cations.[54–57] One exception amongst the AAILs is diallylammonium formate ([DAA]Fmt) with Walden product values well below the ideal KCl line. The question can be raised as to whether this compound can still be described as an ionic liquid, confirming the doubts of a successful reaction between the starting materials as discussed above (*vide supra*). To summarize, most of the studied AAILs show Walden products comparable to non-protic ILs.

**Comparison with literature data and suggestions for the presentation of ancillary information**

Eight publications are available with reports of either the density, the viscosity or the electrical conductivity of the ILs investigated.[23,30–33,35–37] Almost none of the separately measured data agrees with each other and significant deviations are not uncommon. Most literature densities agree within 6 % relative to our results, but outliers show relative deviations of 23 %.[31] Our measured densities are consistent with the data of Burrell *et al.*[30] and the relative deviations to Cota *et al.*[23] range from (0.5 to 4.5) %, depending on the AAIL one whishes to compare. With regard to viscosities, relative deviations of literature data are very significant with outliers differing as much as 800 %.[32] However, our measurements agreed most with the results reported by Burrell *et al.*[30] The reported electrical conductivities show relative deviations of up to 120 % and the results of Burrell *et al.*[30] are, once again, among the literature reports that agree best with our data (see ESI 3† for a full error analysis).

In order to evaluate the reasons for the significant differences in the reported data, we summarized all the relevant experimental background information including the IL synthesis, purification steps, water contents, measurement methods and associated uncertainties (see ESI 2†). First of all, it becomes obvious that many reports only possess limited credibility due to their lack of accurate information, such as temperatures for example. Second, different methods with often unreported uncertainty were employed to obtain property data, and information about instruments used and temperature calibration is scarce. Third, the water content has not always been determined prior to measurement, and very little information is given on whether or not the measurements were conducted in a moisture-free atmosphere. In addition, none of the literature data did measurements of the water content of the IL after the property measurement. Considering the highly hygroscopic nature of these AAILs, due to the presence of a number of hydroxy groups, absorption of ambient moisture during the measurement can be a major reason for the reported differences in AAIL property data. Fourth, information about degassing prior to the measurement is rarely given. Fifth, reported syntheses and drying methods do vary significantly, and, in our opinion, it could be the harsh drying conditions that account for the large differences in the reported property data. Common drying techniques for the preparation of AAILs are vacuum drying at elevated temperatures or freeze drying. However, heating is most likely to promote proton-back transfer of these protic ILs with the possibility of evaporation of the volatile acid component, resulting in a mixture of IL and unreacted amine.[34] Both, Burrell *et al.*[30] and Cota *et al.*[23] prepared their AAILs without applying harsh drying techniques, however no IL water content was determined by the latter group. The fact that our experimental results agree best with those of Burrell *et al.*[30] and Cota *et al.*[23] strongly suggests that the drying method can have a major influence on the purity of protic AAILs containing volatile acid components.

In order to improve the presentation of experimental results and ancillary data in the literature, we believe that it is helpful to provide a tabulated summary of the experimental results including: CAS registry number, purity of the compound, water content before and after the measurement, instruments and methods used, associated uncertainties of variables, calibration procedures, atmosphere during the measurement, fit function with standard deviation, a tabulation of the experimental results including fitting constants, available literature data along with comments on their experimental procedures, and deviation plots of (i) the fit function and (ii) available literature data with respect to the presented experimental results. The availability of such data in a summarized form offers several advantages: (i) it facilitates data comparison, (ii) it allows quick evaluation of the experimental procedures used by other groups, and (iii) the use of CAS registry numbers helps to avoid confusion due to

nomenclature issues. An example of the suggested data representation is provided in the ESI 3.†

## Experimental

### Materials and methods

The synthesis and characterization (including NMR, FT-IR, TGA, and Karl-Fischer water analysis) of the investigated ILs has been reported previously.[34] The reference ionic liquid 1-hexyl-3-methylimidazolium bis(trifluoromethylsulfonyl) amide ([HMIM]$Tf_2N$) was prepared according to the literature[58] and contained a water mass fraction of $2 \times 10^{-5}$. The commercial ILs 1-ethyl-3-methylimidazolium acetate ([EMIM]Ac) and 1-butyl-3-methylimidazolium acetate ([BMIM]Ac) were from Fluka and dried by evacuation at 353 K for 48 h prior to use. All studied ILs were degassed at room temperature at a pressure of less than 0.1 kPa for at least 12 h prior to measurements. If necessary, sample temperatures were increased to a maximum of 333 K to facilitate degassing of those ILs with higher viscosities. In cases of limited thermal stability,[34] the pressure was raised to 20 kPa to avoid deprotonation of the cation and subsequent evaporation of the resulting volatile organic acid. To minimize water uptake from the environment all samples were kept under inert gas atmosphere ($N_2$) at all times. Prior to measurements the instrument sample chambers were cleaned with (i) purified water from a Millipore Elix 5 with a final resistivity of 15 MΩ cm and (ii) distilled acetone. Subsequently the sample chambers were flushed with ambient air overnight to ensure complete solvent removal. All instrument sample chambers were then flushed with dry nitrogen gas prior to sample injection. IL sample volumes of 1 mL were required for each instrument.

All IL samples were generally aimed to be measured over a temperature range of (278.15 to 358.15) K at intervals of 10 K, unless restrictions applied due to the thermal stability or the viscosity of the sample. The temperature of the densimeter was measured with an industrial grade platinum resistance thermometer of nominal resistance 100 Ω that had been calibrated against a standard platinum thermometer of nominal resistance 25 Ω, which itself had been calibrated on ITS-90. The temperature of the conductivity cell was measured with the 25 Ω thermometer. Thus, the uncertainty in temperature for the density measurements was estimated to be ±0.02 K, while the uncertainty in temperature for the electrical conductivity measurements was estimated to be ±0.01 K. The temperature of the viscometer was determined with its built-in resistance temperature detector with a stated uncertainty of ±1.0 K.

### Density

Densities were measured with an Anton Paar DMA 602 H vibrating tube densimeter. Prior to measurement, the densimeter was calibrated over a temperature range from (278.15 to 358.15) K with water and air. For this purpose the water was degassed and deionized, and its calculated density values were retrieved from the NIST Chemistry WebBook.[59] Ambient air with a relative humidity of 44.3 % at a temperature of 295.05 K and a pressure of 101.3 kPa was used for calibration, and the density values of the moist air were calculated with consideration of its water content.[60] The calibration was verified with the IUPAC reference ionic liquid [HMIM]$Tf_2N$.[61] The combined expanded ($k = 2$) relative uncertainty of the density measurements was estimated to be 0.3 %.

### Viscosity

Viscosities were measured with a cone and plate Brookfield DV-II + Pro viscometer (model LVDV-11) with a CPE-40 cone spindle. Prior to measurement, the viscometer was calibrated over a temperature range from (278.15 to 333.15) K with reference oils (Canon S20 and S60, and Paragon N10, N100 and N1000) covering a viscosity range from (6 to 865) mPa·s, and verified with the IUPAC reference ionic liquid [HMIM]$Tf_2N$.[61] Only viscosities of less than 1 Pa·s were measurable, and the resulting combined expanded ($k = 2$) relative uncertainty of the viscosity measurements was estimated to be 3.0 %.

### Electrical conductivity

Electrical conductivities were measured with a conductivity flow cell (LKB model 5312 A) made from borosilicate glass with two platinum black electrodes.[62] The maximum operating temperature of the conductivity cell was 348.15 K due to restrictions imposed by its plastic framework. The resistance $R(f)$ of the cell was determined with a Fluke PM 6306 RCL meter at a frequency $f$ of 1 kHz, and the electrical conductivity $\kappa$ was calculated according to

$$\kappa = \frac{K}{R} \tag{2}$$

with a cell constant $K$ of 90.1 $m^{-1}$.[62] Prior to measuring the ILs, the accuracy of the conductivity measurements was checked over a temperature range from (278.15 to 323.15) K with the IUPAC reference ionic liquid [HMIM]$Tf_2N$.[61] The combined expanded ($k = 2$) relative uncertainty of the measurements was estimated to be 2.0 %. Previously, Kandil *et al.* determined the frequency dependency for the IUPAC reference ionic liquid [HMIM]$Tf_2N$ from (0.5 to 10) kHz, and the extrapolation from 1 kHz to infinite frequency as $f^{-1}$ gave an additional relative uncertainty of less than 0.5 %.[62]

## Conclusion

Establishing structure–property relationships of ILs enhances our understanding of this fascinating class of solvents which still offers many opportunities for exploration. Such knowledge will assist our efforts to use computational calculations in order to systematically screen for novel ILs with task specific properties. However, computational chemists prefer agreement with the experimental data sets for this purpose, but literature data on experimental properties can vary significantly, especially with regard to newer compounds which lack commonly accepted procedures for their preparation and purification. Due to the lack of standards in the presentation of experimental data and ancillary information, it can be very difficult to account for the differences in the reported literature values.

In order to address these issues, we investigated the structure–property relationship of a set of protic ILs that are of interest for their use in gas separation processes or as electrolytes in fuel cells. Our study explored the properties of

 

hitherto unstudied ILs and it extended the property knowledge of ILs that have already been targeted for potential industrial applications. However, the limited thermal stability of this type of protic ILs will restrict their use to operating temperatures below 373 K (see ESI 1†). Detailed comparison of the experimental procedures, applied by different groups to obtain AAIL property data, did offer explanations for the, sometimes significant, disagreement in the reported data. Finally, we presented an example for the improved presentation of experimental data with the aim to motivate other researchers to adopt and further refine our suggestions.

## Acknowledgements

The authors wish to thank Owen Curnow from the UoC Chemistry Department for permission to use the Brookfield viscometer. Funding from the New Zealand Foundation for Research, Science and Technology (FRST) is gratefully acknowledged.

## References

1 E. E. Barton, D. M. Rampulla and A. B. Bocarsly, *J. Am. Chem. Soc*., 2008, **130**, 6342–6344.
2 B. Halford, *Chem. Eng. News*, 2010, **88**, 40–41.
3 J. E. Bara, D. E. Camper, D. L. Gin and R. D. Noble, *Acc. Chem. Res*., 2009, **43**, 152–159.
4 N. McCann, M. Maeder and M. Attalla, *Ind. Eng. Chem. Res*., 2008, **47**, 2002–2009.
5 J. Alejandre, J. L. Rivera, M. A. Mora and V. de la Garza, *J. Phys. Chem. B*, 2000, **104**, 1332–1337.
6 R. López-Rendón, M. A. Mora, J. Alejandre and M. E. Tuckerman, *J. Phys. Chem. B*, 2006, **110**, 14652–14658.
7 K. E. Gutowski and E. J. Maginn, *J. Am. Chem. Soc*., 2008, **130**, 14690–14704.
8 E. F. da Silva and H. F. Svendsen, *Ind. Eng. Chem. Res*., 2005, **45**, 2497–2504.
9 *Ionic Liquids, Industrial Applications to Green Chemistry*, ed. J. D. Holbrey and R. D. Rogers, Oxford University Press and The American Chemical Society, Washington, DC, 2002.
10 J. Adams Christopher, in *Ionic Liquids*, ed. R. D. Rogers and K. R. Seddon, American Chemical Society, Washington, DC, 2002, vol. 818, ch. 2, pp. 15–29.
11 K. R. Seddon, *J. Chem. Technol. Biotechnol*., 1997, **68**, 351.
12 A. Yokozeki, M. B. Shiflett, C. P. Junk, L. M. Grieco and T. Foo, *J. Phys. Chem. B*, 2008, **112**, 16654–16663.
13 S. Raeissi and C. J. Peters, *Green Chem*., 2009, **11**, 185–192.
14 A. P. S. Kamps, D. Tuma, J. Xia and G. Maurer, *J. Chem. Eng. Data*, 2003, **48**, 746–749.
15 M. B. Shiflett, D. J. Kasprzak, C. P. Junk and A. Yokozeki, *J. Chem. Thermodyn*., 2008, **40**, 25–31.
16 L. E. Barrosse-Antle and R. G. Compton, *Chem. Commun*., 2009, 3744–3746.
17 P. Husson-Borg, V. Majer and M. F. Costa Gomes, *J. Chem. Eng. Data*, 2003, **48**, 480–485.
18 Y. Zhao, X. Zhang, S. Zeng, Q. Zhou, H. Dong, X. Tian and S. Zhang, *J. Chem. Eng. Data*, 2010, **55**, 3513–3519.
19 C. Wang, S. M. Mahurin, H. Luo, G. A. Baker, H. Li and S. Dai, *Green Chem*., 2010, **12**, 870–874.
20 B.-J. Hwang, S.-W. Park, D.-W. Park, K.-J. Oh and S.-S. Kim, *Sep. Sci. Technol*., 2009, **44**, 1574–1589.
21 K. A. Kurnia, F. Harris, C. D. Wilfred, M. I. Abdul Mutalib and T. Murugesan, *J. Chem. Thermodyn*., 2009, **41**, 1069–1073.
22 X. Yuan, S. Zhang, J. Liu and X. Lu, *Fluid Phase Equilib*., 2007, **257**, 195–200.
23 I. Cota, R. Gonzalez-Olmos, M. Iglesias and F. Medina, *J. Phys. Chem. B*, 2007, **111**, 12468–12477.
24 C. Yue, A. Mao, Y. Wei and M. Lü, *Catal. Commun*., 2008, **9**, 1571–1574.
25 Y. O. Sharma and M. S. Degani, *Green Chem*., 2009, **11**, 526–530.
26 J. Wang, X. Li, H. Meng, C. Li and Z. Wang, *J. Chem. Thermodyn*., 2009, **41**, 167–170.
27 M. Iglesias, A. Torres, R. Gonzalez-Olmos and D. Salvatierra, *J. Chem. Thermodyn*., 2008, **40**, 119–133.
28 J. P. Mann, A. McCluskey and R. Atkin, *Green Chem*., 2009, **11**, 785–792.
29 B. Nuthakki, T. L. Greaves, I. Krodkiewska, A. Weerawardena, M. I. Burgar, R. J. Mulder and C. J. Drummond, *Aust. J. Chem*., 2007, **60**, 21–28.
30 G. L. Burrell, I. M. Burgar, F. Separovic and N. F. Dunlop, *Phys. Chem. Chem. Phys*., 2010, **12**, 1571–1577.
31 T. L. Greaves, D. F. Kennedy, S. T. Mudie and C. J. Drummond, *J. Phys. Chem. B*, 2010, **114**, 10022–10031.
32 C. Zhao, G. Burrell, A. A. J. Torriero, F. Separovic, N. F. Dunlop, D. R. MacFarlane and A. M. Bond, *J. Phys. Chem. B*, 2008, **112**, 6923–6936.
33 X. L. Yuan, S. J. Zhang and X. M. Lu, *J. Chem. Eng. Data*, 2007, **52**, 596–599.
34 A. Pinkert, K. N. Marsh and S. Pang, *Ind. Eng. Chem. Res*., 2010, **49**(22), 11809–11813.
35 N. Bicak, *J. Mol. Liq*., 2004, **116**, 15–18.
36 T. L. Greaves, A. Weerawardena, C. Fong, I. Krodkiewska and C. J. Drummond, *J. Phys. Chem. B*, 2006, **110**, 22479–22487.
37 K. A. Kurnia, C. D. Wilfred and T. Murugesan, *J. Chem. Thermodyn*., 2009, **41**, 517–521.
38 M.-M. Huang and H. Weingaertner, *ChemPhysChem*, 2008, **9**, 2172–2173.
39 D. Hekmat, D. Hebel, S. Joswig, M. Schmidt and D. Weuster-Botz, *Biotechnol. Lett*., 2007, **29**, 1703–1711.
40 M. Khodadadi-Moghaddam, A. Habibi-Yangjeh and M. R. Gholami, *J. Mol. Catal. A: Chem*., 2009, **306**, 11–16.
41 J. O. Valderrama and P. A. Robles, *Ind. Eng. Chem. Res*., 2007, **46**, 1338–1344.
42 X. Yuan, S. Zhang, J. Liu and X. Lu, *Fluid Phase Equilib*., 2007, **257**, 195–200.
43 B. Cichy, K. Gabarski and J. Wojciechowski, *Polish Patent PL* 162859 B1, 1994.
44 J. H. Zhang, J. R. Faryniarz and M. C. Cheney, *World Patent WO* 2003099250 A1, 2003.
45 J. R. Faryniarz, P. E. Miner, M. C. Cheney and J. Zhang, *World Patent WO* 2003099254 A1, 2003.
46 K. K. Subramanyan, J. R. Faryniarz and J. H. Zhang, *World Patent WO* 2004082652 A1, 2004.
47 J. R. Faryniarz, M. C. Cheney and A. W. Johnson, *World Patent WO* 2004082651 A1, 2004.
48 J. R. Faryniarz, M. C. Cheney and A. W. Johnson, *US Patent US* 2005202054 A1, 2005.
49 J. R. Brand and P. M. Story, *US Patent US* 4752340 A, 1988.
50 A. J. Walker, *British Patent GB* 2412912 A, 2005.
51 A. L. Jenny and J. H. Curtis, *German Patent* DE 1918246, 1969.
52 T. Suga, K. Saito, R. Kato and S. Yamagata, *US Patent US* 2004000355 A1, 2004.
53 M. Diguillo, R. J. Lee, S. T. Shaaeffer, L. L. Brasheri and A. S. Teja, *J. Chem. Eng. Data*, 1992, **37**, 239–242.
54 D. R. MacFarlane, M. Forsyth, E. I. Izgorodina, A. P. Abbott, G. Annat and K. Fraser, *Phys. Chem. Chem. Phys*., 2009, **11**, 4962–4967.
55 M. Yoshizawa, W. Xu and C. A. Angell, *J. Am. Chem. Soc*., 2003, **125**, 15411–15419.
56 C. A. Angell, N. Byrne and J.-P. Belieres, *Acc. Chem. Res*., 2007, **40**, 1228–1236.
57 K. J. Fraser, E. I. Izgorodina, M. Forsyth, J. L. Scott and D. R. MacFarlane, *Chem. Commun*., 2007, 3817–3819.
58 J. A. Widegren and J. W. Magee, *J. Chem. Eng. Data*, 2007, **52**, 2331–2338.
59 NIST Chemistry WebBook, http://webbook.nist.gov/chemistry/fluid/ (accessed Nov. 2009).
60 The Engineering ToolBox, http://www.engineeringtoolbox.com/density-air-d_680.html (accessed Nov. 2009).
61 K. N. Marsh, J. F. Brennecke, R. D. Chirico, M. Frenkel, A. Heintz, J. W. Magee, C. J. Peters, L. P. N. Rebelo and K. R. Seddon, *Pure Appl. Chem*., 2009, **81**, 781–790.
62 M. E. Kandil, K. N. Marsh and A. R. H. Goodwin, *J. Chem. Eng. Data*, 2007, **52**, 2382–2387.

# Appendix D – Characterisation of alkanolammonium ionic liquids

See atom labelling in Figure 13 (page 37) for NMR data assignment.

**2-Hydroxyethylammonium formate, [HEA]Fmt** (CASRN 53226-35-0). $^1$H NMR (DMSO-$d_6$, $\delta$/ppm): 8.34 (s, 1H, H-a), 7.74 (broad, 4H, H-1 & H-4), 3.53 (t, J = 5.5 Hz, 2H, H-3), 2.81 (t, J = 5.5 Hz, 2H, H-2). FT-IR (KBr, $\nu_{max}$/cm$^{-1}$): 2934, 2144, 1589, 1347, 1074, 1023, 869, 766. Thermal decomposition temperatures ($T_{D,1K}$/K, $T_{D,10K}$/K): 336, 384.

**2-Hydroxyethylammonium acetate, [HEA]Ac** (CASRN 54300-24-2). $^1$H NMR (DMSO-$d_6$, $\delta$/ppm): 6.59 (broad, 4H, H-1 & H-4), 3.51 (t, J = 5.5 Hz, 2H, H-3), 2.74 (t, J = 5.5 Hz, 2H, H-2), 1.69 (s, 3H, H-a). FT-IR (KBr, $\nu_{max}$/cm$^{-1}$): 2964, 2162, 1558, 1409, 1339, 1073, 1019, 924, 654. Thermal decomposition temperatures ($T_{D,1K}$/K, $T_{D,10K}$/K): 368, 405.

**2-Hydroxyethylammonium malonate, [HEA]Mal** (CASRN 29870-14-2). $^1$H NMR (DMSO-$d_6$, $\delta$/ppm): 7.79 (broad, 5H, H-1 & H-4 & H-b), 3.55 (t, J = 5.5 Hz, 2H, H-3), 2.93 (s, 2H, H-a), 2.84 (t, J = 5.5 Hz, 2H, H-2). FT-IR (KBr, $\nu_{max}$/cm$^{-1}$): 2921, 2351, 1729, 1155, 1071, 1012, 898, 754. Thermal decomposition temperatures ($T_{D,1K}$/K, $T_{D,10K}$/K): 381, 409.

**3-Hydroxypropylammonium formate, [HPA]Fmt** (CASRN 1246472-52-5). $^1$H NMR (DMSO-$d_6$, $\delta$/ppm): 8.43 (s, 1H, H-a), 6.52 (broad, 4H, H-1 & H-5), 3.45 (t, J = 6.0 Hz, 2H, H-4), 2.81 (t, J = 7.0 Hz, 2H, H-2), 1.68 (m, 2H, H-3). FT-IR (KBr, $\nu_{max}$/cm$^{-1}$): 3264, 3055, 2950, 2830, 2127, 1590, 1365, 1134, 1067, 961, 908, 774. Thermal decomposition temperatures ($T_{D,1K}$/K, $T_{D,10K}$/K): 373, 424.

**3-Hydroxypropylammonium acetate, [HPA]Ac** (CASRN 160819-27-2). $^1$H NMR (DMSO-$d_6$, $\delta$/ppm): 6.92 (broad, 4H, H-1 & H-5), 3.55 (t, J = 6.0 Hz, 2H, H-4), 2.87 (t, J = 7.0 Hz, 2H, H-2), 1.79 (s, 3H, H-a), 1.76 (m, 2H, H-3). FT-IR (KBr, $\nu_{max}$/cm$^{-1}$): 2947, 2171, 1568, 1404, 1337, 1140, 1071, 1015, 966, 921, 654, 618 Thermal decomposition temperatures ($T_{D,1K}$/K, $T_{D,10K}$/K): 373, 415.

**3-Hydroxypropylammonium malonate, [HPA]Mal** (CASRN 630095-22-6). $^1$H NMR (DMSO-$d_6$, $\delta$/ppm): 6.92 (broad, 5-H, H-1 & H-5 & H-b), 3.58 (t, J = 5.5 Hz, 2H, H-4), 2.94 (t, J = 7.0 Hz, 2H, H-2), 2.87 (s, 2H, H-a), 1.78 (m, 2H, H-3). FT-IR (KBr, $\nu_{\max}$/cm$^{-1}$): 2953, 2643, 2604, 1970, 1723, 1582, 1550, 1372, 1243, 1161, 1068, 1033, 959, 905, 759, 667, 584. Thermal decomposition temperatures ($T_{\mathrm{D,1K}}$/K, $T_{\mathrm{D,10K}}$/K): 381, 414.

**Bis(2-hydroxyethyl)ammonium formate, [DEA]Fmt** (CASRN 68391-54-8). $^1$H NMR (DMSO-$d_6$, $\delta$/ppm): 8.46 (s, 1H, H-a), 5.58 (broad, 4H, H-1 & H-4), 3.70 (t, J = 5.5 Hz, 4H, H-3), 2.98 (t, J = 5.5 Hz, 4H, H-2). FT-IR (KBr, $\nu_{\max}$/cm$^{-1}$): 3282, 2805, 1590, 1455, 1378, 1347, 1070, 950, 765. Thermal decomposition temperatures ($T_{\mathrm{D,1K}}$/K, $T_{\mathrm{D,10K}}$/K): 393, 431.

**Bis(2-hydroxyethyl)ammonium acetate, [DEA]Ac** (CASRN 23251-72-1). $^1$H NMR (DMSO-$d_6$, $\delta$/ppm): 6.13 (broad, 4H, H-1 & H-4), 3.65 (t, J = 6.0 Hz, 4H, H-3), 2.89 (t, J = 6.0 Hz, 4H, H-2), 1.87 (s, 3H, H-a). FT-IR (KBr, $\nu_{\max}$/cm$^{-1}$): 3352, 2852, 1564, 1410, 1341, 1100, 1070, 1020, 945, 654 Thermal decomposition temperatures ($T_{\mathrm{D,1K}}$/K, $T_{\mathrm{D,10K}}$/K): 379, 417.

**Bis(2-hydroxyethyl)ammonium malonate, [DEA]Mal** (CASRN 29870-26-6). $^1$H NMR (DMSO-$d_6$, $\delta$/ppm): 5.80 (broad, 5H, H-1 & H-4 & H-b), 3.61 (t, J = 6.0 Hz, 4H, H-3), 2.94 (s, 2H, H-a), 2.83 (t, J = 5.5 Hz, 4H, H-2). FT-IR (KBr, $\nu_{\max}$/cm$^{-1}$): 3365, 2956, 2879, 1720, 1614, 1428, 1361, 1256, 1070, 948, 860, 615. Thermal decomposition temperatures ($T_{\mathrm{D,1K}}$/K, $T_{\mathrm{D,10K}}$/K): 370, 415.

**Tris(2-hydroxyethyl)ammonium formate, [TEA]Fmt** (CASRN 24794-58-9). $^1$H NMR (DMSO-$d_6$, $\delta$/ppm): 8.26 (s, 1H, H-a), 5.32 (broad, 4H, H-1 & H-4), 3.52 (t, J = 5.5 Hz, 6H, H-3), 2.78 (t, J = 5.5 Hz, 6H, H-2). FT-IR (KBr, $\nu_{\max}$/cm$^{-1}$): 3313, 3158, 2939, 2903, 2831, 1599, 1488, 1459, 1403, 1367, 1328, 1258, 1199, 1096, 1081, 1067, 1033, 1006, 918, 775, 666, 608. Thermal decomposition temperatures ($T_{\mathrm{D,1K}}$/K, $T_{\mathrm{D,10K}}$/K): 383, 427.

**Tris(2-hydroxyethyl)ammonium acetate, [TEA]Ac** (CASRN 14806-72-5). $^1$H NMR (DMSO-$d_6$, $\delta$/ppm): 5.00 (broad, 4H, H-1 & H-4), 3.51 (t, J = 6.0 Hz, 6H, H-3), 2.67 (t, J = 6.0 Hz, 6H, H-2), 1.98 (s, 3H, H-a). FT-IR (KBr,

$\nu_{max}$/cm$^{-1}$): 3312, 3160, 2939, 1573, 1488, 1459, 1404, 1328, 1258, 1096, 1081, 1067, 1033, 1006, 918, 607. Thermal decomposition temperatures ($T_{D,1K}$/K, $T_{D,10K}$/K): 357, 392.

**Tris(2-hydroxyethyl)ammonium malonate, [TEA]Mal,** (CASRN 117225-80-6). $^1$H NMR (DMSO-$d_6$, $\delta$/ppm): 6.02 (broad, 5H, H-1 & H-4 & H-b), 3.71 (t, J = 5.5 Hz, 6H, H-3), 3.10 (t, J = 5.5 Hz, 6H, H-2), 2.88 (s, 2H, H-b). FT-IR (KBr, $\nu_{max}$/cm$^{-1}$): 3313, 3160, 2939, 1732, 1590, 1403, 1368, 1246, 1154, 1096, 1067, 1032, 1006, 917, 751, 692, 609. Thermal decomposition temperatures ($T_{D,1K}$/K, $T_{D,10K}$/K): 379, 409.

**Diallylammonium formate, [DAA]Fmt** (CASRN 701913-13-5). $^1$H NMR (DMSO-$d_6$, $\delta$/ppm): 8.20 (s, 1H, H-a), 5.92 to 5.75 (m, 2H, H-3), 5.29 to 5.20 (m, 4H, H-4), 3.93 (d, J = 6.0 Hz, 4H, H-2). FT-IR (KBr, $\nu_{max}$/cm$^{-1}$): 3504, 3083, 2985, 2919, 2866, 1672, 1420, 1398, 1281, 1222, 1187, 1125, 994, 972, 927, 728. Thermal decomposition temperatures ($T_{D,1K}$/K, $T_{D,10K}$/K): 323, 363.

**Diallylammonium acetate, [DAA]Ac** (CASRN 108501-63-9). $^1$H NMR (DMSO-$d_6$, $\delta$/ppm): 7.02 (broad, 2H, H-1), 5.97 to 5.91 (m, 2H, H-3), 5.32 to 5.20 (m, 4H, H-4), 3.31 (d, J = 6.0 Hz, 4H, H-2), 1.93 (s, 3H, H-a). FT-IR (KBr, $\nu_{max}$/cm$^{-1}$): 2986, 2578, 2452, 1710, 1560, 1404, 1333, 1263, 996, 938, 880, 654, 617. Thermal decomposition temperatures ($T_{D,1K}$/K, $T_{D,10K}$/K): 311, 335.

**Diallylammonium malonate, [DAA]Mal** (CASRN 1246472-53-6). $^1$H NMR (DMSO-$d_6$, $\delta$/ppm): 7.16 (broad, 3H, H-1 & H-b), 5.98 to 5.92 (m, 2H, H-3), 5.51 to 5.42 (m, 4H, H-4), 3.57 (d, J = 6.5 Hz, 4H, H-2), 2.85 (s, 2H, H-a). FT-IR (KBr, $\nu_{max}$/cm$^{-1}$): 3405, 2989, 2793, 2447, 1716, 1575, 1424, 1365, 1161, 994, 942, 756, 661, 617. Thermal decomposition temperatures ($T_{D,1K}$/K, $T_{D,10K}$/K): 324, 371.

# Appendix E – Experimental scheme for extracting wood lignin

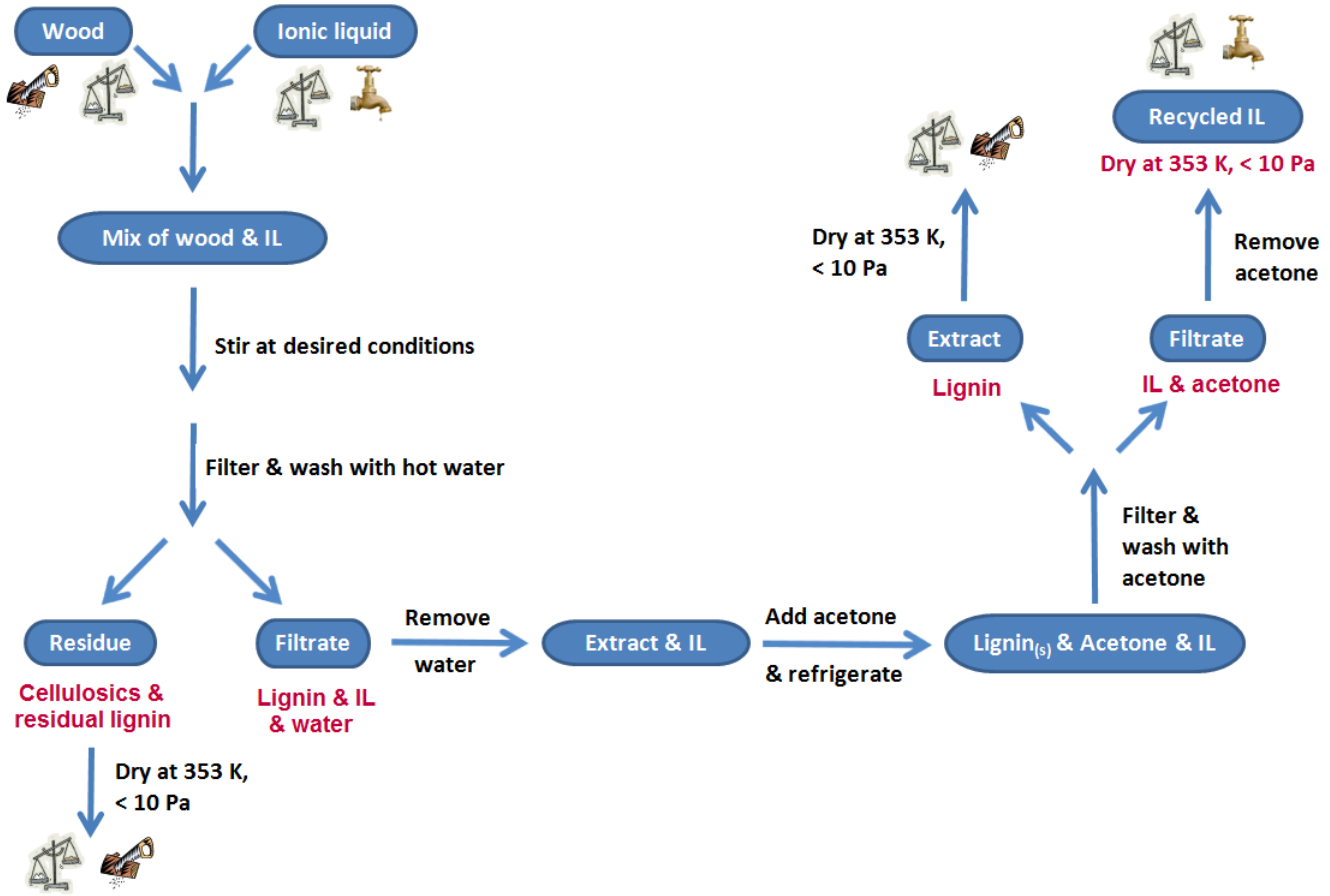


**Figure 61.** Experimental scheme for extracting wood lignin with acesulfamate ionic liquids. The wood symbol stands for acid insoluble lignin analysis, the scale stands for mass determination, and the water tap represents the measurement of the water content.

# Appendix F – Infrared spectra

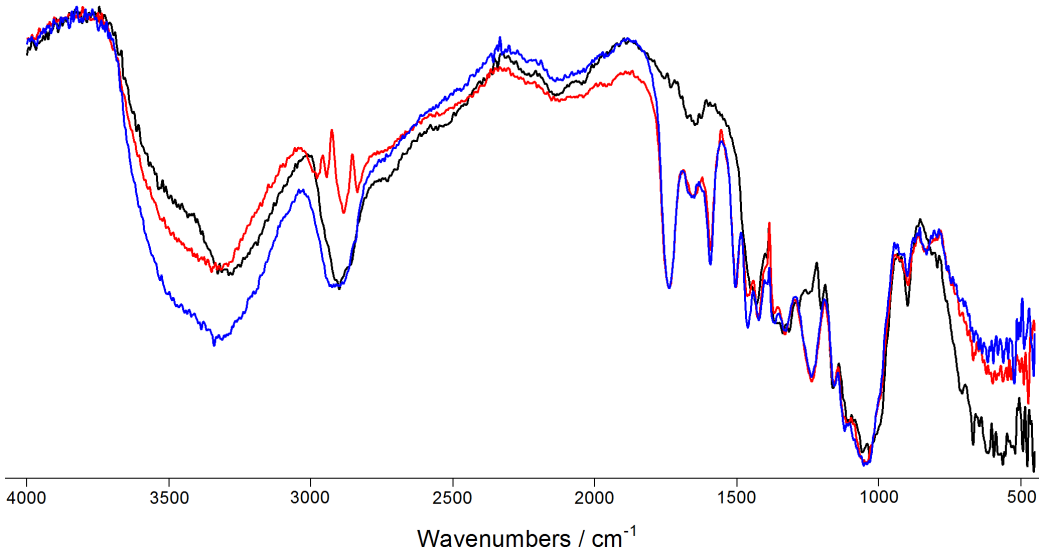


**Figure 62.** Infrared spectra of (i) the cellulosic-rich wood residue obtained from [BMIM]Ace treatment of *Eucalyptus nitens* at 373 K (red), (ii) native *Eucalyptus nitens* wood (blue), and (iii) microcrystalline cellulose (black).